LBL-36819
UC-414

Lawrence Berkeley Laboratory

UNIVERSITY OF CALIFORNIA

Physics Division

Broken Flavor Symmetries in High Energy Particle Phenomenology

A. Antaramian
(Ph.D. Thesis)

February 1995

U. C. Lawrence Berkeley Laboratory
Library, Berkeley

FOR REFERENCE

Not to be taken from this room

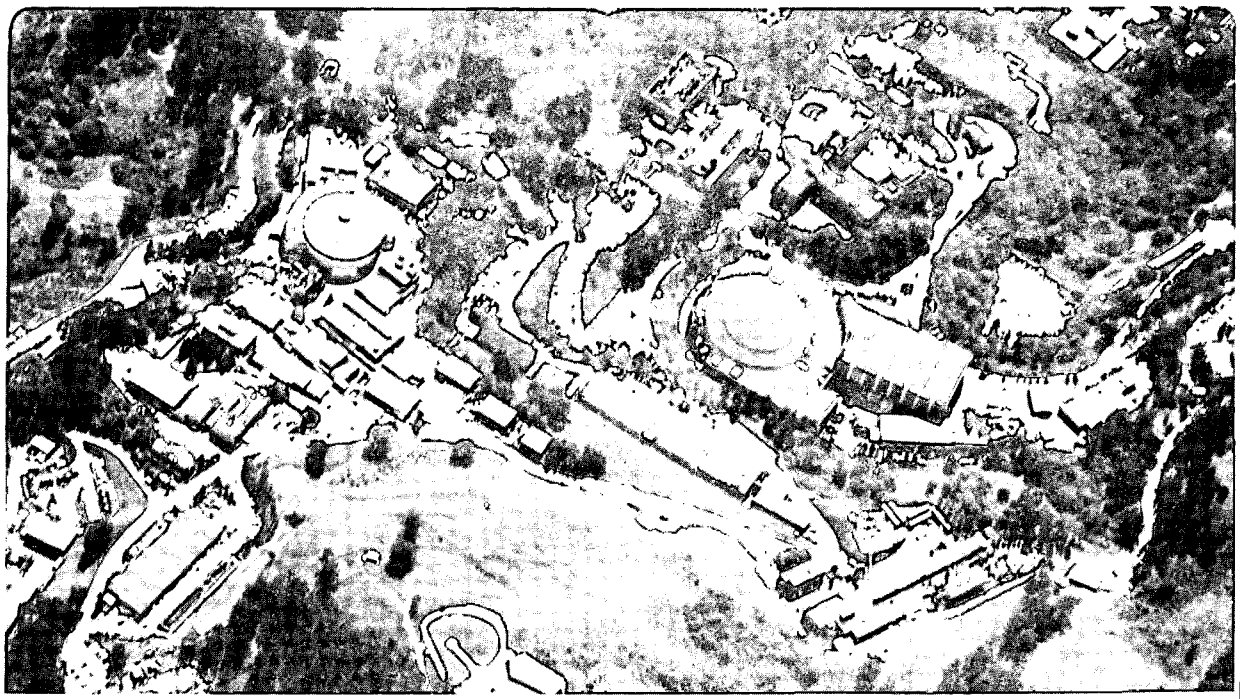

REFERENCE COPY
Does Not
Circulate
Bldg. 50 Library.
LBL-36819
Copy 1

Prepared for the U.S. Department of Energy under Contract Number DE-AC03-76SF00098

DISCLAIMER

This document was prepared as an account of work sponsored by the United States Government. While this document is believed to contain correct information, neither the United States Government nor any agency thereof, nor the Regents of the University of California, nor any of their employees, makes any warranty, express or implied, or assumes any legal responsibility for the accuracy, completeness, or usefulness of any information, apparatus, product, or process disclosed, or represents that its use would not infringe privately owned rights. Reference herein to any specific commercial product, process, or service by its trade name, trademark, manufacturer, or otherwise, does not necessarily constitute or imply its endorsement, recommendation, or favoring by the United States Government or any agency thereof, or the Regents of the University of California. The views and opinions of authors expressed herein do not necessarily state or reflect those of the United States Government or any agency thereof or the Regents of the University of California.

February 22, 1995

LBL-36819
UCB-PTH-95/05

Broken Flavor Symmetries in High Energy Particle Phenomenology

(Ph.D. Thesis) *

Aram Antaramian

Department of Physics
University of California
and
Theoretical Physics Group
Lawrence Berkeley Laboratory
University of California
Berkeley, California 94720

Abstract

Over the past couple of decades, the Standard Model of high energy particle physics has clearly established itself as an invaluable tool in the analysis of high energy particle phenomenon. However, from a field theorists point of view, there are many dissatisfying aspects to the model. One of these, is the large number of free parameters in the theory arising from the Yukawa couplings of the Higgs doublet.

In this thesis, we examine various issues relating to the Yukawa coupling structure of high energy particle field theories. We begin by exam-

*This work was supported by the Director, Office of Energy Research, Office of High Energy and Nuclear Physics, Division of High Energy Physics of the U.S. Department of Energy under Contract DE-AC03-76SF00098.

ining extensions to the Standard Model of particle physics which contain additional scalar fields. By appealing to the flavor structure observed in the fermion mass and Kobayashi-Maskawa matrices, we propose a reasonable phenomenological parameterization of the new Yukawa couplings based on the concept of approximate flavor symmetries. It is shown that such a parameterization eliminates the need for discrete symmetries which limit the allowed couplings of the new scalars. New scalar particles which can mediate exotic flavor changing reactions can have masses as low as the weak scale.

Next, we turn to the issue of neutrino mass matrices, where we examine a particular texture which leads to matter independent neutrino oscillation results for solar neutrinos. Using a nonstandard basis for our parameterization, we argue that such a mass matrix has a far larger allowed parameter space than the standard see-saw mass matrices. We propose a model which gives rise to such a matrix, finding that approximate flavor symmetries are an important tool in its construction. The experimental consequences of this model are discussed in detail.

We, then, examine the basis for extremely strict limits placed on flavor changing interactions which also break lepton- and/or baryon-number. These limits are derived from cosmological considerations. Such interactions, when in equilibrium simultaneously with electroweak instantons, can destroy an existing asymmetry in baryon number. We find that it is a simple matter to avoid these limits entirely, and that one need not impose a symmetry which has a baryon number component in order to do so.

Finally, we embark on an extended analysis of proton decay in supersymmetric $SO(10)$ grand unified theories. In such theories, the dominant decay diagrams involve the Yukawa couplings of a heavy triplet superfield. We argue that past calculations of proton decay which were based on the minimal supersymmetric $SU(5)$ model require reexamination because the Yukawa couplings of that theory are known to be wrong. By analyzing the flavor structure of a class of $SO(10)$ theories which do not suffer form this problem , we determine that proton decay branching ratios and dominant diagrams can differ substantially from previous expectations. We discuss, in some generality, the circumstances in which charged lepton decay modes have large branching ratios and in which gluino diagrams

become dominant. We find that both possibilities are more likely for the models we analyze. In addition, we examine some commonly made assumptions concerning squark mass matrices and discuss how the possible changes arising from very high energy radiative effects and nonminimal boundary conditions can effect proton decay.

Contents

1 Introduction **1**

2 Flavor Symmetries and Flavor Changing Scalar Interactions **5**
2.1 Introduction 5
2.2 Approximate Flavor Symmetries 6
2.3 Experimental Consequences 9
2.4 The Glashow-Weinberg Criterion for Multihiggs Models 11
2.5 Conclusions 12

3 Maximally Mixed Neutrinos **13**
3.1 Introduction 13
3.2 The MSW Solution 14
3.2.1 Vacuum Oscillations 14
3.2.2 Matter Oscillations 16
3.2.3 Maximal Mixing 20
3.2.4 "Averaging" Over Oscillations 23
3.3 The Model 24
3.4 Experimental Limits 28
3.4.1 Applying Limits 30
3.5 Conclusion 32

4 Hypercharge and the Cosmological Baryon Asymmetry **33**
4.1 Introduction 33
4.2 General Condition for Survival of a Baryon Asymmetry. 35
4.3 A Simple Model. 40
4.4 Conclusion 44

5 Proton Decay in SUSY SO(10) **46**
5.1 Introduction 46
5.2 What is Wrong with the MSGUT? 48
5.3 The ADHRS Model 50
5.4 Dimension-Five Operators and Discussion 57

5.5 Squark Masses 61
5.5.1 Preliminaries and the MSSM 61
5.5.2 Beyond MSGUT Masses 64
5.6 Calculational Preliminaries 68
5.7 Gluino Dressed Diagrams 69
5.7.1 Neutrino Modes 70
5.7.2 Charged Lepton Modes 76
5.7.3 Gluino Conclusions 80
5.8 Chargino and Neutralino Dressed Diagrams 81
5.8.1 Chargino Dressing 81
5.8.2 Neutralino Dressing 87
5.8.3 Chargino and Neutralino Conclusions 88
5.9 Discussion of Branching Ratios 89
5.10 Conclusion 90

Bibliography **92**

A Yukawa Matrices **99**

B Branching Ratios **102**

Acknowledgements

I extend my most sincere thanks to my advisor, Professor Lawrence J. Hall. I could not have hoped for a more enthusiastic, kind, and helpful teacher. He has given me both the space and freedom I needed and the insight and direction I required to complete my research efforts. Around him, I have learned never to pronounce a problem hopeless for fear of quickly being proven wrong. I consider myself incredibly privileged to have had the opportunity to learn from such a gifted physicist.

I am eternally grateful to my collaborator and fellow student, Andrija Rašin, who has shared in so much of the research I have done. On many occasions, his keen mind and good humor have been the difference between a fruitful endeavor and a catastrophic waste of time. His imagination, warmth, and intelligence will be sorely missed.

I am forever in the debt of the students, postdocs, and professors of the Berkeley physics department and LBL theory group. In particular, Markus Luty, Hitoshi Murayama, Bill Kilgore, Greg Anderson, Uri Sarid, Raman Sundrum, and Matt Austern have provided me with the answers to uncountabley many questions. Their help has been invaluable. Also, the teaching skill and love for physics which Professors Orlando Alvarez, David Jackson, Korkut Bardakci, and William Bialek have brought into the classroom and office have served to make my experience as a graduate student a deeply rewarding and enjoyable one.

It is difficult to express the depth of my gratitude to my friends and family who have, whether they liked it or not, been sucked into the world of physics graduate school as silent partners. Their unflagging support and patience has carried me through the difficult times with hardly a psychic scratch. Special thanks go to Matt Hendricks, Jamal Rayyis, Robin Thomas, Claudia Hoffberg, Jeff Rubin, Aaron Gladman, and Michelle Guy for all knowing exactly when I needed a good kick in the pants. Together with Nova Antaramian, Pat and Tim Burns, Mark Howorth, Lenna Gozurian, Amy Thomas, and Dean Cook these people helped to make the last few years very special. For inspiring me and driving me throughout

the first half of my graduate career as well as involving me in a series of unwise sporting pursuits, I am deeply in debt to Wati Taylor. To my parents I express the deepest gratitude for their unswerving confidence and backing.

I also wish to extend special thanks to Anne Takizawa, Betty Moura, Luanne Neumann, and the late Ken Miller. If it were not for each of them, I would have never made it in the door, let alone out.

Finally, my most heartfelt thanks go to Kimberly Drake. She has been my best friend and constant companion for the last three years, and, without her, I surely would have gone completely insane.

Chapter 1

Introduction

The Standard Model of particle interactions is a triumph of theoretical physics. It has enjoyed amazing success in describing the vast majority of high energy particle phenomenon. However, it leaves many fundamental questions unanswered. For example, is there a way of reducing the large number of free parameters in the Standard Model (SM), and can we explain their origin? What decides the particle content of the universe and the gauge charges for these particles? How can we account for the large particle mass hierarchies? For years, theorists have sought additional insight beyond the physics in the SM to help answer these questions. The task has proven to be a difficult one. The fundamental explanation may rest in superstring theories, at energies which we have little or no hope of reaching.

For phenomenologists, additional symmetries have been the tool of choice for addressing these issues. The gauge group of the SM has been enlarged to account for the particle content and charge structure. Supersymmetry has been added to solve the hierarchy problem. New global symmetries which govern the flavor structure of the theory have been imposed to help relate the 13 free parameters in the Kobayashi-Maskawa matrix and the fermion mass matrices. These additional symmetries give rise to new and interesting phenomenon, absent in the SM. In some instances, experiments bolster hopes of possible new physics, such as the observed deficit in solar neutrinos. In others, experiments are probing the limits of expected new phenomenon. Such is the case in recent and planned nucleon decay experi-

ments, where minimal supersymmetric grand unified theories are being challenged.

In this thesis, we will examine various effects and constraints that arise from the quest for a more fundamental understanding of the structure of the SM. The issue of broken symmetries is a consistent theme throughout. In particular, many of the chapters deal directly with flavor symmetries, which govern the interactions between different generations of fermions. These symmetries and the degree to which they may be broken are the natural language with which to deal with unknown Yukawa couplings in a theory. In Chapters 2 and 3, we use a phenomenological parametrization of flavor symmetry breaking parameters to gain insight into new Yukawa interactions. In Chapter 5, we employ an explicit flavor symmetry scheme to help in understanding proton decay in realistic supersymmetric Grand Unified Theories. Chapter 4 examines stringent bounds on flavor breaking interactions which also break baryon- and/or lepton-number.

We begin by re-examining the experimental constraints imposed on new scalar particles and their interactions. By using approximate flavor symmetries to parameterize the Yukawa couplings of these new scalars, we find that present experimental bounds allow them to have masses on the order of the weak scale. The use of discrete symmetries, in a wide array of models, to insure small flavor changing effects is rendered unnecessary. We discuss the resulting exotic flavor changing phenomenon which provide powerful probes for these new scalar interactions.

Chapter 3 proposes a solution to the solar neutrino deficit. An observed deficit in the flux of electron neutrinos coming from the sun has been a persistent and ever more convincing puzzle to physicists over the past few years as more groups independently confirm the results of the Homestake experiment [1]. Although the extremely low neutrino rate count and the high precision and huge scale of these experiments leave much doubt as to the reliability of the reported results, many believe that a deficit exists. Mikheyev, Smirnov, and Wolfenstein have proposed a popular and ingenious mechanism by which small mixing between two different neutrino flavor eigenstates can account for a large deficit [2]. Their theory relies on a subtle effect relating to the propagation of neutrinos through matter. Matter effects, however, are relevant only for a very constrained set of the free parameters in

the theory. In Chapter 3, we propose a model which gives a "matter independent" explanation for a dramatic deficit in solar electron neutrinos. The neutrino mass matrix we employ requires a reverse hierarchy between its diagonal and off-diagonal elements. We modify a model first proposed by Zee [3] by including the effects of approximate flavor symmetries. This allows us to naturally achieve the desired neutrino mass matrix.

In Chapter 4, we examine some of the cosmological constraints on baryon- and lepton-number violating interactions. Specifically, we analyze the circumstances in which the violation of these symmetries leads to a destruction of a cosmological baryon asymmetry produced at an extremely high temperature in the big bang. Stringent bounds on baryon- and lepton-number-violating interactions have been derived from the requirement that such interactions, together with electroweak instantons, preserve such an asymmetry. These bounds require coupling constants which are much smaller than are dictated by our previous flavor symmetry considerations. However, while these bounds apply in specific models, we find that they are generically evaded. In particular, the only requirement for a theory to avoid these bounds is that it contain charged particles which, during a certain cosmological epoch, carry a non-zero hypercharge asymmetry. Hypercharge neutrality of the universe then dictates that the remaining particles must carry a compensating hypercharge density, which is necessarily shared amongst them so as to give a baryon asymmetry. Hence the generation of a hypercharge density in a sector of the theory forces the universe to have a baryon asymmetry.

In Chapter 5, we look at an assortment of issues concerning proton decay in supersymmetric grand unified theories. We examine a specific class of models which provide an understanding of the mass and flavor structures of the SM particles. These models offer a concrete example of the mechanics of high energy flavor physics which govern the Yukawa couplings of a theory. We use the models as a guide in discussing the implications of flavor physics for proton decay in theories based on the gauge group $SO(10)$. We find that the neglect of these issues in previous proton decay calculations can be a grave error. In particular, proton decay calculations based on the minimal supersymmetric $SU(5)$ theory are reevaluated and found to

be incorrect in many circumstances.

It is well known that the minimal supersymmetric $SU(5)$ model fails to give correct fermion masses. In the theories which we analyze, solving this problem inevitably effects the commonly used symmetry relations between the Yukawa couplings which give fermions mass and those which govern the branching structure of nucleon decay. The new relations allow for interesting deviations from the standard nucleon decay predictions. Entire classes of diagrams, previously ignored, are likely to be dominant in many cases. For example, diagrams which involve the exchange of virtual gluinos are no longer negligible under the same assumptions about supersymmetric particle masses. In addition, the relative branching ratio of charged lepton decay modes to neutrino decay modes can be considerably larger than previously expected. Some models even predict that charged lepton modes are likely to be discovered at the same time as neutrino modes. We also discuss how high energy flavor symmetries can dramatically effect squark mass matrices and how these effects may further alter standard proton decay expectations.

Chapter 2

Flavor Symmetries and Flavor Changing Scalar Interactions

2.1 Introduction

As more and more tests of the standard model confirm its predictions to ever higher accuracy, it becomes tempting to believe that new physics, especially if it involves flavor changing neutral currents, can only occur at energy scales very much larger than the weak scale. For example, $\Delta S = 2$ four fermion operators with coefficients $1/\Lambda^2$ give a $K_L - K_S$ mass difference $\Delta m_K/m_K \simeq (f_K/\Lambda)^2$ implying that $\Lambda \geq 1000$ TeV. The purpose of this chapter is to show that it is perfectly natural for physics involving new heavy scalars to occur at scales as low as the weak scale, 250 GeV, and to show that rare leptonic B meson decays will provide an excellent probe of this new physics.

In this chapter, we introduce a specific form for the way that approximate flavor symmetries act on quarks and leptons. We then use this as a guide to infer the expected size of couplings between the known fermions and hypothetical, heavy scalar particles. The scalar mass M is then the only unknown parameter in the coefficient of the four fermion interactions induced by the exchange of this scalar. We derive the experimental limits on M from a variety of rare processes. The most powerful of these limits are of order the weak scale, giving hope to the possibility

that we may discover physics at the weak scale to be much richer than in the minimal standard model. There are two important advantages of our general approach. The scalar mass limits depend only on symmetry arguments and not on any specific model. Secondly, we can identify the most promising processes for discovering new physics in the next few years. In particular, we find that rare leptonic B decays are a very powerful probe of these new scalar interactions. For the case of leptoquarks, these B decays will probe masses far above the present experimental limits.

An important application of our results is to flavor changing effects in models with many Higgs doublets[5]. We find that the approximate flavor symmetries, which we already know must be a part of any successful model of particle physics, are sufficient to make it natural to have any number of Higgs doublets coupling to up and down type quarks. In other words it is completely unnecessary to introduce discrete symmetries which act on Higgs doublets, as is so frequently done.

2.2 Approximate Flavor Symmetries

In the standard model, the gauge interactions of the fermions:

$$\mathcal{L}_0 = i\bar{Q}\not{D}Q + i\bar{U}\not{D}U + i\bar{D}\not{D}D + i\bar{L}\not{D}L + i\bar{E}\not{D}E \tag{2.1}$$

have a global symmetry $U(3)_Q \times U(3)_U \times U(3)_D \times U(3)_L \times U(3)_E$, where Q_i and L_i are $SU(2)$ doublet quarks and leptons while U_i , D_i and E_i are $SU(2)$ singlets and $i = 1, 2, 3$ is a generation label.

The Yukawa couplings:

$$\mathcal{L} = \mathcal{L}_0 + (\lambda^U_{ij}\bar{Q}_i U_j \frac{\tilde{H}}{\sqrt{2}} + \lambda^D_{ij}\bar{Q}_i D_j \frac{H}{\sqrt{2}} + \lambda^E_{ij}\bar{L}_i E_j \frac{H}{\sqrt{2}} + h.c.) \tag{2.2}$$

break the symmetry by varying degrees down to $U(1)_e \times U(1)_\mu \times U(1)_\tau \times U(1)_B$. We parameterize the approximate flavor symmetries by a set of small parameters $\{\epsilon\}$, one for each of the above chiral fermion fields, which describes the breaking of phase rotation invariance on each fermion. Thus λ^U_{ij} is suppressed by both ϵ_{Q_i} and ϵ_{U_j} . The idea is that the pattern of fermion masses and mixing angles can be

described by the set $\{\epsilon\}$. However, this is not a precise numerical theory for fermion masses; equations of the form $\lambda^U_{ij} \approx \epsilon_{Q_i}\epsilon_{U_j}$ are only meant to be order of magnitude relations.

The Yukawa matrices $\lambda^U, \lambda^D, \lambda^L$ contain a great deal of information about the form of the breaking of flavor symmetry. Unfortunately, we cannot reconstruct these matrices from the information which can be obtained from experiments, namely from the fermion masses (i.e. the Yukawa matrix eigenvalues) and the Kobayashi-Maskawa (KM) matrix. This information is insufficient to derive the form of the approximate flavor symmetries which the underlying theory must have. Nevertheless it provides a strong guideline for giving a simple predictive ansatz for the symmetry breaking parameters.

The lightness of the up quark tells us that flavor symmetries strongly suppress the $\bar{Q}_1 U_1$ operator. However, the mass eigenvalue does not allow us to infer whether this is because the approximate flavor symmetry is acting only on Q_1, only on U_1, or on both. However, we need to know whether the coefficient of a scalar coupling to $Q_1 X$ (where X is any fermion other than U_1) is strongly suppressed because the up quark is very light.

We now argue that the approximate symmetries act both on left- and right-handed fields:

- The flavor symmetries do not act just on the right-handed fields because otherwise $U_3 \approx t_R$ couples to $(\alpha Q^u_1 + \beta Q^u_2 + \gamma Q^u_3) = t_L$ and $D_3 \approx b_R$ couples to $(\alpha' Q^u_1 + \beta' Q^u_2 + \gamma' Q^u_3) = b_L$ where $\alpha, \beta, \gamma, \alpha', \beta', \gamma'$ are arbitrary mixing angles of order one, so that t_L and b_L would have no reason to be very nearly in the same $SU(2)_L$ doublet.

- The flavor symmetries do not act just on the left-handed fields because in this case the approximate flavor symmetries make no distinction between λ^U and λ^D. A large m_t/m_b ratio could be due to a large ratio of vevs v_2/v_1 in a two Higgs theory, but this would lead to an unacceptably large m_u/m_d ratio. In addition the KM angles are given by linear mass relations such as $\theta_c \approx m_d/m_s$ rather than the more successful square root form $\theta_c \approx \sqrt{m_d/m_s}$

Therefore we conclude that *the underlying theory must have approximate flavor symmetries that act on both left- and right-handed fields* .

The approximate flavor symmetries and the associated set of small symmetry breaking parameters $\{\epsilon\}$ are defined on flavor eigenstates. In practice it is much more useful to know what suppression factors are induced on the mass eigenstates. Consider the up-type quarks. Assume that $\epsilon_{Q_i} \ll \epsilon_{Q_j}$ and $\epsilon_{U_i} \ll \epsilon_{U_j}$ for $i < j$, as suggested by $m_{U_i} \ll m_{U_j}$. Then the mass matrix is diagonalized by unitary rotations on the Q_i by a matrix with elements $|V_{ij}| \approx \epsilon_{Q_i}/\epsilon_{Q_j}$ $(i < j)$ and on the U_i by a matrix with elements $|V^R_{ij}| \approx \epsilon_{U_i}/\epsilon_{U_j}$ $(i < j)$. Relations between flavor and mass eigenstates (Q'_i) are of the form: $Q'_1 = Q_1 + O(\epsilon_{Q_1}/\epsilon_{Q_2})Q_2 + O(\epsilon_{Q_1}/\epsilon_{Q_3})Q_3$. This shows the important result that the flavor breaking parameters $\{\epsilon\}$ apply to mass eigenstates as well as to flavor eigenstates. For example, the three flavor eigenstate contributions to Q'_1 all carry the same approximate flavor symmetry suppression factor of ϵ_{Q_1}.

The actual structure of the approximate low energy flavor symmetries is likely to involve many parameters: the fermion masses and mixing angles have very few obvious regularities. A simple predictive ansatz is shown in Table 2.1. It involves both left- and right-handed fermions and is predictive because it only involves quark and lepton masses.

Table 2.1: The ansatz for flavor symmetry breaking parameters associated to the chiral fermion fields. $\eta_i = \sqrt{\frac{m_{U_i}}{v_2}}$ and $\xi_i = \sqrt{\frac{m_{D_i}}{v_1}}$.

FIELD	FLAVOR SYMMETRY BREAKING PARAMETER
Q_i	$\sqrt{\eta_i \xi_i}$
U_i	$\sqrt{\frac{\eta_i}{\xi_i}}\eta_i$
D_i	$\sqrt{\frac{\xi_i}{\eta_i}}\xi_i$
L_i, E_i	$\sqrt{\frac{m_{E_i}}{v_1}}$

The rationale behind our choice is as follows. For the leptons the flavor symmetries on L_i and E_i are equally responsible for suppressing the Yukawa cou-

plings. For quarks, we have again tried to have both left- and right- handed flavor symmetries equally responsible for suppressing Yukawa couplings. However since Q_i appears in both up and down mass operators, we have taken the symmetry breaking parameter ϵ_{Q_i} to be the geometric mean of that expected from m_{U_i} and that expected from m_{D_i}. Note that we have allowed for a two Higgs doublet model. With only one Higgs boson $v_1 = v_2 = 250GeV$.

The ansatz gives reasonable values for the CKM mixing angles. $V_{ij} \approx \epsilon_{Q_i}/\epsilon_{Q_j} \approx (m_{U_i}m_{D_i}/m_{U_j}m_{D_j})^{\frac{1}{4}}, i < j$, which is correct at the factor of 2 level.

One must keep in mind that the ansatz, despite its simplicity, is hardly unique. A more complicated ansatz might use the KM matrix as input as well as the fermion masses. However this extra complexity is not warranted since our ansatz is quite consistent with the KM matrix. We use the ansatz only to *estimate* the magnitudes of unknown Yukawa couplings.

2.3 Experimental Consequences

We use our ansatz to estimate the size of the Yukawa couplings and then the corresponding rates for various processes induced by the effective four fermion couplings. In Table 2.2, we list the limits on the exchanged scalar mass [6] obtained from a variety of experiments . For now we assume the scalar exchange does induce each process and that the flavor symmetry acts only on fermions. Once again, we obtained these numbers using our ansatz to estimate the Yukawa couplings, so we expect the values to be reliable up to a factor of perhaps 2 or 3.

The factor κ represents the ratio of the matrix element of the new four fermion operator relative to its vacuum insertion value. In the radiative μ decay, the τ-lepton contribution dominates in the loop because it has the largest Yukawa couplings.

Table 2.2: Experimental lower limits on the exchanged scalar masses

process	$M/GeV(250GeV/v_1)$
$\mu \to 3e$	1
$\mu \to e\gamma$	4
$\mu N \to eN$	10
$K_L^0 \to \mu^\pm e^\mp$	20
$B_d \to \tau^+\tau^-$	20 $(\frac{10^{-4}}{B.R.})^{\frac{1}{4}}$
$B_s \to \mu^+\mu^-$	70 $(\frac{10^{-8}}{B.R.})^{\frac{1}{4}}$
$\Delta m(B_d^0 - \bar{B}_d^0)$	400 $\sqrt{\kappa}$
$\Delta m(K^0 - \bar{K}^0)$	500 $\sqrt{\kappa}$

First, we can see that these limits are nowhere near as strong as those for vector exchange [7]. Flavor nonconserving theories at the weak scale are not ruled out at all. Secondly, if the uncertainty factors of 2 or 3 go the right way, it is possible that the rare leptonic B_s decay will be the first place to discover this new physics, considering that branching ratios $10^{-7} - 10^{-8}$ will be obtained in the near future [8]. The branching ratio prediction for $B_s \to \mu^+\mu^-$ is about 10^{-9} in the standard model, and in two Higgs doublet models with discrete symmetries [9].

There are cases where the scalar cannot induce all the processes considered, as in leptoquark models. The tree level exchange of leptoquarks generates four fermion operators which contain two quarks and two leptons. The limits from $K\bar{K}$ and $B\bar{B}$ mixing are therefore removed. In this case our results are particularly important: the rare leptonic B decay modes provide the most stringent test of models with scalar leptoquarks.

We discuss briefly the case in which approximate flavor symmetries act on the exchanged scalar too. Such is the case in R-parity violating supersymmetric models [10] where the exchanged scalar is a slepton or a squark which carries the same approximate flavor symmetry as its fermion partners. Then, in Table 2.2, all mass limits from simple scalar exchange diagrams are lowered by an additional symmetry breaking factor ϵ_a, where the approximate symmetry of type "a" is carried

by the scalar. It is even less likely that such theories could have been excluded.

Recently, stringent cosmological bounds have been placed on the size of baryon and lepton number violating interactions in certain theories. These bounds require much smaller Yukawa interactions for scalars which violate baryon and/or lepton number than are implied by our approximate flavor symmetries. However, these bounds are easily evaded. In Chapter 4, we look in detail at this subject.

We have not mentioned limits arising from CP-violating effects in the $K - \overline{K}$ system. These limits can be quite severe if we allow for large phases in the scalar couplings of the theory. Hall and Weinberg discuss this issue in reference [4]. They examine the consequences of assuming that CP is also an approximate symmetry, thereby insuring very small phase factors.

2.4 The Glashow-Weinberg Criterion for Multi-higgs Models

In this section we apply our results to the case of the minimal standard model extended only by the addition of an arbitrary number of Higgs doublets. In this case it is already known that, for the special case of Fritzsch-like Yukawa matrices, the additional scalars need not be heavier than a TeV [11]. However, our results are independent of the particular texture and depend only on the approximate flavor symmetry.

To avoid problems with large flavor-changing neutral currents, Glashow and Weinberg [5] argued that only one Higgs doublet could couple to up-type quarks and only one Higgs to down-type quarks. However, this naturality constraint, known as the Glashow-Weinberg criterion, was based on an unusual definition of what is "natural". For them the avoidance of flavor-changing neutral currents was natural in a model only if it occurred for all values of the coupling constants of that model. For us a model will be natural provided the smallness of any coupling is guaranteed by approximate symmetries [12], and we find that this implies the Glashow-Weinberg criterion is not necessary.

In a model with many scalar doublets it is convenient to work in a basis where only one doublet, the Higgs doublet, acquires a vev, and all the others are massive scalar particles which play no role in the Higgs mechanism. The couplings of the Higgs meson are flavor-diagonal at tree level, but in general the couplings of the other doublets are not. The limits on the mass M of these extra scalars are given in Table 2.2. This shows that *approximate flavor symmetries are sufficient to allow extra scalar doublets with masses in the 100s of GeV range, there is no need for additional symmetries to act on the scalar fields.*

One reason why this is important is that the vast majority of phenomenology on the multihiggs models has been done assuming symmetries which force only one Higgs to couple to up-type and one to down-type quarks. We conclude that there is no good reason for accepting the predictions of these analyses, except in the case of supersymmetric models.

2.5 Conclusions

In this chapter, we have introduced a simple ansatz for the approximate flavor symmetries as shown in Table 2.2. It reproduces the KM matrix elements at the factor of 2 level. If the interactions of additional scalars respect these approximate symmetries, then the mass limits on the scalars from various experiments are shown in Table 2.2. From this viewpoint, new flavor changing physics at the weak scale is not excluded, and is natural. In particular extra Higgs doublets can couple to both up and down type quarks; there is no need to impose additional discrete symmetries on the scalars. We find that rare leptonic B decay modes, such as $B_s^0 \to \mu^+\mu^-$, could uncover this new scalar-mediated physics in the coming years.

Chapter 3

Maximally Mixed Neutrinos

3.1 Introduction

An observed deficit in the flux of electron neutrinos coming from the sun has been a persistent and ever more convincing puzzle to physicists over the past few years as more groups independently confirm the results of Davis and his associates [1, 25, 35, 34]. Although the extremely low neutrino rate count and the high precision and huge scale of these experiments leave much doubt as to the reliability of the reported results, many believe that a deficit exists.

This deficit, known as the solar neutrino problem, has spurred both astrophysicists and particle physicists to propose a vast array of possible explanations. Mikheyev, Smirnov, and Wolfenstein (MSW) [2] have proposed a popular and ingenious mechanism by which small mixing between two different neutrino flavor eigenstates can account for a large deficit. Their theory, which we describe in greater detail in Section 3.2 , relies on a subtle effect relating to the propagation of neutrinos through matter.

As we will argue however, matter effects are relevant only for a very limited set of the free parameters in the theory. We assume the attitude that although one could constrain the field of possible solutions by giving the experimental results more statistical relevance than they deserve, it is wiser, at this time, to keep open the possibility that many of the proposed solutions are not ruled out. In that spirit,

we have looked for a solution which is both likely in terms of allowed parameter space, and as simple as possible. In Section 3.2.3, we will compare the parameter space of small mixing solutions with that of a maximal mixing scheme. We will argue that the maximal mixing scheme not only has a far greater parameter space, but that it leads to a vastly simplified oscillation explanation for the solar neutrino problem. Thus, according to the guidelines above this solution deserves further study.

In Section 3.3, we propose a specific particle theory model which gives a maximal mixing neutrino mass matrix like the ones discussed in the previous section. In constructing this model, we are naturally lead to the topic of approximate flavor symmetries. Applying one possible set of such symmetries, we examine the consequences of our model and conclude that the only way to check such models in the near future is at new solar neutrino detectors. Our scheme predicts a $\frac{1}{2}$ depletion of the solar electron neutrino flux independent of neutrino energy.

3.2 The MSW Solution

In this section, we will discuss the theory behind the most popular particle theory explanation for the solar neutrino problem, neutrino flavor oscillations. We work in a basis where the charged lepton mass matrix is diagonal and denote the $SU(2)$ partner of the electron/muon/tau by $\nu_{e/\mu/\tau}$ respectively. In these theories, one gives neutrinos small masses and assumes the neutrino mass eigenstates are mixtures of the flavor eigenstates $\nu_{e/\mu/\tau}$. Such a scheme leads to neutrino flavor oscillations.

3.2.1 Vacuum Oscillations

Let us first examine neutrino oscillations in vacuum. For convenience, we will express all neutrinos as two component left handed spinors. We can always do so, since if ν is right handed than $\nu' = \nu^C$ is left handed, where ν^C is the charge conjugate of ν. We will look at the case of oscillations involving only two flavors

and will assume CP is a good symmetry. Then, the mass matrix in this basis is symmetric and can be made real. Relaxing our assumption of CP being valid does not change any of the results in this section because CP violation can not be detected in neutrino oscillations involving only two flavors [20]. The mass matrix can be diagonalized by an orthogonal matrix which we call O. the mass eigenstates, ν_i, are then related to the neutrinos of a given flavor, ν_α, in the following way.

$$\nu_i = O_{i\alpha}\nu_\alpha \qquad O_{i\alpha} = \begin{pmatrix} \cos\theta & \sin\theta \\ -\sin\theta & \cos\theta \end{pmatrix}$$

where θ is the angle of rotation.

The diagonal mass matrix which results, however may have negative masses. This can be remedied by defining the unitary matrix U where $U_{i\alpha} = O_{i\alpha}e^{i\frac{\pi}{4}(\rho_i-1)}$ where ρ_i is the sign of the mass eigenvalue m_i.

If an electron neutrino is emitted in a plane wave state with momentum $\vec{k}$ at time $t = 0$, we can decompose it in terms of mass eigenstates. At some later time t the state is given by

$$\nu(\vec{x},t) = \nu_1 \cos\theta\, e^{i\frac{\pi}{4}(\rho_1-1)}e^{-iE_1t+i\vec{k}\cdot\vec{x}} - \nu_2 \sin\theta\, e^{i\frac{\pi}{4}(\rho_2-1)}e^{-iE_2t+i\vec{k}\cdot\vec{x}} \tag{3.1}$$

It would be more exact to deal with wave packets and coherence lengths but, for our purposes, this simplified approach is more instructive and leads to the same conclusions [21]. The probability of detecting an electron neutrino at $\vec{x}$ and t is then given by

$$P_{\nu_e\to\nu_e} = \frac{1}{2}\left(1 + \cos^2 2\theta + \sin^2 2\theta \cos((E_1 - E_2)t)\right), \tag{3.2}$$

where t is the distance the beam has travelled divided by its velocity, which we take to be the speed of light, $c = 1$. For highly relativistic neutrinos, we can express $(E_2 - E_1)$ as $\frac{\Delta m^2}{2k}$ where

$$\Delta m^2 = m_2^2 - m_1^2. \tag{3.3}$$

The combination

$$l \equiv \left(\frac{\Delta m^2}{2k}\right) \tag{3.4}$$

is known as the vacuum oscillation length.

A great deal of care can be taken to include the coherence length and dispersion of the neutrino wave packets, but the only consequence we will be concerned with is the effects on the "averaging" of the term proportional to $\cos((E_1 - E_2)t)$ in equation 3.2. We refer to this term as the oscillating term.

Solar neutrino experiments give a result which is an average over a finite range of neutrino energies as well as over the position of emission of the neutrino. This translates into an average over the factor $(E_1 - E_2)t$ above. The average over energy will kill the term $\cos((E_1 - E_2)t)$ as long as $R_e \frac{\Delta m^2}{2k^2} \delta k > 10$ where δk is the spread in energy and R_e is the earth sun distance.

Similarly, for mass differences with which we shall be interested a solar neutrino wave packet after traveling to the earth may separate into two nonoverlapping wave packets corresponding to the two different mass eigenstates, which travel at different speeds. This leads to the vanishing of quantum interference terms and again kills the $\cos((E_1 - E_2)t)$ term. If we can drop this term, we are left with the averaged result

$$P_{\nu_e \to \nu_e} = \frac{1}{2}\left(1 + \cos^2 2\theta\right). \tag{3.5}$$

3.2.2 Matter Oscillations

The situation changes when propagation through the sun is taken into account. What Mikheyev, Smirnov, and Wolfenstein noticed was that charged-current interactions between the propagating neutrinos and the electrons in the sun contribute an effective mass term to electron neutrinos. The relevant Lagrangian is

$$\begin{aligned} \mathcal{L} &= \nu_e^\dagger (i\partial_0 - i\boldsymbol{\sigma} \cdot \boldsymbol{\nabla})\nu_e + \nu_\mu^\dagger (i\partial_0 - i\boldsymbol{\sigma} \cdot \boldsymbol{\nabla})\nu_\mu \\ &\quad -\frac{m_e}{2}(\nu_e^T i\sigma_2 \nu_e) - \frac{m_\mu}{2}(\nu_\mu^T i\sigma_2 \nu_\mu) - m_{e\mu}(\nu_e^T i\sigma_2 \nu_\mu) \\ &\quad -V\nu_e^\dagger \nu_e + h.c. \end{aligned} \tag{3.6}$$

where $V = \sqrt{2}\, G_F N_e$ and G_F is the fermi constant, N_e is the number density of electrons in the medium, and m_e, m_μ, and $m_{e\mu}$ are neutrino majorana masses.

For relativistic neutrinos, the equations of motion can be simplified by eliminating the positive helicity states [22]. We are left with an effective equation of motion, which, in the flavor basis ν_α is given by

$$i\partial_t \begin{bmatrix} \nu_e \\ \nu_\mu \end{bmatrix} = \left[U^\dagger \begin{pmatrix} k + \frac{m_1^2}{2k} & 0 \\ 0 & k + \frac{m_2^2}{2k} \end{pmatrix} U + \begin{pmatrix} V & 0 \\ 0 & 0 \end{pmatrix} \right] \begin{bmatrix} \nu_e \\ \nu_\mu \end{bmatrix}$$

The rotation which diagonalizes this Hamiltonian is

$$\tan 2\theta_m = \frac{\Delta m^2 \sin 2\theta}{\Delta m^2 \cos 2\theta - 2kV}, \tag{3.7}$$

where θ is the vacuum rotation angle. We denote the eigenstates of this Hamiltonian by ν_{mi} where $i = 1,\ 2$. Their masses are given by m_{mi}.

$$\begin{aligned} m_{m2}^2, m_{m1}^2 &= \tfrac{1}{2}(m_1^2 + m_2^2 + 2kV) \\ &\pm \tfrac{1}{2}\left[(\Delta m^2 \cos 2\theta - 2kV)^2 + (\Delta m^2)^2 \sin^2 2\theta\right]^{\frac{1}{2}} \end{aligned} \tag{3.8}$$

Up to a term proportional to the identity, this Hamiltonian is of the same form as that of a spin $\frac{1}{2}$ particle in a uniform magnetic field with off diagonal interactions [23]. The potential V above plays the role of the magnetic field. As is well known in the spin $\frac{1}{2}$ system, a small off-diagonal perturbation can have dramatic effects. If the magnetic field is varied slowly in the proper manner, almost complete spin flip can occur. This is the well known avoided level crossing phenomenon.

The exact same mechanism is at work in the neutrino case. For small rotation angles θ the Hamiltonian is almost diagonal. Varying V in the proper way can lead to almost complete conversion of ν_e to ν_μ. This is easy to see from equation (3.7). If V is large, then θ_m is close to $\frac{\pi}{2}$, and ν_e is primarily ν_{2m}. If V is varied slowly, then there are no transitions between the local eigenstates ν_{m1} and ν_{m2}, and the neutrino stays in the state ν_{m2}. For V equal to zero, $\nu_{m1} \simeq \nu_e$ and $\nu_{m2} \simeq \nu_\mu$. Thus, if V is slowly varied from a large value to zero, an electron neutrino can be transformed almost entirely to a muon neutrino. This can be the situation for neutrinos travelling through the sun. The potential V is given by the local electron density along the neutrino's path. The value of V at which the level

crossing is avoided is known as the resonance density and is given by equation (3.7) for the case where $\theta_m \simeq \frac{\pi}{4}$.

As in the vacuum case, oscillating terms which arise from interference between mass eigenstates can be averaged to zero in most cases. If this is the case, the probability of a ν_e surviving the trip from the sun is just a combination of classical probability factors.

$$P_{\nu_e \to \nu_e} = \begin{pmatrix} 1 & 0 \end{pmatrix} \begin{pmatrix} c_m^2 & s_m^2 \\ s_m^2 & c_m^2 \end{pmatrix} \begin{pmatrix} c^2 & s^2 \\ s^2 & c^2 \end{pmatrix} \begin{pmatrix} 1 \\ 0 \end{pmatrix}, \tag{3.9}$$

where $c_m^2 = \cos^2\theta_m$, $s_m^2 = \sin^2\theta_m$ and c^2, s^2 are similar for θ.

The above results must be corrected however to account for possible transitions between the matter eigenstates caused by the variation of the matter density along the neutrino's path. We may write the Hamiltonian equation for ν_{m1} and ν_{m2} in the following form

$$i\partial_t \begin{bmatrix} \nu_{m1} \\ \nu_{m2} \end{bmatrix} = \begin{bmatrix} k + \frac{m_{1m}^2}{2k} & i\dot{\theta}_m \\ -i\dot{\theta}_m & k + \frac{m_{2m}^2}{2k} \end{bmatrix} \begin{bmatrix} \nu_{m1} \\ \nu_{m2} \end{bmatrix},$$

where $\dot{\theta}_m$ is the spacial derivative of θ_m along the direction of travel of the neutrino. Thus, the approximation of no transitions, commonly called the adiabatic approximation, is only good as long as

$$\dot{\theta}_m << \frac{\Delta\tilde{m}^2}{4k}, \tag{3.10}$$

where $\Delta\tilde{m}^2 = m_{m2}^2 - m_{m1}^2$ is given by

$$\tilde{m}^2 = \left[(2VE)^2 + (\Delta m^2)^2\right]^{1/2} \tag{3.11}$$

Since θ_m is changing most rapidly at the resonance density and $\Delta\tilde{m}^2$ is smallest at the same time, any violation of the above condition will be most dramatic there. One can take into account the likelihood of a transition between ν_{m1} and ν_{m2} by introducing a nonadiabatic transition matrix into equation (3.9).

$$\begin{aligned} P_{\nu_e \to \nu_e} &= \begin{pmatrix} 1 & 0 \end{pmatrix} \begin{pmatrix} c_m^2 & s_m^2 \\ s_m^2 & c_m^2 \end{pmatrix} \begin{pmatrix} 1-P_j & P_j \\ P_j & 1-P_j \end{pmatrix} \begin{pmatrix} c^2 & s^2 \\ s^2 & c^2 \end{pmatrix} \begin{pmatrix} 1 \\ 0 \end{pmatrix} \\ &= \frac{1}{2} + (\frac{1}{2} - P_j)\cos 2\theta \cos 2\theta_m, \end{aligned} \tag{3.12}$$

where P_j is the probability of a jump between the states ν_{m1} and ν_{m2}, and depends on the position of origin of the neutrinos involved. P_j has been computed for various density profiles.

One can refine equation (3.12) to take into account phase effects which might enter if the neutrino wave packet is still coherent when it enters the resonance region or to incorporate corrections to account for neutrinos produced on the far side of the sun which may have to travel through two resonance regions, etc. However, we will stop here in our explanation of the MSW mechanism, having adequately highlighted the main subtleties involved.

The result, equation (3.12), depends critically on matter effects both through P_j and θ_m. Although quite beautiful in its intricacy, the MSW solution also points to a much more simple and straightforward solution as long as we accept a solar neutrino depletion factor of about $\frac{1}{2}$. From equation (3.12), we see that if $\theta = \frac{\pi}{4}$, then $P_{\nu_e \to \nu_e} = \frac{1}{2}$, independent of any matter effects.

If $\theta = \frac{\pi}{4}$, then no matter what linear combination of mass eigenstates in which the original neutrino arrives at earth, $P_{\nu_e \to \nu_e} = \frac{1}{2}$ as long as we can neglect the oscillating interference terms. If the neutrino state at the earth is given by

$$\nu = \nu_{m1} \cos\alpha \, e^{-i\beta_1} + \nu_{m2} \sin\alpha \, e^{-i\beta_2},$$

where β_i is an oscillating phase, the average probability of finding a ν_e at earth is just $\frac{1}{2}(\cos^2\alpha + \sin^2\alpha) = \frac{1}{2}$.

Let us look for a mass matrix which results in $\theta \approx \frac{\pi}{4}$. For a general neutrino mass matrix,

$$\begin{pmatrix} m_e & m_{e\mu} \\ m_{e\mu} & m_\mu \end{pmatrix}, \tag{3.13}$$

the angle of rotation is given by $\tan 2\theta = \frac{2m_{e\mu}}{m_\mu - m_e}$. Barring fine tuning of the difference $m_\mu - m_e$, one should look for a matrix in which the diagonal elements are much smaller than $m_{e\mu}$. We can not allow $m_e = m_\mu$, for in this case no oscillations take place; we are left with two degenerate neutrino states which we can combine into a single Dirac neutrino [24].

3.2.3 Maximal Mixing

We will call a matrix which leads to a mixing angle of $\frac{\pi}{4}$ a maximal mixing mass matrix. In the next section, we shall discuss a model which leads to such a matrix. But first, we will briefly discuss our philosophy concerning the result $P_{\nu_e \to \nu_e} = \frac{1}{2}$. Taking the central theoretical values for Bahcall and Pinsonneault's Standard Solar Model calculations [33], the experimental data from Kamiokanda [25], Gallex [34], and Sage [35] are all within 1σ of 0.5. (See Table 3.1). Davis's chlorine experiment, however, has a central value which is 36% below 0.5. Nevertheless, we believe that at the present time the lack of calibration for the chlorine experiment and the poor statistics for all four experiments make $\frac{1}{2}$ a result which should not be neglected. The simplicity of such a solution together with the existence of a particle model which leads to it provide enough reason to pursue the possibility.

Table 3.1: The solar neutrino observation rates over Standard Solar Model predictions for the models of Bahcall-Pinsonneault (BP) [33] and Turck-Chièze (TC) [36]. GALLEX and SAGE data are as reported in July 1994 [37]. The errors given are at one standard deviation.

Experiment	BC	TC
Chlorine	$0.32 \pm .05$	$0.40 \pm .09$
Kamiokanda	$0.50 \pm .07$	$0.66 \pm .09$
GALLEX	$0.60 \pm .10$	$0.63 \pm .10$
SAGE	$0.52 \pm .09$	$0.55 \pm .10$

In addition, we believe that the large mixing solution is a far more likely solution than the small mixing ones. We can plot the parameter space for a general model in a nontraditional, but more transparent, basis. Once we have subtracted a term proportional to the identity, the mass matrix for two neutrino oscillations can be written as follows;

$$\begin{pmatrix} 0 & m \\ m & M \end{pmatrix}. \tag{3.14}$$

Figure 3.1 is a rough plot which illustrates our claim. Using m and M as free parameters, we plot the approximate parameter space compatible with various values of $P_{\nu_e \to \nu_e}$ in a typical experiment. The area enclosed within the solid lines is the allowed solution space for a matrix giving the result $P_{\nu_e \to \nu_e} \simeq \frac{1}{2} \pm 10^{-2}$. The large trapezoidal area dominating the right half of the diagram corresponds to the maximal mixing solution. Here $M < 2 \times 10^{-3}\, m$ and the vacuum mixing angle is very close to $\frac{\pi}{4}$; $\cos 2\theta < 2 \times 10^{-2}$. The parameters enclosed within the annular triangular region in Figure 3.1, which also lead to $P_{\nu_e \to \nu_e} \simeq \frac{1}{2}$, correspond to smaller angle solutions which depend critically on matter effects.

The parameter space for all values of $P_{\nu_e \to \nu_e} < \frac{1}{2} - 10^{-2}$ is contained within the triangular region. The area enclosed in the dotted line corresponds to $\frac{9}{10} > P_{\nu_e \to \nu_e} > \frac{8}{10}$ for a typical experiment. The allowed parameter space corresponding to $\frac{8}{10} > P_{\nu_e \to \nu_e} > \frac{1}{2} + 10^{-2}$ is the region in between the dotted area and the solid outline. Figure 3.1 makes it obvious that the solution space, parameterized in terms of m and M strongly favor $P_{\nu_e \to \nu_e} \simeq \frac{1}{2}$ and $\theta \approx \frac{\pi}{4}$.

In fact, this conclusion is even stronger than it appears, because Figure 3.1 is plotted on a log-log scale. The triangular region occupies a tiny fraction of the total solution space. We note that the restriction $\Delta m^2 < 1.4 \times 10^{-2} eV^{-2}$, coming from the nonobservation of neutrino oscillations in reactor experiments, means that M can not be too large. For small m, we have $\Delta m^2 \simeq M^2$. Thus, M is restricted to be less than $0.12 eV$. There is no corresponding restriction on m since, for large m, $\Delta m^2 = 2mM$.

We find this parameter space analysis to be a compelling reason to investigate models which lead to maximal mixing.

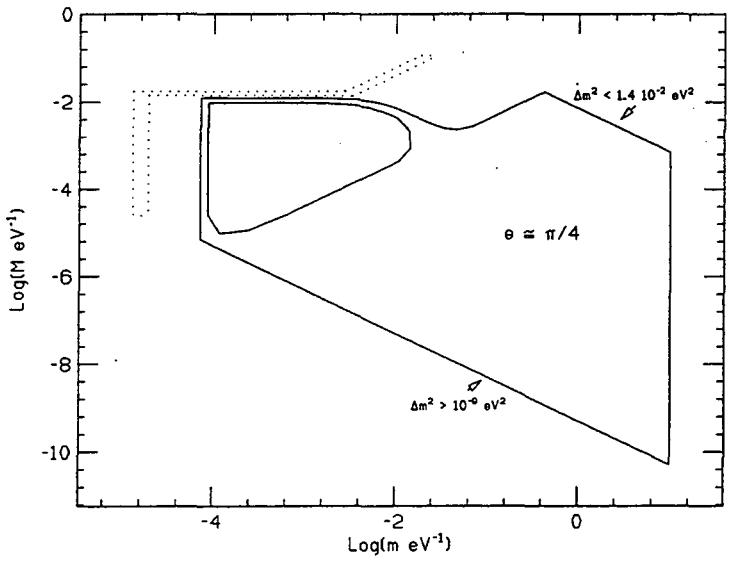

Figure 3.1: We draw the allowed parameter space in terms of m and M from Equation 3.14 which results in a given range for the survival probability of solar electron neutrinos at the earth. The area enclosed in the solid curve corresponds to a survival probability within 10^{-2} of the result $P_{\nu_e \to \nu_e} = \frac{1}{2}$ for a typical experiment. This is a reparameterized version of the standard MSW triangle. Within the large trapezoidal region, the vacuum mixing angle is very near $\frac{\pi}{4}$; $\cos 2\theta < 2 \times 10^{-2}$. The annular triangular region corresponds to smaller mixing angles and is determined in detail by matter effects. The right hand limit results from demanding that the lightest neutrino have a mass less than $10eV$ (See Eq. 3.24). The area enclosed in the dotted curve corresponds to a survival probability which satisfies $\frac{9}{10} > P_{\nu_e \to \nu_e} > \frac{8}{10}$ for a typical experiment.

3.2.4 "Averaging" Over Oscillations

Before we discuss the model in Section 3.3, we will briefly examine the conditions under which we can ignore the oscillatory term in $P_{\nu_e \to \nu_e}$. Anada and Nishimura [26] argue that the coherence length of a neutrino packet originating in a dense medium is limited by the time between collisions, τ_c, of the emitting particles. Assuming that the coherence length d is given by its maximal value, $d \simeq c\tau_c$, where c is the speed of light, they estimate it to be about $9 \times 10^{-8} cm$ (for neutrinos originating from ^8B reactions).

A neutrino wavepacket decomposes into its mass eigenstates which travel at different velocities. In travelling from a point R_o to earth, R_e, the mass eigenstates separate by a distance

$$L = \frac{1}{E} \int_{R_o}^{R_e} \frac{\Delta \tilde{m}^2}{2E} dx, \tag{3.15}$$

where $\tilde{m}^2 = m_{m2}^2 - m_{m1}^2$ is given by equation (3.11), and we have taken $\theta \approx \frac{\pi}{4}$. If $L > d$, then the neutrino has separated into two nonoverlapping wavepackets, and no interference can occur. Under these circumstances, we can ignore the oscillating term in $P_{\nu_e \to \nu_e}$.

Taking $n_e(x) = 245\ N_A\ exp(-\frac{10x}{R_\odot})\ (cm)^{-3}$, where N_A is Avogadro's number, and assuming $R_o \simeq 0$, we can compute the integral in equation (3.15) and get

$$L = \left(\frac{\Delta m^2}{2E^2}\right)\left(\frac{R_\odot}{20}\right)\left[2s + \ln\left(\frac{s-1}{s+1}\right)\right]\Big|_{s_i}^{s_f},$$

where $s = 1 + (V_0 l)^2 exp(-\frac{10x}{R_\odot})$. Here, V_0 is the value of the potential V at the point of origin of the neutrino, l is the vacuum neutrino wavelength (See Eq. 3.4), and s_f and s_i correspond to the final and initial values of s.

For small Δm^2, the product $V_0 l$ is large and we have

$$L = \frac{\Delta m^2}{2e^2} R_e + \frac{1}{5} R_\odot \left(\frac{V_0}{E} - \frac{1}{V_0 l}(1 + \ln(V_o l/2))\right).$$

The natural log term is irrelevant. For neutrino energies less than an MeV, which are seen in the radiochemical experiments, this distance L is always larger than the

coherence length given above. For $E \simeq 7MeV$, we find that the mass eigenstates separate for $\Delta m^2 > 3.3 \times 10^{-7} eV^2$.

However, this is not the only effect which kills the oscillating terms. As we have already mentioned, the finite energy resolution of neutrino experiments causes an averaging over the oscillatory terms. For resolution of order δE, the phase varies by $\delta\phi = R_e \frac{\Delta m^2}{2E^2} \delta E$. For oscillations to be washed out, we demand that $\delta\phi > 100$ or $R_e/l > (100\ to\ 1000)$. This gives $\Delta m^2 > (4\ to\ 40) \times 10^{-10} eV^2$.

Although there exist so called "just so" solutions [27] to the solar neutrino problem which require values of Δm^2 on the order of $10^{-10} eV^2$ and for which the oscillating term is relevant, we are interested in the much larger solution space associated with larger Δm^2. In the next section, we will impose the limit $\Delta m^2 > 10^{-9}\ eV^2$ so that we can safely neglect the oscillating terms.

3.3 The Model

The model we will use was first proposed by Zee [3]. To the standard model, Zee added two scalar multiplates; a doublet ϕ' with the same quantum numbers as the Higgs doublet, and a $SU(3) \times SU(2)$ singlet h^+ with unit electric charge.

With two doublets, we are naturally led into the realm of broken flavor symmetries. In fact, as we will see, we must impose approximate flavor symmetries to achieve a neutrino mass matrix which leads to maximal mixing.

We will apply the results of Section 2.2 to give an acceptable flavor structure to Zee's model. Unfortunately, the flavor structure we will impose is slightly more complicated than the examples discussed in that section. In order to achieve a neutrino mass matrix of the kind discussed in the previous section, we must prohibit mixing for one of the neutrinos. We do so by requiring that τ number be an extremely good or unbroken symmetry, so that we can neglect the mixing of ν_τ with either ν_e or ν_μ.

We will work in a basis of scalar doublet fields where ϕ takes a VEV

equal to $\frac{v}{\sqrt{2}}$ while the VEV of ϕ' is zero. We also work in a lepton basis in which the Yukawa couplings of ϕ are diagonal. This corresponds to the charged lepton mass basis. We identify neutrinos by a subscript corresponding to their charged lepton partners. Under these assumptions, the Lagrangian contains the following important terms

$$\underset{\sim}{c}_{\alpha\beta} h^+ (l_\alpha^T \epsilon C l_\beta) \; + \; \overline{M} \phi \epsilon \phi' \, h^+ \; + \; \frac{\sqrt{2} m_\alpha}{v} \bar{l}_\alpha \phi r_\alpha \; + \; f_{\alpha\beta} \bar{l}_\alpha \phi' r_\beta \; + \; h.c., \qquad (3.16)$$

where Greek letters refer to lepton generations, and we have suppressed $SU(2)$ indices. In this equation, l_α and r_α are left and right handed lepton fields , respectively, ϵ is the unit antisymmetric matrix in $SU(2)$ space, and C is the charge conjugation matrix $C = i\gamma^2\gamma^0$.

The $SU(2)$ structure of the first term in equation (3.16) forces $\underset{\sim}{c}_{\alpha\beta}$ to be antisymmetric. Taking into account our assumption that τ number is a good symmetry, we can write this term for the first two flavors as follows

$$2f \, h^+ (\nu_e^T C \mu_L \; - \; \nu_\mu^T C e_L), \qquad (3.17)$$

where $f \equiv (\underset{\sim}{c}_{e\mu} = -\underset{\sim}{c}_{\mu e})$.

Neutrinos acquire mass radiatively via the diagram in Figure 3.2. We can see that the Lagrangian terms in equation (3.17) naturally lead to a maximum mixing neutrino mass matrix.

There is a subtlety, however. For such a scheme to work we must impose approximate flavor symmetries. If we only allowed one scalar doublet to couple to leptons, then electron-number-minus-muon-number would be an exact symmetry of the theory. Thus, the neutrino mass matrix would have zeros on its diagonal, and we would be left with a single Dirac neutrino, as was discussed following equation (3.13).

Now, we use approximate flavor symmetries to estimate the value of $f_{\alpha\beta}$. There are more than one set of flavor symmetries which will result in the desired neutrino mass matrix. We will choose one and work out the consequences for it. For the first two generations, we will impose the same approximate flavor symmetry as we discussed in Section 2.2. Thus, if a term in the Lagrangian breaks left/right

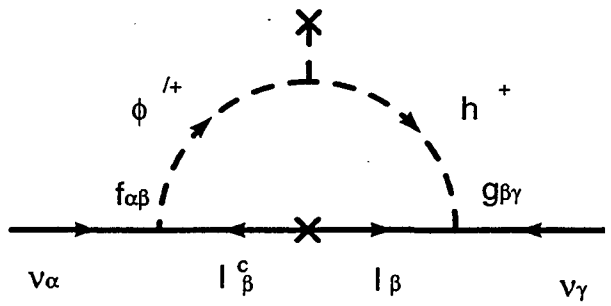

Figure 3.2: The diagram giving neutrinos mass in the model of section 3.3.

handed lepton number for flavor i, then it is proportional to $\epsilon_{iL/R} = \frac{\sqrt{m_i}}{v/\sqrt{2}}$. Although such a model succeeds quite well, as we will see, it leaves no freedom in choosing the couplings of our theory. We wish to investigate the allowed parameter space of our model more thoroughly. Thus, we will introduce the possibility of further approximate flavor symmetries which lead to suppression of the flavor changing terms in our Lagrangian.

Once we have diagonalized the couplings of ϕ to the leptons, the charged gauge couplings to leptons are diagonal. In this basis, the only flavor changing reactions left are ϕ''s and h^+'s couplings to leptons. We introduce the parameters ϵ_1 and ϵ_2 and assume that $f_{e\mu} \propto \epsilon_1$, $f_{\mu e} \propto \epsilon_1$, and $f \propto \epsilon_2$. For now, we will not assume ϵ_i is small , but if we impose approximate flavor symmetries which enforce flavor conservation, they will be. For example, we can impose the two approximate flavor symmetries $L_e - L_\mu$ number and $L_e + L_\mu$ number. In this case, ϵ_1 will reflect the small violation of $L_e - L_\mu$ and ϵ_2 the small violation of $L_e + L_\mu$. Throughout, we will keep the approximate flavor symmetries of table 2.2. Thus, the relevant couplings of our theory are

$$f_{\alpha\beta} \simeq \frac{\sqrt{2}}{v} \begin{pmatrix} m_e & \sqrt{m_e m_\mu}\epsilon_1 \\ \sqrt{m_e m_\mu}\epsilon_1 & m_\mu \end{pmatrix} \tag{3.18}$$

$$f \simeq \frac{\sqrt{m_e m_\mu}}{v\sqrt{2}}\epsilon_2. \tag{3.19}$$

New CP violation effects do exist in a two majorana neutrino model [20] as well as in the two higgs doublet models. However, CP violating effects do not appear in the oscillation of the neutrinos. Since we are interested in neutrino oscillations, we will assume CP is a very good symmetry and ignore CP violating phases in the following.

The neutrino mass matrix, computed from Figure 3.1, is

$$M^{\nu}_{\alpha\beta} = \frac{G_F}{4\pi^2}\epsilon_2\sqrt{m_e m_\mu}\frac{\mu v}{M_1^2 - M_2^2}\ln\left(\frac{M_1^2}{M_2^2}\right)\begin{pmatrix} 2m_\mu\sqrt{m_e m_\mu}\epsilon_1 & m_\mu^2 - m_e^2 \\ m_\mu^2 - m_e^2 & \sqrt{m_e m_\mu}\epsilon_1 \end{pmatrix}, \quad (3.20)$$

where the M_1 and M_2 are the masses of the two physical charged scalar fields, μ is the mass mixing between ϕ'^+ and h^+ and G_F is the Fermi constant. Equation 3.20 made use of the identity

$$\tilde{U}^{\dagger}_{hi}\ln(M_i^2)\tilde{U}_{i\phi} = \tfrac{1}{2}\sin(2\alpha)\ \ln\left(\frac{M_1^2}{M_2^2}\right),$$

where $\tilde{U}$ is the mixing matrix for the two physical charged scalars h^+ and ϕ'^+ and α is the corresponding mixing angle.

Taking $\sin(2\alpha)$ to be of order 1, and assuming that all the scalar mass parameters are of order $100GeV$, the above matrix results in the following mass values.

$$M^{\nu}_{\alpha\beta} = \begin{pmatrix} 0.24\epsilon_1\epsilon_2 & 3.4\epsilon_2 \\ 3.4\epsilon_2 & 1.2\times 10^{-3}\epsilon_1\epsilon_2 \end{pmatrix}\times 10^{-2}eV^2 \quad (3.21)$$

Such a matrix does not give a mixing angle exactly equal to $\frac{\pi}{4}$. Thus $P_{\nu_e\to\nu_e}$ differs from $\frac{1}{2}$. This difference is at most $\frac{1}{2}\cos 2\theta$ which is equal to $3.5\times 10^{-2}\epsilon_1$. Demanding that this correction is less than 10^{-2}, we find that

$$\epsilon_1 < 0.29. \quad (3.22)$$

We will see that this is by far the most severe limit on ϵ_2.

We compute Δm^2 from equation (3.21) and get $\Delta m^2 = 8.1\times 10^{-5}\epsilon_1{\epsilon_2}^2\,eV^2$. Reactor experiments constrain Δm^2 to be less than about $1.4\times 10^{-2}\ eV^2$. In addition, we require $\Delta m^2 > 10^{-9}\ eV^2$, as discussed in Section 3.2.4. These constraints

translate to

$$1.2 \times 10^{-5} < \epsilon_1 {\epsilon_2}^2 < 1.7 \times 10^2 \tag{3.23}$$

Requiring the mass of the neutrinos to be less than about $10eV$ [28], we obtain the following requirement;

$$\epsilon_2 < 5.9 \times 10^2 \tag{3.24}$$

3.4 Experimental Limits

Because all flavor violating interactions are proportional to our symmetry breaking parameters, experimental bounds from such reactions are easily met.

The lepton number nonconserving μ decays of the form $\mu \to e\nu\nu$, which occur via the exchange of a virtual scalar, have branching ratios on the order of

$$B \approx \left(\frac{\frac{f_1 f_2}{\overline{M}^2}}{\frac{g^2}{2M_W^2}} \right)^2 \approx 9.2(f_1 f_2)^2 \left(\frac{100GeV}{\overline{M}} \right)^4, \tag{3.25}$$

where f_1 and f_2 are the relevant Yukawa couplings. In this equation, $\frac{1}{\overline{M}^2}$ is given by $\tilde{U}^\dagger_{\alpha i} \tilde{U}_{i\beta} \frac{1}{M_i^2}$, where α, β refer either to h^+ or ϕ'^+. Assuming that $\overline{M}$ is about $100GeV$, we arrive at the following branching fractions.

1. $B(\mu \to e\nu_\mu\nu_\mu) \approx 4.6(f_{\mu\mu} f)^2 \approx 3.0\ 10^{-15}\epsilon_2^2$
2. $B(\mu \to e\nu_e\nu_\mu) \approx 9.2(f_{e\mu} f)^2 \approx 2.9\ 10^{-17}\epsilon_1^2\epsilon_2^2$
3. $B(\mu \to e\overline{\nu}_e\overline{\nu}_\mu) \approx 9.2(f f_{\mu e})^2 \approx 2.9\ 10^{-17}\epsilon_1^2\epsilon_2^2$
4. $B(\mu \to e\overline{\nu}_e\overline{\nu}_e) \approx 4.6(f f_{ee})^2 \approx 7.0\ 10^{-20}\epsilon_2^2$
5. $B(\mu \to e\nu_e\overline{\nu}_\mu) \approx 9.2(f_{e\mu} f_{\mu e})^2 \approx 2.9\ 10^{-17}\epsilon_1^4$

These branching fractions are extremely small. The only quoted bound for these reactions is $B(\mu \to e\nu_e\overline{\nu}_\mu) \leq 5\%$ [18].

The standard μ decay, $\mu \to e\overline{\nu}_e\nu_\mu$ has additional contributions from charged scalar exchange. The coupling constant c^V_{LL} which reflects the strength of the left-handed-vector $\times$ left-handed-vector amplitude,

$$\frac{4G_F}{\sqrt{2}} c^V_{LL} (\overline{e}_L \gamma^\alpha \nu_e)(\overline{\nu_\mu} \gamma_\alpha \mu_L),$$

is given by

$$\varrho^V_{LL} = 1 - \frac{\sqrt{2}}{8G_F}\frac{f^2}{\tilde{M}^2},$$

where $\tilde{M}^{-2} = \cos^2\alpha M_1^{-2} + \sin^2\alpha M_2^{-2}$. The coupling constant ϱ^S_{RR} which reflects the strength of the right handed scalar-scalar amplitude,

$$\frac{4G_F}{\sqrt{2}}\varrho^S_{RR}(\overline{e}_R\nu_e)(\overline{\nu_\mu}\mu_R),$$

is given by

$$\varrho^S_{RR} = \frac{\sqrt{2}}{4G_F}\frac{f_{ee}f_{\mu\mu}}{\overline{M}^2},$$

where

$$\overline{M}^{-2} = \sin^2\alpha M_1^{-2} + \cos^2\alpha M_2^{-2}. \tag{3.26}$$

The limit $\varrho^V_{LL} > 0.96$ [29] gives

$$\epsilon_2 < 3.8 \times 10^3. \tag{3.27}$$

The limit $\varrho^S_{RR} < 0.066$ [30] is easily met.

The decay $\mu \to e\gamma$ involves a loop of charged scalars and neutrinos. The rate for this reaction is

$$R(\mu \to e\gamma) = \frac{m_\mu^5}{16\pi^2}\left|A^2\right|$$

where

$$A = \frac{e}{384\pi^2}\frac{f^*_{\mu\alpha}f_{\alpha e}}{\overline{M}^2},$$

and $\overline{M}^{-2}$ is as in equation (3.26). This results in a branching fraction relative to the standard decay of

$$B(\mu \to e\gamma) = 3.6 \times 10^{-20}{\epsilon_1}^2$$

Applying the bound $B < 4.9 \times 10^{-11}$ we get

$$\epsilon_1 < 4 \times 10^4.$$

The exotic decay $\mu \to ee\overline{e}$ proceeds through the exchange of the neutral scalar. Its branching ratio is given by

$$B(\mu \to 3e) = \frac{3}{4}\frac{m_e^3 m_\mu}{m_{H_0}^4}{\epsilon_1}^2,$$

where m_{H^0} is the mass of the neutral scalar. Applying the limit $B(\mu \to 3e) < 10^{-12}$ we get

$$\epsilon_1{}^2 < 10^7.$$

Neutrinoless double beta decay is allowed in our model, but proceeds at a small rate because it is proportional to the square of the electron-electron element of the neutrino mass matrix. The resulting constraint from the limit $M^{\nu}_{ee} < 6.3eV$ [31] is

$$\epsilon_1 \epsilon_2 < 2.6 \times 10^3 \tag{3.28}$$

Finally, we will briefly discuss the transition magnetic moment of our neutrino pair and the lifetime of the heavier neutrino. (The magnetic and dipole moments of Majorana neutrinos are zero by CTP invariance. In the case of CP being a good symmetry, our neutrinos have zero transition electric dipole moments because they have opposite CP parities [24]). We follow the work of Petcov [32] below. The amplitude for the decay $\nu_2 \to \nu_1 + \gamma$ is given by

$$A(\nu_2 \to \nu_1 + \gamma) \approx -e\epsilon^{\lambda}_{\alpha} \left(\overline{\nu_2}\, \sigma_{\alpha\beta} q_{\beta}\, \nu_1\right) \left\{ 50 \frac{M^{\nu}_{\mu e}}{\overline{M}^2} \right\}, \tag{3.29}$$

where $\overline{M}^2$ is an approximate average of the two charged scalar masses squared and $M^{\nu}_{\mu e}$ is the μe element of the neutrino mass matrix. The transition magnetic moment can be read from equation (3.29) and is equal to

$$\mu_{21} = 8.7 \times 10^{-17} \epsilon_1 \times \frac{e}{2m_e}$$

The lifetime for the decay of ν_2 is

$$\tau_(\nu_2 \to \nu_1 + \gamma) = 2 \times 10^{28} \epsilon_1{}^{-3} \epsilon_2{}^{-5} \ \ years.$$

3.4.1 Applying Limits

The only limit which requires either ϵ_1 or ϵ_2 to be less that 1 is equation (3.23), which requires $\epsilon_1 \approx 2/5$. Thus, as we have previously claimed, it is not necessary to impose approximate flavor symmetries to make ϵ_1 and ϵ_2 small.

We plot the allowed values of ϵ_1 and ϵ_2 in Figure 3.3. The limits in this plot come solely from equations (3.22), (3.23), and (3.24). All of the limits calculated in this section are already met by these equations, most by many orders of magnitude. The closest are the limits in equation (3.27) and equation (3.28). The former is met by a factor of 10, and the latter by a factor of 100.

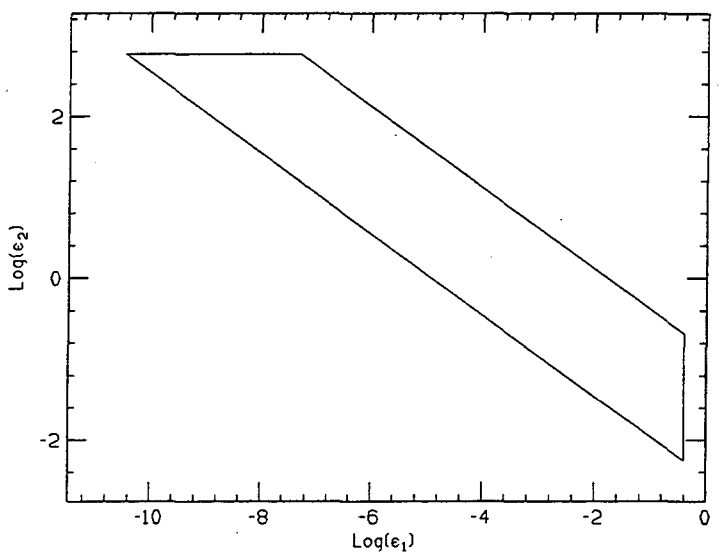

Figure 3.3: The allowed parameter space for the model in section 3.3. The diagonal lines are limits from $10^{-9} < \Delta m^2 < 1.4 \times 10^{-2}$ (See Eq. 3.23). The horizontal line comes from demanding that $\frac{1}{2}\cos 2\theta < 10^{-2}$ (See Eq. 3.22), and the vertical line comes from $m_\nu < 10eV$ (See Eq. 3.24).

Thus, the only real signature for such a scheme is a value of $P_{\nu_e \to \nu_e} \approx \frac{1}{2}$ which has no dependence on either matter effects or neutrino energy.

Using the above approximate flavor symmetries, it is unreasonable to expect that ϵ_2 is much larger than 1. However, there are a number of alternate approximate flavor symmetry schemes which allow for larger values of f. (Recall that $f = \epsilon_{\mu L}\epsilon_{eL}\epsilon_2$.) For example we could have chosen to impose approximate flavor symmetries for right-handed electron and right-handed muon number along with

(electron$\pm$muon) number. The consequences closely parallel the above analysis but require small values for all ϵ_i.

3.5 Conclusion

We have pointed out that to account for the solar electron neutrino flux discrepancy a maximal mixing scheme greatly expands the limited allowed parameter space of other more popular schemes, as well as makes a definite prediction concerning the magnitude of the discrepancy. Any such model predicts a depletion factor of $\frac{1}{2}$ for electron neutrinos over the examined parameter space. In constructing a model which leads naturally to a maximal mixing scheme, it was necessary to introduce approximate flavor symmetries. The very same approximate symmetries introduced in Section 2.2 work remarkably well in achieving the correct form for the neutrino mass matrix. By introducing new approximate flavor symmetries, we were able to explore the relevant parameter space of the theory.

Chapter 4

Hypercharge and the Cosmological Baryon Asymmetry

4.1 Introduction

Various authors [38, 39] have placed cosmological bounds on the size of baryon and lepton number violating interactions in theories where baryogenesis occurs before the electroweak phase transition. The baryon asymmetry of the universe is threatened by a combination of these interactions and a large electroweak instanton rate [40, 41]. Electroweak instanton interactions are expected to be in equilibrium for temperatures above T_{min}, approximately the weak breaking scale, up to some very high temperature $T_{max} \simeq 10^{12} GeV$. Such reactions create $SU(2)_L$ transforming fermions out of the vacuum [40]. Lepton and baryon violating interactions, such as R-parity breaking terms in supersymmetry [42] or Majorana neutrino masses, when in equilibrium simultaneously with instanton reactions, can break all linear combinations of conserved quantum numbers which involve baryon number. Naively, one is led to believe that the baryon asymmetry of the universe is, therefore, washed away. In this chapter, we examine the general circumstances in which this outcome is avoided. We find that in many models there will be additional symmetries and, even though these symmetries apparently have nothing to do with baryon number, they automatically lead to a protection of it.

Electroweak instanton interactions respect the symmetries $B - 3L_i$, where L_i is lepton number for the ith generation. Let us examine the constraints which can arise in a supersymmetric model containing the lepton violating interactions

$$\lambda_{ijk}\,(L_i L_j E_k^c)_F, \tag{4.1}$$

where L_i and E_k^c are the superfields containing the ith generation left-handed lepton and right-handed antilepton, respectively. The claim is that if these interactions cause processes which violate L_i for all i, then an existing baryon asymmetry is threatened. Let us try to save the baryon asymmetry by insuring that $B - 3L_e$ is a good symmetry of the theory. Electron number is violated if reactions, such as $\tilde{\tau} \rightleftharpoons \overline{\nu}_e\,\tau$, are in equilibrium, where $\tilde{\tau}$ is a scalar tau particle. The reaction rate for such a process is $\Gamma \sim \lambda^2 T$ for temperatures, T, greater than the mass of the $\tilde{\tau}$. It is in equilibrium if its rate is larger than the Hubble expansion parameter $H \approx 20\frac{T^2}{M_p}$. Taking the scalar tau mass to be $1TeV$, we arrive at the limit

$$\lambda_{133} < 4 \times 10^{-8} \tag{4.2}$$

On the other hand, our flavor symmetry ansatz of Chapter 2 indicates that

$$\lambda_{ijk} \approx \left(\frac{m_{E_i}}{v}\right)^{1/2} \left(\frac{m_{E_j}}{v}\right)^{1/2} \left(\frac{m_{E_k}}{v}\right)^{1/2}. \tag{4.3}$$

(See table 2.2). This gives a value for λ_{133} which is three orders of magnitude larger than the one in equation (4.2). If, instead, we preserved $B - L_\mu$ or $B - L_\tau$ the discrepancy would be even larger. It is important, then, to examine the applicability of these cosmological limits in detail.

It is well known that a symmetry involving baryon number itself can preserve the baryon asymmetry [39]. Approximate symmetries involving B have been found in the minimal supersymmetric standard model which can be used to help prevent erasure of the baryon asymmetry [43] and, thus, evade these limits. We have found that the protection of the baryon asymmetry is extremely common and is a typical feature of theories with extra symmetries, even when those symmetries do not transform quarks. We illustrate this by a very simple example: assume that there exists a particle, X, which carries hypercharge but not $SU(2)$ or $SU(3)$ gauge

interactions. Assume that reactions occurring at temperatures well above T_{min} generate an asymmetry in the X species, and that at lower temperatures the reactions which change X number are sufficiently weak that this X asymmetry persists. A crucial role is played by the requirement that the early universe is hypercharge neutral. Because X particles carry hypercharge, the asymmetry in their number contributes to the hypercharge density of the universe. The remaining particles in the theory must carry an opposite hypercharge density to cancel this. Chemical equilibrium equations specify how this hypercharge density is shared. A baryon asymmetry can develop either through added B violating interactions or once the weak instanton becomes effective. In general, any X asymmetry together with chemical equilibrium requires a baryon asymmetry[1]. This illustrates just how easy it is to preserve the baryon asymmetry and, to our way of thinking, puts the issue of direct detection of baryon and lepton number violation back where it belongs: with the experimentalists.

4.2 General Condition for Survival of a Baryon Asymmetry.

In this section, we discuss, in a very general way, the conditions under which an extra $U(1)$ symmetry preserves the cosmological baryon asymmetry.

In thermodynamic equilibrium the number density of particle species i is determined by its chemical potential, μ_i. If a given reaction, say $p_1 + p_2 \rightleftharpoons p_3 + p_4$, is in equilibrium, then $\mu_1 + \mu_2 = \mu_3 + \mu_4$. It is straightforward, yet tedious, to solve all chemical equilibrium equations. One can simplify the process by noticing that these equations are the same equations one would write down to determine the $U(1)$ symmetries of the equilibrium theory. One need only replace μ_i with q_i, the charge of particle i. Solving for q_i determines the possible assignments of $U(1)$ charge to each particle so that all equilibrium reactions conserve that charge. In general, such $U(1)$ symmetries need not be exact symmetries of the Lagrangian.

[1]Implicit in this discussion is the assumption that the universe is homogeneous.

They are symmetries of those interactions in thermal equilibrium at temperature T, and we refer to them as effective $U(1)$ symmetries at this temperature.

Thus, a solution to the chemical equilibrium equations corresponds to an assignment of effective $U(1)$ charges to each particle, and the possible effective $U(1)s$ in a given theory are usually easy to identify. Suppose that at a certain temperature there are N such effective $U(1)$s: $U(1)_A, A = 1, ...N$, then the most general solution is

$$\mu_i = \sum_A C^A q_i^A \tag{4.4}$$

where q_i^A is the charge of particle i under $U(1)_A$. The constant C^A we refer to as the asymmetry constant for $U(1)_A$. As soon as some interaction which violates $U(1)_A$ comes into thermal equilibrium, C^A rapidly tends to zero: $U(1)_A$ is no longer able to support particle asymmetries.

This general solution is restricted, however. We assume that the universe is homogeneous and that no charge asymmetry has developed for the unbroken gauged $U(1)s$ of the theory[2]. This forces the charge density for these $U(1)s$ to zero. We can write the charge density for $U(1)_A$ as follows,

$$Q^A = \sum_i q_i^A n_i \tag{4.5}$$

where n_i is the particle asymmetry density of species i. If particle asymmetry densities are small, then they can be written, for $T \gg m_i$, as

$$n_i \simeq \frac{T^2}{6} \tilde{g}_i \mu_i \tag{4.6}$$

where $\tilde{g}_i$ is the number of internal degrees of freedom of particle i, g_i, multiplied by a factor of two for bosons. (However, see reference [45] for an interesting look at small mass effects.) Under these conditions the charge density constraint is a simple linear equation in the μ_is. Q^A can be written using n_i from equation (4.6) and μ_i from equation (4.4):

$$Q^A \simeq \frac{T^2}{6} \sum_B C^B \sum_i \tilde{g}_i q_i^B q_i^A = \frac{T^2}{6} \sum_B C^B \, \overline{B} \cdot \overline{A} \tag{4.7}$$

[2]This requirement avoids the problems inherent in giving a massless gauge boson a chemical potential.

where we define $\overline{B} \cdot \overline{A}$ by

$$\overline{B} \cdot \overline{A} = \sum_i \tilde{c}_i q_i^B q_i^A. \tag{4.8}$$

Should the diagonal generators of non-Abelian gauge groups, such as T_{3L}, be included in the list of effective $U(1)s$? The answer is no, as can be seen easily from the above equations. Call such a generator α, then neutrality of the universe with respect to this charge requires

$$\sum_A C^A \overline{A} \cdot \overline{\alpha} = 0 \tag{4.9}$$

where

$$\overline{A} \cdot \overline{\alpha} = \sum_i \tilde{c}_i q_i^A q_i^\alpha. \tag{4.10}$$

When A refers to a $U(1)$ generator (not embedded in a non-Abelian gauge group), then $\overline{A} \cdot \overline{\alpha} = 0$. This is because the $\tilde{c}_i$ and q_i^A are the same for all components of an irreducible representations of α, and hence the sum in equation (4.10) can be written as a sum of zero terms, one for each irreducible multiplet of α. When $A = \beta$ is a diagonal generator of a non-Abelian group, the orthogonality property of the generators within each multiplet ensures that $\sum_i q_i^\alpha q_i^\beta$ vanishes for $\beta \neq \alpha$. Hence, the sum in equation (4.9) just has one term: $C^\alpha \overline{\alpha} \cdot \overline{\alpha} = 0$. Since $\overline{\alpha} \cdot \overline{\alpha} \neq 0$, we have proved that $C^\alpha = 0$ follows from $Q^\alpha = 0$. This implies that such $U(1)s$ need not be included in the list of effective $U(1)s$.

Now, let's apply this formalism. We are interested in the situation in which additional particles and interactions have been added to the standard model such that at temperatures T, $T_c < T < T_{max}$, where T_c is the weak breaking temperature, there are just two effective $U(1)s$: Y and X, where $Y = 2(Q - T_3)$ denotes hypercharge and X is an ungauged effective symmetry. The charge neutrality condition equation (4.9) when applied to hypercharge gives

$$C^Y = -\frac{\overline{X} \cdot \overline{Y}}{\overline{Y}^2} C^X. \tag{4.11}$$

Using equation (4.11) in equation (4.7), the asymmetry in baryon number is just

$$n_B \simeq \frac{T^2}{6} C^X \left(\overline{X} - \frac{\overline{X} \cdot \overline{Y}}{\overline{Y}^2} \overline{Y} \right) \cdot \overline{B}, \tag{4.12}$$

where we have rewritten Q^B, the baryon density, as n_B. This is the general result of this chapter. Any effective $U(1)_X$, whether it contains a piece of baryon number or not, will in general contribute to n_B if $C^X \neq 0$. The extension of equation (4.12) to many extra X symmetries is straightforward. If such a $U(1)_X$ exists, there is no limit to how large the B and L violating interactions can be.

We will examine the case in which X particles carry no baryon number themselves. Then,

$$n_B \simeq \frac{T^2}{6} C^X \left(-\frac{\overline{Y} \cdot \overline{B}}{\overline{Y}^2} \right) \overline{X} \cdot \overline{Y}. \tag{4.13}$$

In the standard model, $\overline{Y} \cdot \overline{B}/\overline{Y}^2 = \frac{1}{11}$. Additional particles will change this, but would generally give some non-zero value which we call α. Then, $n_B \simeq -\frac{T^2}{6}\alpha C^X \left(\overline{X} \cdot \overline{Y}\right)$. Thus, to obtain $n_B \neq 0$, we require that some particles with $X_i \neq 0$ have $Y_i \neq 0$. Hypercharge neutrality then forces other particles to have an asymmetry, some of which carry baryon number, thus providing a baryon asymmetry.

Cline *et al.* [44] point out that the standard model interactions conserve right handed electron number down to a temperature of about $10\,TeV$. If no other operators violate this symmetry, then right handed electrons can act as X particles. However, couplings such as in equation (4.1) would still be strictly limited. In Section 4.3, we discuss another possibility, an X symmetry which does not transform any standard model particles. In this case, equation (4.11) can be rewritten in terms of the hypercharge density carried by the standard model sector, $Q^Y(SM)$, and by the X sector, $Q^Y(X) \equiv \sum_i q_i^Y n_{X_i}$.

$$Q^Y(SM) = Q^Y(X) \tag{4.14}$$

In terms of $Q^Y(X)$, equation (4.13) becomes

$$n_B \simeq -\frac{1}{11} Q^Y(X). \tag{4.15}$$

(We have assumed that $T < 10TeV$ so that right handed electrons are in equilibrium.)

Equation (4.15) doesn't assume that X number density is small or proportional to its chemical potential. Thus, it is valid even when the temperature drops below the mass of certain X particles. When this happens, the heavier species carrying X might decay into lighter ones. Nevertheless, providing the particles with $X \neq 0$ possess a hypercharge asymmetry the baryon asymmetry will survive. In particular, the $X \neq 0$ particles must continue to carry such an asymmetry until a temperature T_0, beneath which B and L violating reactions are sufficiently weak that a symmetry having a baryon number component has become an effective $U(1)$. The resulting baryon asymmetry after X decay depends on the specifics of the model. In the least complicated scenario, in which baryon number is a good symmetry below T_0, today's baryon asymmetry is simply derived form equation (4.15) and entropy considerations.

We note that it is not necessary for our X sector to be neutral under $SU(2)$. Adding additional $SU(2)$ transforming fermions to the standard model will mean that these particles also take part in instanton mediated reactions. Nevertheless, in a consistent theory, instanton reactions will conserve the hypercharge asymmetry carried by the X sector of the theory. This is true because instantons neither violate hypercharge in the standard model sector nor in the theory overall, and thus must conserve hypercharge in the X-sector.

In this section, we have tacitly assumed that some component of baryon number is a good symmetry below T_c, the weak breaking temperature. If this is not the case, then, for temperatures T, $T_0 < T < T_c$, the role of hypercharge is played by electric charge. In this case, the X sector must carry an electric charge asymmetry.

An intriguing possibility exists if the lightest X particle is stable and electrically neutral. If this is the case, the particle is a candidate for the dark matter in the universe [46, 47]. To realize such a scenario, the X sector would still have to maintain a hypercharge asymmetry for temperatures above T_0. (For convenience, we have assumed $T_0 \geq T_c$.). However, at a lower temperature, charged X particles would decay to standard model particles plus these electrically neutral X particles. If Ω_X is the fraction of the critical density contributed by the electrically neutral

X particles, then their mass is given by

$$\frac{m_X}{m_{proton}} \simeq \frac{\langle q_X \rangle}{11} 10^2 \Omega_X$$

where $\langle q_X \rangle$ is the appropriate average of X-particle hypercharges. Low-background Ge detector experiments [48, 49] indicate that an electrically neutral dark matter particle with nonzero hypercharge must have a mass greater than $\sim 1000\ GeV$. Thus, we can effectively rule out a dark matter X particle with nonzero hypercharge. One possible candidate is the neutral component of a new hyperchargeless $SU(2)$ multiplet. Such a particle is expected to interact via loop diagrams with nuclei and thus its cross section with Ge is approximately $10^{-35} cm^2$ or smaller [47], effectively evading relevant experimental limits [48]. Another candidate is a new particle with no gauge interactions whatsoever [46].

4.3 A Simple Model.

In this section, we illustrate the general ideas discussed above with a very simple model. We add to the standard model a single fermion X, of mass m_X, which is $SU(2)$ neutral but has three units of electric charge. It is unstable, decaying to three charged leptons via the effective interaction

$$\frac{1}{2}\frac{1}{M^2} \sum_{ijk} f_{ijk} \left(\overline{X}\, e_R^i\right) \left((e_R^j)^T C e_R^k\right) \quad + \quad h.c.,$$

where e_R^i is the right handed lepton field of flavor i, X is the X particle field, C is the charge conjugation matrix, M is a constant with units of energy, and f_{ijk} $(= f_{ikj})$ is a flavor dependent constant of order 1. In addition, we let our model include unspecified lepton and/or baryon violating terms which together with the instanton reaction break all linear combinations of B and L numbers.

Both the mass of the X particle, m_X, and the constant M are constrained by the various requirements of our theory. First, we must insure that the X asymmetry develops before all baryon violating interactions fall out of equilibrium. Otherwise, the X asymmetry has no effect on baryon number. Let T_X be the temperature

at which X violating reactions drop out of equilibrium. Without specifying the exact scenario, we assume that an X asymmetry develops at some temperature lower than T_X but above the temperature at which instantons freeze out (See [50] and references therein for numerous methods by which number asymmetries can develop). In this way, the instanton reaction provides the baryon violation required for our mechanism to work. This is a convenient choice, but not a necessary one if other baryon violation exists in the theory.

It is interesting to note that the only baryon violation required in this model is instantons. If an X asymmetry exists or develops during the epoch in which instantons are in equilibrium, then it will necessarily generate a proportional baryon asymmetry.

In our example, X particles will eventually decay into standard model particles. Various constraints must be imposed on this decay. To make things simple, we require X particles to survive past the temperature at which instantons freeze out. We assume that after this temperature baryon number is a good symmetry. Thus, the only possible effect on the produced baryon density comes from the change in entropy of the universe upon X decay.

The standard nucleosynthesis scenario places limits on this decay [50]. If X particles decay after nucleosynthesis, they must not dump more than a factor of ~ 15 times the entropy density present at the time of nucleosynthesis. If they did, then the observed baryon to photon density would be incompatible with standard nucleosynthesis. Also, if the mass of the X particle is larger than a few MeV, which it must be to avoid strict limits on the width of the Z boson, then energetic photons from X decay can destroy too much deuterium. Further, depending on the era of decay, photons from X decay can destroy the uniformity of the cosmic microwave background radiation or contribute too much to the diffuse photon background. If X particles decay before nucleosynthesis, their mass and density prior to decay must be compatible with the known baryon to photon ratio, η, during nucleosynthesis.

Let us examine our first constraint. The rate for X violating 4-fermion

interactions is given by

$$\Gamma_X \simeq \frac{49 f^2 \pi^5}{12960\zeta(3)} \frac{T^5}{M^4}$$

where f^2 is an average of terms like $f^*_{ijk} f_{lmn}$, and we have dropped terms of order $\frac{m_X}{T}$.

The Hubble constant, H, is $17\frac{T^2}{M_p}$. The 4-fermion interaction drops out of equilibrium when its rate falls below the Hubble expansion rate[3]. Calling the temperature at which this occurs T_X, we have

$$M^4 \simeq \frac{49 f^2 \pi^5}{220320\zeta(3)} M_p T_X^3. \tag{4.16}$$

Although X number changing interactions freeze out at T_X, X particles stay in thermodynamic equilibrium below this temperature through their gauge interactions. These gauge interactions freeze out at a much lower temperature given by the standard cold relic freeze out criteria.

Now, we examine the decay of the X particles. The decay rate for these particles is given by

$$\Gamma \simeq \frac{f^2}{256\pi^3} \frac{m_X^5}{M^4}$$

where we have ignored terms of order the temperature over m_X since they will be seen to be negligible. The X particles decay when this rate is approximately equal to the Hubble expansion rate. Calling the temperature at which these rates become equal T_D, we have

$$M^4 \simeq \frac{f^2}{4352\pi^3} \frac{m_X^5}{T_D^2} M_p. \tag{4.17}$$

If significant entropy is generated by X decay, then T_D is the "reheat" temperature after decay.

Equations (4.16) and (4.17) can be combined to give

$$m_X^5 \simeq 7.6 \times 10^3 \, T_X^3 T_D^2$$

[3]For convenience, and because we are interested in the order of magnitude of our results, we assume $g_* \simeq 106$ independent of the temperature.

In Figure 4.1, we plot the allowed parameter space by considering the constraints discussed above. (We have assumed $T_D \leq T_{min} \simeq 10^2 GeV$ and required $T_X > 10T_{min}$.)

The diagonal dotted lines in this figure are lines of constant T_X and are labeled in GeV. The allowed region is divided up into three regimes. The first, corresponding to $T_D > 10^{-3}GeV$, covers the case in which X particles decay before the onset of nucleosynthesis. In this case, X density just before decay may be quite large, leading to an early matter dominated era and a significant increase in entropy density upon X decay. This is because for large m_X, X particle gauge interactions freeze out when there is still a large anti-X particle density. In this situation, the X number asymmetry is a small fraction of the symmetric relic freeze out density. A large symmetric relic density leads to large entropy dumping when X particles decay. Let us call the factor by which entropy is increased R. Since, in our model, today's observed baryon asymmetry is proportional to the X asymmetry divided by R, a large X asymmetry is required when R is large. We have plotted a dot-dashed line which corresponds to the onset of significant entropy generation when X particles decay. At this line, entropy is increased by 10% upon X decay. As we rise above this line, the amount of entropy generated when the X particles decay increases. At the top boundary of our allowed region, the X asymmetry required to generate todays observed baryon asymmetry becomes infinite. Above this line, there is no way to generate enough baryon asymmetry.

In the second regime, $10^{-4}GeV < T_D < 10^{-3}GeV$, during which nucleosynthesis is taking place, we impose the conservative requirement that X decay increases the universe's entropy by less than 10%. This is shown as a dip in the top boundary of the allowed region.

The last regime, $T_D < 10^{-4}GeV$, in which X particles decay after nucleosynthesis, is bounded on the left by the requirement that decay products don't destroy too much deuterium [51]. The curved line marked with an arrow takes account of this limit (We have used Lindley's rough calculation for heavy dark matter particles [51]). This constraint is more severe than those arising from cosmic microwave background and diffuse photon background observations. The top limit

of this region is determined by entropy dumping considerations. Since, in this case X particles are still present during nucleosynthesis, we know that the required X asymmetry is equal to $\frac{-q_X}{11}$ times the baryon asymmetry at the time of nucleosynthesis. When X particles decay, they can increase the entropy and thus decrease the value of η today relative to its value during nucleosynthesis. We allow at most a decrease by a factor of 15, and this gives us our top limit. Figure 4.1 illustrates how general our mechanism is. The X particle's mass can range over 12 orders of magnitude, from 45 GeV to 10^{12} GeV.

4.4 Conclusion

We have shown that in order to avoid the strict cosmological limits placed on lepton and baryon number violating interactions it is not necessary to resort to low temperature baryon generation or to the addition of new symmetries which affect baryons. Any symmetry which allows one sector of the theory to acquire a net hypercharge density will suffice. This includes a symmetry under which standard model particles are neutral, as our example shows. The key observation is that, although this new symmetry seems decoupled from the rest of the theory, the gauged $U(1)$ symmetries can connect it. Thus, an asymmetry in X particles, because they are charged, is enough to ensure a proportional asymmetry in all charged particles independent of whether their particle number is conserved or not.

If a scenario similar to the one proposed here was realized in the early universe, then experimental searches for lepton and baryon violating interactions may prove successful. Such a success would not only directly signal exciting new L and/or B number violating physics, but would also indirectly signal the existence of a baryon number protection mechanism.

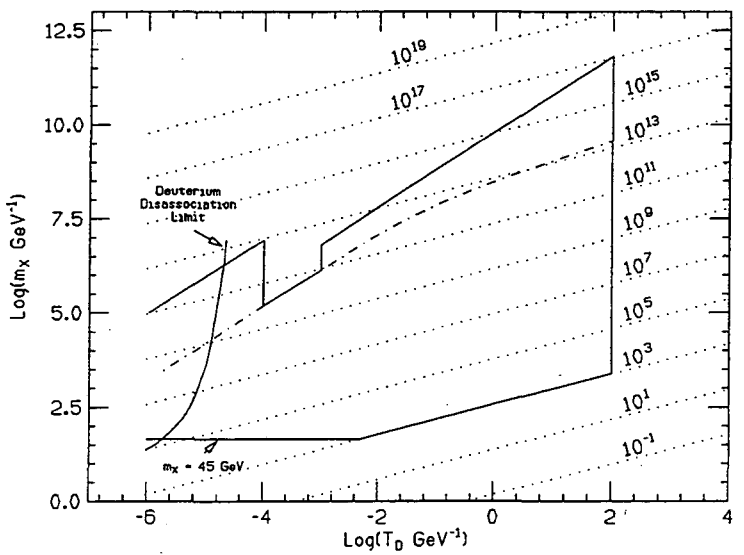

Figure 4.1: The allowed parameter space in our example is shown, bounded by solid lines. We have assumed $T_D \leq T_{min} \simeq 10^2 GeV$ and required $T_X > 10T_{min}$ and $m_X > 45\ GeV$. The diagonal dotted lines are lines of constant T_D, and are labeled in GeV. Our parameter M is also constant on these dotted lines, $M = 2.9 \times 10^4 \left(\frac{T_X}{GeV}\right)^{3/4}\ GeV$. On the dot-dashed line the entropy of the universe is increased by 10% when X particles decay. In determining this line, as well as the top boundary line, we have assumed that X particle gauge interactions freeze out according to the standard cold relic freeze out criteria [50]. We have made conservative assumptions in determining the relative increase in entropy upon X decay; allowing the cosmic scale factor to scale as t^n where n ranges from 1/2 to 2/3. We have used a value for η at the time of nucleosynthesis equal to $\left(\frac{11}{4}\right) 3 \times 10^{-10}$.

Chapter 5

Proton Decay in SUSY SO(10)

5.1 Introduction

While successfully addressing various theoretical problems and correctly predicting the weak angle, $\sin\theta_W$[54], in the Standard Model, supersymmetric (SUSY) grand unified theories (GUTS) also introduces a large assortment of new phenomenon and unknown parameters [55] which make predictions difficult. Chief among the new phenomenon is the instability of the proton. In SUSY GUTS, in addition to the standard heavy gauge boson mediated decays, proton decay can occur via the exchange of heavy chiral superfields [56]. This process results in baryon violating four-fermion operators which are suppressed by only one power of a GUT scale mass, in contrast to the gauge boson mediated processes, which have two powers.

Determining these operators, which dominate the proton decay rate, is a two step process. First, one evaluates a diagram in which a heavy superfield is exchanged, resulting in dimension-five operators which involve two Standard Model (SM) fermion fields and two SUSY scalar partners. Then, one dresses the scalars, using either gluinos, neutralinos, or charginos to convert them into fermions. Unlike their gauge boson mediated counterparts, the resulting operators depend upon new Yukawa couplings, whose values, in general, are unrelated to known parameters. Most past attempts at predicting the rates and branching ratios involved in proton

decay have relied on simplifying assumptions to relate the new Yukawa couplings to those of the standard model, predictions based on the minimal supersymmetric $SU(5)$ theory (MSGUT)[57] being the most common [58].

Unfortunately, this is a poor choice to base real world predictions upon, as it fails to correctly predict the mass spectrum of the known fermions. To solve this problem, one is forced to introduce new Yukawa couplings beyond those of the MSGUT. Within the context of an $SO(10)$ theory, this new structure will have definite effects on the couplings which determine proton decay rates and branching ratios. Thus, it seems important to examine the repercussions of a model which is both predictive and correctly accounts for the known fermion spectrum.

We can not choose one such model without limiting the applicability of our predictions. Nevertheless, because factors of two and three will be important, and because we will be dealing with issues which require us to understand the origin of our couplings, we do not simply impose a phenomenological flavor symmetry ansatz of the form used in Chapter 2. Instead, we will examine a particular model which explains the hierarchical nature of the Yukawa couplings in the theory in terms of a specific flavor symmetry structure. The model we choose is outlined in reference [59], and we refer to it throughout this chapter as the ADHRS model, after the initials of the authors.

This choice is not as limiting as one might think. The ADHRS model actually encompasses a whole class of models which, though sharing the same universal Yukawa texture, differ in the specific values for the couplings. The Yukawa matrices which result are very similar to ones derived from a simple phenomenological flavor symmetry ansatz, and, in much of this chapter, we use an approximate parameterization which makes the generality of our results apparent. In addition, we have the added benefit of being able to determine the specific Clebsch factors involved for a whole series of models.

In our calculations, we find a large number of expected phenomena which differ substantially from the results of standard MSGUT proton decay calculations, foremost among them being the dominance of certain gluino dressed diagrams and the increased branching fraction for charged lepton decay modes under common

circumstances. In addition, we conclude that certain neutralino diagrams contribute substantially to certain proton decay modes, and should not be ignored. We do not calculate the overall rate for proton decay, as this depends on theory details which are more specific than we deal with here. Instead, we examine relative branching ratios and compare the size of differently dressed operators to make our conclusions.

We note that the results stated above are not a special case peculiar to the ADHRS flavor scheme alone. In fact, the ADHRS scheme gives comparatively conservative results, as it is a simple matter to apply flavor symmetry schemes, such as that of Section 2.2, which give far more dramatic deviations form MSGUT proton decay calculations. Thus, the fact that we find significant deviations, is a testament to the fragility of previous calculations based on the MSGUT.

In addition to the expected changes brought about by our Yukawa matrices, we examine the possible repercussions for proton decay of nonstandard squark mass matrices, which are either a consequence of nonminimal Planck scale boundary conditions or of high energy radiative corrections. In Sections 5.5 and 5.7, we discuss how the implementation of a flavor symmetry scheme based on the ADHRS philosophy can very easily lead to flavor mixing effects in the squark mass matrices which make gluino dressed diagrams dominant for all nucleon decay modes. We point out that only very modest flavor changing effects, well within experimental limits, are required to make most gluino dressed diagrams dominant in most circumstances.

5.2 What is Wrong with the MSGUT?

We begin by discussing Yukawa couplings relevant to proton decay in the MSGUT. Thus, we assume that a single 5 and $\bar{5}$ of $SU(5)$ are responsible for fermion masses. The superpotential terms which give the relevant Yukawa couplings are

$$W_Y = \frac{1}{4} h_{ij}\, \epsilon_{\alpha\beta\gamma\delta\epsilon}\ \psi_i^{\alpha\beta}\psi_j^{\gamma\delta}H^{\epsilon} + \sqrt{2} f^{ij}\ \psi_i^{\alpha\beta}\phi_{j\alpha}\overline{H}_{\beta}, \tag{5.1}$$

where latin indices refer to families, Greek indices to $SU(5)$, and h_{ij}, f^{ij} are dimensionless coupling constants.

The Higgs superfields are the 5 and $\overline{5}$, $H = (H_c, H_c, H_c, H_{f^+}, H_{f^0})$ and $\overline{H} = \left(\overline{H}_c, \overline{H}_c, \overline{H}_c, \overline{H}_{f^-}, -\overline{H}_{f^0}\right)$, respectively. Above, H_c and $\overline{H}_c$ are the Higgs triplet superfields. H_f and $\overline{H}_f$ are the doublets.

The matter field, ψ, is a 10 of $SU(5)$,

$$\psi = \frac{1}{\sqrt{2}} \begin{pmatrix} 0 & u^c & -u^c & u & d \\ -u^c & 0 & u^c & u & d \\ u^c & -u^c & 0 & u & d \\ -u & -u & -u & 0 & e^c \\ -d & -d & -d & -e^c & 0 \end{pmatrix},$$

and ϕ is a $\overline{5}$ of $SU(5)$,

$$\phi^T = (d^c, d^c, d^c, e, -\nu).$$

Above, u, d, e, ν are chiral superfields which contain the left handed up quark, charged lepton, and neutrino respectively. The chiral superfields u^c, d^c, e^c contain the right handed fermions.

The Yukawa couplings in the superpotential in terms of the component fields

$$e^c,\ u^c,\ d^c,\quad Q = \begin{pmatrix} u \\ d \end{pmatrix},\ L = \begin{pmatrix} \nu \\ e \end{pmatrix},$$

are given by

$$\begin{aligned} W_Y \ = \ & \lambda^u_{ij}\, u^c_i\, Q_j\, H_f \ + \ \lambda^d_{ij}\, d^c_i\, Q_j\, \overline{H}_f \ + \ \lambda^e_{ij}\, e^c_i\, L_j\, \overline{H}_f \\ & + \tfrac{1}{2} U^Q_{ij}\, (Q_i Q_j H_c) \ + \ U^L_{ij}\, (Q_i L_j \overline{H}_c) \ + \ U^E_{ij}\, (u^c_i e^c_j H_c) \ + \ U^D_{ij}\, (u^c_i d^c_j \overline{H}_c). \end{aligned} \tag{5.2}$$

We will work in the convenient basis in which the Yukawa matrices λ^u, λ^e, and $\lambda^d K$ are diagonal. K is the Kobayashi Maskawa (KM) matrix [60]. In this basis, we have

$$\begin{aligned} Q_i &= \begin{pmatrix} u_i \\ d'_i \end{pmatrix} = \begin{pmatrix} u_i \\ K_{ij}\, d_j \end{pmatrix} \\ L_i &= \begin{pmatrix} \nu_i \\ e_i \end{pmatrix}, \end{aligned} \tag{5.3}$$

and u_i, d_i, e_i, u_i^c, d_i^c, e_i^c are each in a basis which diagonalizes their fermion component's mass matrix. We will use this basis extensively in this chapter, referring to it as the d' basis.

Proton decay proceeds through the exchange of the Higgs triplet superfields. Thus, the Yukawa matrices, U^G, for $G = Q, L, E, D$, determine the structure of these decays.

If $SU(5)$ is unbroken, the following equalities hold at the GUT scale in the basis above ;

$$\begin{aligned} U^Q_{ij} &= \delta_{ij}\, \lambda^u_{jj}\, e^{i\phi_j} \\ U^L_{ij} &= \lambda^d_{ij} \\ U^E_{ij} &= \lambda^u_{ii}\, K_{ij} \\ U^D_{ij} &= e^{-i\phi_i}\, \lambda^d_{ij} \\ \lambda^e_{ij} &= \delta_{ij}\, (\lambda^d\, K)_{jj}, \end{aligned} \tag{5.4}$$

where the phases ϕ_i satisfy $\sum_i \phi_i = 0$ and there is no sum on i or j.

Equation (5.4), however, embodies the very boundary conditions which lead to incorrect fermion mass relations. The last equation, relating the mass matrices of down quarks and charged leptons, gives the unacceptable result $\frac{m_d}{m_s} = \frac{m_e}{m_\mu}$. Solutions to this problem invariably introduce new, possibly effective operators into equation (5.2), at the very least, altering this last relation. In $SO(10)$ theories, solving this problem disturbs all of the equalities in equation (5.4), as we will see in the next section. Even in GUT theories based on other gauge groups, arranging for acceptable fermion masses will often disrupt these relations. Proton decay calculations in the MSGUT which rely on these $SU(5)$ equations must therefore be reexamined.

5.3 The ADHRS Model

With a vast assortment of schemes designed to explain the known flavor structure of the light fields, we require further assumptions if we wish to make any predictions about proton decay. Eventually, we will choose to parametrize the Yukawa couplings of our theory in terms of different Clebsch factors multiplying the

various elements of a single matrix with a specific texture. Though this form has been explained within the context of other theories, we will examine the theory of ADHRS, using it as a guidepost for the analysis of this chapter.

In arriving at their Yukawa matrices, ADHRS employ philosophical assumptions which include;

a) maintaining the successful prediction of $\sin\theta_W$ in the MSGUT.

b) maximizing the predictivity of the theory.

c) " explaining " the hierarchical nature of the Yukawa matrices.

This last requirement precludes the use of small dimensionless couplings in the theory.

To reduce the number of free flavor parameters in the theory, ADHRS begin with the gauge group $SO(10)$, which relates the Yukawa matrices for up quarks, down quarks, and leptons. They assume that the theory below the $SO(10)$ breaking scale, v_{10}, has the same particle content as the MSGUT, thus preserving the $\sin\theta_W$ prediction. To improve predictivity of the model, their theory contains only one 10 multiplet, which is responsible for both the up and down type masses.

ADHRS introduce a number of 45 multiplets which participate in the breaking of $SO(10)$ and $SU(5)$. These 45s are assumed to take vacuum expectation values (vevs) in one of the four following directions in the two dimensional subspace of $SO(10)$ which preserves $SU(3) \times SU(2) \times U(1)$;

$$X, \;\; Y, \;\; B-L, \;\; T_{3R}. \tag{5.5}$$

Above, X is the $SO(10)$ generator which commutes with the $SU(5)$ Georgi-Glashow subgroup, Y is hypercharge, $B-L$ is baryon number minus lepton number, and T_{3R} is the T_3 generator of $SU(2)_R$.

The Yukawa couplings of the theory are derived from a set of operators of the following form;

$$O_{ij} = 16_i \, \frac{<45_1>}{M_1} \cdots \frac{<45_k>}{M_k} \, 10 \, \frac{<45_{k+1}>}{M_{k+1}} \cdots \frac{<45_l>}{M_l} \, 16_j, \tag{5.6}$$

where 16_i is the 16 multiplet for the ith generation of fermions, and 45_j is one of the 45s. Such operators are the result of integrating out heavy 16 and $\overline{16}$ multiplets.

The resulting gauge structure leads to very simple values for these operators; If a 45 takes a vev in the X direction it just couples to various members of the adjacent 16 with a strength proportional to the X value of that member. A hierarchy is generated by arranging that the vevs in the numerator are smaller than the masses in the denominator.

We refer to the generation basis used in equation (5.6) as the flavor basis.

Beginning with the operator $O_{33} = 16_3\ 10\ 16_3$, ADHRS search for the minimal number of operators which are compatible with known experimental information. The result of the search is a group of possible models, each of which has just four such operators. The resulting theory has six free parameters (4 real constants, 1 phase, and $\tan\beta$ [1]), and thus can be used to make seven predictions.

We will examine the nucleon decay branching ratios that result from a group of 54 models, all with the Yukawa structure $O_{33} + O_{23} + O_{22} + O_{12}$. The different theories are listed in Appendix A. One example is given below.

$$\begin{aligned}
O_{12} &= 16_1 \left(\tfrac{45_X}{M}\right)^3 10 \left(\tfrac{45_X}{M}\right)^3 16_2 \\
O_{22} &= 16_2\, 10\, \tfrac{45_{B-L}}{45_X}\, 16_2 \\
O_{23} &= 16_2\, \tfrac{45_Y}{45_X}\, 10\, \tfrac{45_{B-L}}{45_X}\, 16_3 \\
O_{33} &= 16_3\, 10\, 16_3.
\end{aligned} \tag{5.7}$$

The 45s in this equation are vevs taken in the indicated directions.

Such a structure can be justified by the imposition of an approximate $U(1)$ flavor symmetry and appropriate choices for the corresponding $U(1)$ charges of the relevant fields.

The resulting Yukawa matrices are all of the form

$$\begin{pmatrix} 0 & zC & 0 \\ zC & ye^{i\phi}E & x'B \\ 0 & xB & A \end{pmatrix}, \tag{5.8}$$

with $A \gg B$ and $E \gg C$, reflecting powers of $\frac{v_5}{v_{10}}$ or $\frac{v_5}{m_{pl}}$, where v_5 is the $SU(5)$ breaking scale. The Clebsch factors, x, x', y, and z, are products of $B - L$, Y,

[1] We use the notation $\tan\beta = \frac{v_1}{v_2}$ where v_1 is the vev of H_f and v_2 is the vev of $\overline{H}_f$.

and X values for the 16 multiplets involved. In Appendix A, we list the Yukawa matrices for the 54 models.

The notation of that appendix and the discussion below is as follows. We introduce the matrices $\hat{U}^G$, where $G = Q, L, E, D$, and $\hat{\lambda}^g$ where $g = u, d, e$, which are the Yukawa matrices of equation (5.2) in the flavor basis of this section, the correspondence being obvious from the notation. We denote the Clebsch coefficients for a specific matrix with the appropriate subscript;

$$\hat{U}^G = \begin{pmatrix} 0 & z_G C & 0 \\ z_G C & y_G e^{i\phi} E & x'_G B \\ 0 & x_G B & A \end{pmatrix}, \tag{5.9}$$

with similar relations for the $\hat{\lambda}^g$.

Since the vevs in equation (5.6) differentiate between the $B-L$, Y, and X values of the fields within the 16s they violate the relations in equation (5.4). For example let us examine the relative values of the $(1,2)$ elements of various Yukawa matrices.

All the models listed in Appendix A have the same O_{12} operator,

$$O_{12} = 16_1 \left(\frac{45_X}{M}\right)^3 10 \left(\frac{45_X}{M}\right)^3 16_2. \tag{5.10}$$

The 45 vevs in O_{12} give factors of the X quantum numbers of the various fields in the 16s. The X value for the matter fields $(Q, u^c, d^c, L, e^c, \nu^c)$ are $(1, 1, -3, -3, 1, 5)$, respectively. The values of the $(1,2)$ elements of the up quark, down quark, charged lepton , and neutrino mass matrices in the flavor basis are thus $(1, -27, -27, -27, 125)$, respectively. Similarly, relative to the up mass matrix, the $(1,2)$ element of the matrices $(\hat{U}^Q, \hat{U}^L, \hat{U}^D, \hat{U}^E)$ are $(1, -27, -27, 1)$, respectively. Similar factors distinguish the other elements of the various Yukawa matrices, violating the relations in equation (5.4). See Appendix A.

To determine the triplet Yukawa matrices U^Q and U^L in equation (5.2), we need the matrices V_L^u and V_L^e which rotate the left handed up quarks and charged leptons into their mass basis. Using notation similar to that used by ADHRS [59],

we have

$$V_L^u = \begin{pmatrix} c_2 & -s_2 & 0 \\ s_2 & c_2 & 0 \\ 0 & 0 & 1 \end{pmatrix} \begin{pmatrix} e^{-i\phi_u} & 0 & 0 \\ 0 & 1 & 0 \\ 0 & 0 & 1 \end{pmatrix} \begin{pmatrix} 1 & 0 & 0 \\ 0 & \bar{c}_3 & -\bar{s}_3 \\ 0 & \bar{s}_3 & \bar{c}_3 \end{pmatrix} \tag{5.11}$$

$$V_L^e = \begin{pmatrix} c_{2e} & -s_{2e} & 0 \\ s_{2e} & c_{2e} & 0 \\ 0 & 0 & 1 \end{pmatrix} \begin{pmatrix} e^{-i\phi_e} & 0 & 0 \\ 0 & 1 & 0 \\ 0 & 0 & 1 \end{pmatrix} \begin{pmatrix} 1 & 0 & 0 \\ 0 & \bar{c}_{3e} & -\bar{s}_{3e} \\ 0 & \bar{s}_{3e} & \bar{c}_{3e} \end{pmatrix}, \tag{5.12}$$

where $s_i = \sin\theta_i$, $c_i = \cos\theta_i$, $\bar{\theta}_3 = x_u B/A$, $\bar{\theta}_{3e} = x_e B/A$, $\theta_2 = z_u C/\hat{y}_u E$, and $\theta_{2e} = z_e C/\hat{y}_e E$. We have introduced the notation $\hat{y}_u E$ for the $(2,2)$ entry of the matrix λ^u, and ϕ_u for the phase of $\hat{y}_u$. Similar relations hold for $\hat{y}_e E$ and ϕ_e.

Using these rotation matrices, we can calculate the matrices $U^Q = V_L^{u*}\hat{U}^Q V_L^{u\dagger}$ and $U^L = V_L^{u*}\hat{U}^L V_L^{e\dagger}$. Taking note of the fact that U^Q is symmetric, we have

$$U^Q = \begin{pmatrix} -2s_2 z_Q C e^{i\phi_u} + s_2^2 \hat{y}_Q E & z_Q C e^{i\phi_u} - s_2 \hat{y}_Q E & -s_2(x'_Q - x_u)B \\ & \hat{y}_Q E_Q & (x'_Q - x_u)B \\ & & A \end{pmatrix}, \tag{5.13}$$

$$U^L = \begin{pmatrix} -s_{2e} z_L C e^{i\phi_u} - s_2 z_L C e^{i\phi_e} + s_{2e} s_2 \hat{y}_L E & z_L C e^{i\phi_u} - s_2 \hat{y}_L E & -s_2(x'_L - x_u)B \\ z_L C e^{i\phi_e} - s_{2e}\hat{y}_L E & \hat{y}_L E & (x'_L - x_u)B \\ -s_{2e}(x_L - x_e)B & (x_L - x_e)B & A \end{pmatrix} \tag{5.14}$$

where

$$\begin{aligned} \hat{y}_Q E &= y_Q E e^{i\phi} + \frac{B^2}{A} x_u (x_u - x_L - x'_L) \\ \hat{y}_L E &= y_L E e^{i\phi} + \frac{B^2}{A}(x_u x_e - x_u x_L - x_e x'_L). \end{aligned} \tag{5.15}$$

Analogous results hold for the matrices U^E and U^D.

The formulas above are messy. We are interested in determining the relative importance of various diagrams leading to proton decay, a result which depends on the choices for the Clebsches above. However, rather then simply using numerical calculations, we wish to make our results more transparent. We thus introduce

a rough parameterization for our Yukawa matrices similar to the phenomenological parametrization of the KM matrix introduced by Wolfenstein [61].

With $\lambda \approx 0.2 \approx \sin\theta_c$, we have for the rough magnitude of the matrix elements

$$\left|U^Q_{ij}\right| = A \begin{pmatrix} \frac{1}{18}\lambda^4 & \frac{1}{6}\lambda^3 & \frac{1}{3}\lambda^3 \\ \frac{1}{6}\lambda^3 & \frac{1}{2}\lambda^2 & \lambda^2 \\ \frac{1}{3}\lambda^3 & \lambda^2 & 1 \end{pmatrix} \qquad \left|U^L_{ij}\right| = A \begin{pmatrix} \frac{1}{2}\lambda^4 & \frac{1}{2}\lambda^3 & \frac{1}{3}\lambda^3 \\ \lambda^3 & \frac{1}{2}\lambda^2 & \lambda^2 \\ \lambda^3 & \lambda^2 & 1 \end{pmatrix} \tag{5.16}$$

$$|K_{ij}| = \begin{pmatrix} 1 & \lambda & \lambda^3 \\ \lambda & 1 & \lambda^2 \\ \lambda^3 & \lambda^2 & 1 \end{pmatrix}, \tag{5.17}$$

with $\left|U^E_{ij}\right| \approx \left|U^Q_{ij}\right|$ and $\left|U^D_{ij}\right| = \left|U^L_{ij}\right|$.

This approximate form for the Yukawa matrices agrees, to within a few percent, with the actual matrices for some of the ADHRS models. For other models it is a poor approximation. Nevertheless, it is a helpful tool in evaluating the relative importance of various diagrams. In all cases discussed below, we will also indicate the precise results for the ADHRS models given in Appendix A. The form of these approximations make it clear that we are, in effect, employing a very familiar flavor symmetry scheme for our Yukawa matrices, one that is similar to the examples in Chapter 2.

Most of the various factors of λ, $\frac{1}{3}$, and $\frac{1}{2}$, that appear above arise from relatively simple considerations. For example, from the form of the up and down quark mass matrices, we have $K_{cb} \approx (x_d - x_u)\frac{B}{A}$, which gives us our order of magnitude approximation for the $(2,3)$ and $(3,2)$ elements of the matrices above, as long as the Clebsch's, x_G, are of order one.

The factor of $\frac{1}{3}$, raised to various powers, that appears throughout the matrices, will play a crucial role in certain diagrams. It arrises from the fact that the rotation angle, θ_2, in the light generation sector of the matrix V^u_L (see equation (5.11)), is approximately one third of the corresponding angle in the down

sector. This is a simple consequence of the relations

$$\begin{aligned} \sin\theta_2 &\approx \sqrt{\tfrac{m_u}{m_c}} \\ \sin\theta_1 &\approx \sqrt{\tfrac{m_d}{m_s}}, \end{aligned} \tag{5.18}$$

where θ_1 is the corresponding rotation in the matrix V_L^d, which diagonalizes the down quark mass matrix. Since the flavor basis Yukawa matrix $\hat{U}^L$ has a zero in its $(1,3)$ entry, a factor of a third naturally appears in the $(1,3)$ entry of $U^L = V_L^{u*}\,\hat{U}^L\,V_L^{e\dagger}$. The same holds for the matrices U^Q, U^E, and U^D. Similarly, because the $(1,2)$ entry of the matrix $\hat{U}^Q$ is small, smaller than the $\sin\theta_2\hat{y}_u E$ contribution which comes from rotating the light sector, as we show below, the factor of $\frac{1}{3}$ also appears in the $(1,2)$ entry of $U^Q = V_L^{u*}\,\hat{U}^Q\,V_L^{u\dagger}$.

We can see why $\hat{U}_{12}^Q$ must be small by taking the determinant of the up and down Yukawa matrices

$$\frac{m_u}{m_d} \approx 2\left(\frac{m_t}{m_b}\right)^2 \frac{m_s}{m_c}\left(\frac{z_u}{z_d}\right)^2, \tag{5.19}$$

where m_u, m_d, and m_s are taken at the scale $1GeV$, while the remaining masses are given at their particular mass scale [59]. This equation implies that the combination $(z_u/z_d)^2 \approx 10^{-3}$. This makes the $(1,2)$ entry of $\hat{U}^Q$ small enough so that the rotation contribution dominates U_{12}^Q.

A comment is in order concerning the value of $\tan\beta = \frac{v_1}{v_2}$, where v_1 and v_2 are the Higgs doublet vevs for H_f and $\overline{H}_f$, respectively. In the ADHRS model a single 10 multiplet and a single coupling, $16_3\ 10\ 16_3$, are responsible for top quark, bottom quark, and tau lepton masses. This leads to large values of $\tan\beta$ and large values for the Yukawa couplings in λ^d and U^L. This situation is disfavored in most models, because proton decay rates, which are already severely constrained by experiment, are proportional to U^L. This is not a serious problem, however. It is possible to arrange for an overall suppression factor to enter proton decay diagrams, sacrificing only the prediction of $\tan\beta$ in the process. One way of accomplishing this is to introduce an additional 10 multiplet into the theory and arrange for the proper triplet and doublet mass matrices. Since we are concerned with relative branching ratios, we will not examine the details of such a scheme here. We only

wish to point out that the ADHRS model can be modified to allow $\tan\beta$ to take values on the order of one, and that smaller values of $\tan\beta$ are favored, leading to longer proton lifetimes.

We note that because of the minimality of the theory and the assumed vev structure, ADHRS are forced into models with very particular Clebsch factors in some cases. For example all of the models in Appendix A have an O_{22} operators which result in $y_u = 0$, the familiar Georgi-Yarlskog form. It is certainly possible to add additional operators in a given model. Doing so will affect the predictivity of the model and also the specific proton decay results. As we stated in the introduction of this chapter, the ADHRS structure, in fact, gives very conservative results for proton decay, in the sense that one can easily arrange for larger deviations from the standard MSGUT predictions by introducing different flavor schemes. We discuss some interesting possibilities in Sections 5.8 and 5.9.

5.4 Dimension-Five Operators and Discussion

The superfield exchange of H_c pictured in Figure 5.1 results in the following relevant proton decay superpotential terms;

$$\begin{aligned} W_5 = & \tfrac{1}{2M_{H_c}}\, U^Q_{ij}\, U^L_{lm}\, (Q_i Q_j)(Q_l L_m) \\ & + \tfrac{1}{M_{H_c}}\, U^D_{ij}\, U^E_{lm}\, (u^c_i d^c_j)(u^c_l e^c_m) \end{aligned} \tag{5.20}$$

where the contraction of indices is given by

$$\begin{aligned} (Q_i Q_j)(Q_l L_m) &= \epsilon_{\alpha\beta\gamma}\, (u^\alpha_i d'^\beta_j - d'^\alpha_i u^\beta_j)(u^\gamma_l e_m - d'^\gamma_l \nu_m) \\ (u^c_i d^c_j)(u^c_l e^c_m) &= \epsilon^{\alpha\beta\gamma}\, u^c_{i\alpha}\, d^c_{j\beta}\, u^c_{l\gamma}\, e^c_m \end{aligned} \tag{5.21}$$

with Greek letters representing $SU(3)$ indices. In equation 5.20, we have ignored operators involving the right-handed neutrino superfields because their contribution to proton decay is negligible.

The superfield couplings in equation (5.21) lead to dimension-five vertices connecting two fermion and two scalar fields. In order to arrive at the four-fermion operators which mediate nucleon decay, we must dress the scalar fields, converting

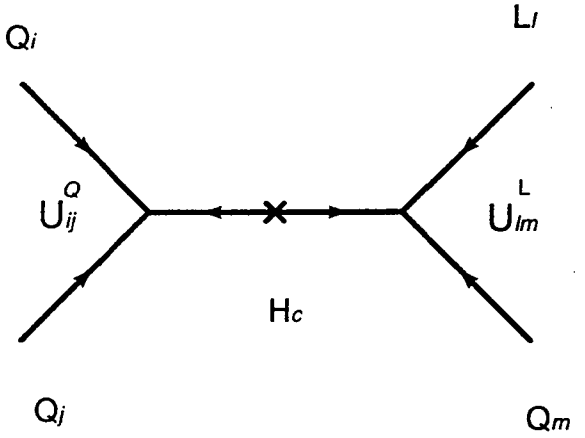

Figure 5.1: The supergraph responsible for the left handed dimension-five proton decay operators. A similar graph gives us the right handed analog.

them to fermions by the exchange of gaugino or higgsino fields. Some examples of the resulting diagrams are shown in Figures 5.4 and 5.5.

In the past, the assumptions of equation (5.4) have been used to conclude that charged wino exchange necessarily dominates over other dressings. To see this, we must note a few points. First, because U^Q is proportional to the up quark mass matrix, the dominant decay modes will involve U^Q_{22} or U^Q_{33}. This will favor dimension-five operators involving 2nd and 3rd generation fermions. It will also require flavor changing in the dressing process.

Flavor changing due to squark flavor mixing is assumed to be small, often by invoking the stringent experimental limits from flavor changing neutral processes such as $K - \bar{K}$ mixing [62]. If one ignores flavor changing effects due to squark exchange, then the dressing of the dimension-five operators by gluinos, neutral winos, or neutral higgsinos does not change the flavor of the fields involved. This immediately kills all contributions from these dressings to charged lepton modes. This is because the only four-fermion operators which contribute to these decays must contain two up quark fields. However, since these is no flavor changing in the dressing process, these operators can only come from dimension-five operators with two up quark superfields, and these vanish by $SU(3)$ antisymmetrization. For neutrino modes, again because of the lack of flavor mixing, neutral gaugino and

gluino dressed diagrams are suppressed. They are proportional $U_{11}^{Q} \propto m_u$. Past calculations have often been based on the assumption of squark mass degeneracy [63]. Under such an assumption, gluino and bino dressed diagrams vanish identically for all proton decay modes; by Fiertzing the four-fermion operators resulting from gluino dressing, one can see that they cancel among themselves. The same holds for bino dressed operators.

Diagrams involving higgsinos are suppressed by small Yukawa couplings in the first and second generation which accompany the higgsino vertices. This leaves charged wino diagrams as the dominant contribution to nucleon decay.

Charged wino diagrams for charged lepton modes involve a factor of U_{11}^{Q}, whereas the diagrams for neutrino modes avoid this suppression factor. Thus, with MSGUT Yukawa matrices and degenerate squarks, we arrive at the standard conclusion, that charged wino diagrams for the decays $(p \to K^+\overline{\nu}_\mu)$ and $(p \to K^+\overline{\nu}_\tau)$ dominate the proton dècay process. In Section 5.8, we will examine this set of circumstances in more detail.

When squark mass splittings are included, it is within the framework of the MSGUT [64, 65], ie. using MSGUT Yukawa couplings and minimal soft supersymmetry breaking squark masses. Results depend crucially on the value of $\tan\beta$. We give a brief overview of the possibilities here, leaving a detailed discussion for later, when we have calculated the relevant four-fermion operators.

For smaller values of $\tan\beta$, all squark matrices are very close to being diagonalized in the d' basis of equation (5.3) [64, 66]. In such a case, little is changed. Although gluino diagrams for neutrino modes no longer vanish, they still invariably involve a factor of m_u. Gluino diagrams for charged lepton modes still vanish, due to $SU(3)$ antisymmetrization (See Section 5.7). Diagrams dressed by neutralinos still invariably involve a factor of m_u. Charged higgsino diagrams still involve Yukawa couplings from the lighter two generations at the higgsino vertices.

For $\tan\beta \gg 1$ significant mixing in the up squark propagators can take place. Although the first two generation squarks remain close to degenerate, effects from the third generation can cause gluino diagrams to become dominant for charged

lepton decay modes [64] (See Section 5.7).

Replacing MSGUT Yukawa matrices with ours dramatically shifts this picture. No longer diagonal, the matrix U^Q now contributes to diagrams involving U^Q_{ij} with $i \neq j$. We briefly outline the results we find in the next few sections.

Assuming degenerate squarks, charged lepton modes generally are less suppressed than in the MSGUT case. In addition, neutral wino diagrams become more important in many models.

With MSGUT squark masses and with $\tan\beta$ not necessarily large, we find that, in addition to the changes above, gluino diagrams for certain decay modes dominate the wino diagrams in many models.

In the next section, we examine the issue of squark mixing in greater detail, revealing that additional assumptions are necessary to insure that either of the simple squark mass scenarios considered above are realized, large squark mass splittings being the norm.

5.5 Squark Masses

5.5.1 Preliminaries and the MSSM

In N=1 supergravity models with flavor blind gravitino couplings to matter, all squarks receive a universal mass at the Plank scale from soft supersymmetry breaking. In this section, we will examine how radiative corrections to this result will effect squark masses [67]. We begin by examining results from the minimal supersymmetric standard model (MSSM).

The squark mass terms in the lagrangian are given by

$$(\tilde{q}, \overline{\tilde{q}^c})\, \tilde{M}_q^2 \begin{pmatrix} \overline{\tilde{q}} \\ \tilde{q}^c \end{pmatrix} = (\tilde{q}, \overline{\tilde{q}^c}) \begin{pmatrix} \tilde{M}_{q,L}^2 & \tilde{M}_{q,LR}^2 \\ \tilde{M}_{q,LR}^{2\dagger} & \tilde{M}_{q,R}^2 \end{pmatrix} \begin{pmatrix} \overline{\tilde{q}} \\ \tilde{q}^c \end{pmatrix}, \tag{5.22}$$

where each of the four entries in the mass matrix is a 3×3 matrix itself in flavor space and $\tilde{q}$ stands for either up or down squarks. The overbar in $\overline{\tilde{q}}$ signifies complex conjugation.

The matrices above are related to soft symmetry breaking parameters and the quark mass matrices m_q in the following way.

$$\begin{aligned} \tilde{M}_{u,L}^2 &= m^u m^{u\dagger} + M_Q^2 + \frac{1}{4}(\tfrac{1}{2}\varrho_2^2 - \frac{1}{6}\varrho_1^2)(v_2^2 - v_1^2), \\ \tilde{M}_{u,R}^2 &= m^{u\dagger} m^u + M_U^2 + \frac{1}{6}\varrho_1^2(v_2^2 - v_1^2), \\ \tilde{M}_{u,LR}^2 &= \mu m^u \cot\beta + A m^u \end{aligned} \tag{5.23}$$

where A is the trilinear scalar soft symmetry breaking matrix, $\tan\beta = \frac{v_1}{v_2}$ (the ratio of vevs of the two Higgs scalars), the matrices M_Q, M_U are the soft symmetry breaking scalar mass matrices, m^u is the fermion mass matrix, and μ is the scalar doublet coupling in the superpotential. Similar results hold for the down sector.

In minimal supergravity models, at the Planck scale, the matrices M_Q and M_U are equal to the universal scalar mass m_0 times the identity matrix. Similarly, A is proportional to the same combination. We see that at the tree level the matrices in equation (5.23) are diagonalized in the quark mass basis.

Radiative running from the Planck scale down to the weak scale gives contributions to the parameters above. In most cases, running from the Planck scale

down to the GUT scale is ignored. The result is that the matrices $\tilde{M}_q^2$ receive contributions from the quark Yukawa matrices λ^q and from gaugino masses. Ignoring the latter contribution, which is identical for all fields with the same gauge charges, we have for the radiative contributions $\Delta\tilde{M}_{q,L}^2$ and $\Delta\tilde{M}_{q,R}^2$,

$$\Delta\tilde{M}_{u,L}^2 \approx m_0^2\left(c_1\lambda^u\lambda^{u\dagger} + c_2\lambda^d\lambda^{d\dagger}\right) \tag{5.24}$$

$$\Delta\tilde{M}_{d,L}^2 \approx m_0^2\left(c_1'\lambda^u\lambda^{u\dagger} + c_2'\lambda^d\lambda^{d\dagger}\right) \tag{5.25}$$

$$\Delta\tilde{M}_{u,R}^2 \approx m_0^2\left(c_3\lambda^{u\dagger}\lambda^u\right) \tag{5.26}$$

$$\Delta\tilde{M}_{d,R}^2 \approx m_0^2\left(c_3'\lambda^{d\dagger}\lambda^d\right), \tag{5.27}$$

$$\tag{5.28}$$

where the constants c_i, c_i' are of order $-\frac{1}{2}$.

Except for the third generation contributions, the off-diagonal matrices $\tilde{M}_{q,LR}^2$ are relatively small compared to the diagonal blocks. We will ignore their contributions throughout most of this chapter.

Mass Splittings in the MSSM

In gluino dressed diagrams, squark degeneracy causes a complete cancellation of the nucleon decay amplitudes. Thus, it is important to determine to what extent squark masses split from one another. Because the lower generational Yukawa couplings are small, the radiative running above has little effects on the squark masses of the first two generations. They remain nearly degenerate, the largest splitting effect coming from the D terms in equation (5.23), which are negligible unless $\tan\beta \gg 1$.

Third generation squarks can be considerably lighter than the first two generations, because the top Yukawa coupling, λ_t, is of order one. This leads to nonvanishing gluino dressed diagrams. However, we will see that if one uses the MSGUT Yukawa couplings, then charged wino diagrams are still much larger. This is not true if we employ our Yukawa matrices (See Section 5.7).

Squark Mixing in the MSSM

Squark flavor mixing, which occurs when squark mass eigenstates do not correspond to quark mass eigenstates, also plays a role in determining the importance of various proton decay diagrams. We introduce some notation which will be helpful in our discussion.

Let $V^{\tilde{q}}$ be the 6×6 unitary matrices which diagonalize the squark mass matrices. With $\tilde{q}$ signifying either up or down squarks, we have

$$V^{\tilde{q}} \tilde{M}_q^2 V^{\tilde{q}\dagger} = diagonal\,(\tilde{m}_{q_i}^2), \quad i = 1, 2, \cdots, 6. \tag{5.29}$$

Gluino couplings involve the matrix $K_{\tilde{q}}$, a product of the matrix $V^{\tilde{q}}$ and the quark rotation matrices $V_{L,R}^q$,

$$K_{\tilde{q}} = V^{\tilde{q}} \begin{pmatrix} V_L^{q\dagger} & 0 \\ 0 & V_R^{q\dagger} \end{pmatrix}. \tag{5.30}$$

We introduce the off-diagonal matrices Δ^q, which parametrize flavor changing neutral current effects.

$$\Delta_{ij}^q = (K_{\tilde{q}\dagger})_{ik} \frac{\delta \tilde{m}_{q_k}^2}{\overline{m}^2} (K_{\tilde{q}})_{kj} \quad i \neq j, \tag{5.31}$$

$$\delta \tilde{m}_{q_k}^2 = \tilde{m}_{q_k}^2 - \overline{m}^2, \tag{5.32}$$

with $\tilde{m}_{q_k}$ as in equation (5.29) and $\overline{m}$ an average squark mass. For future reference, we write Δ^q in terms of its submatrices;

$$\Delta^q = \begin{pmatrix} \Delta_L^q & \Delta_{LR}^q \\ \Delta_{LR}^{q\dagger} & \Delta_R^q \end{pmatrix}. \tag{5.33}$$

From equations (5.28), (5.30), and (5.33), we deduce that the mixing matrix Δ_L^u is of the form

$$\Delta_L^u = c_2 V_L^u \lambda^d \lambda^{d\dagger} V_L^{u\dagger}, \tag{5.34}$$

Similarly, the mixing matrix for the down sector is given by

$$\Delta_L^d = c_1' V_L^d \lambda^u \lambda^{u\dagger} V_L^{d\dagger}. \tag{5.35}$$

The form of equations (5.34) and (5.35) lead to very small flavor changing effects which easily meet the stringent flavor changing neutral current (FCNC) limits below. Unless $\tan\beta \gg 1$, this mixing is also too small to significantly effect the size of gluino diagrams (See Section 5.7).

5.5.2 Beyond MSGUT Masses

High Energy Radiative Corrections

As first noted by Hall, Kostelecky, and Raby [68], the running of squark masses for energies above the GUT scale can lead to large corrections in the squark mass matrices. In almost any theory which explains the hierarchy in fermion masses, there exist couplings between the standard model fields and exotic fields. Diagrams in which the exotic fields are exchanged lead to radiative corrections to squark mass matrices which can be quite large [69].

Most of the scenarios designed to explain fermion masses, such as higher dimensional operators induced by quantum gravity, radiative hierarchy schemes, and see-saw schemes, introduce flavor symmetries to establish the structure of new exotic couplings.

In all of these models, the Yukawa couplings appearing in the low energy theory are effective couplings which conceal the underlying physics. This underlying physics invariably involves vertices coupling light fermion superfields to non-Standard Model multiplets. In addition, the coupling constants for these vertices are of order 1, since otherwise we are not "explaining" the hierarchy.

For example, in schemes such as the ADHRS model, hierarchies are generated by diagonalizing mass matrices which involve both the known fermions and new heavy fermions. This mechanism is common to a large class of models which attribute hierarchies to various factors of small mass ratios of the form $\lambda\frac{v}{M}$ where λ is a coupling constant of order 1, v is a vev relating to flavor symmetry breaking, and M is the mass of a heavy particle. In such models, lower generation fermion masses have higher powers of the suppression factor. In effect, the diagrams connecting fermions involve more heavy propagators and flavor breaking vevs as we

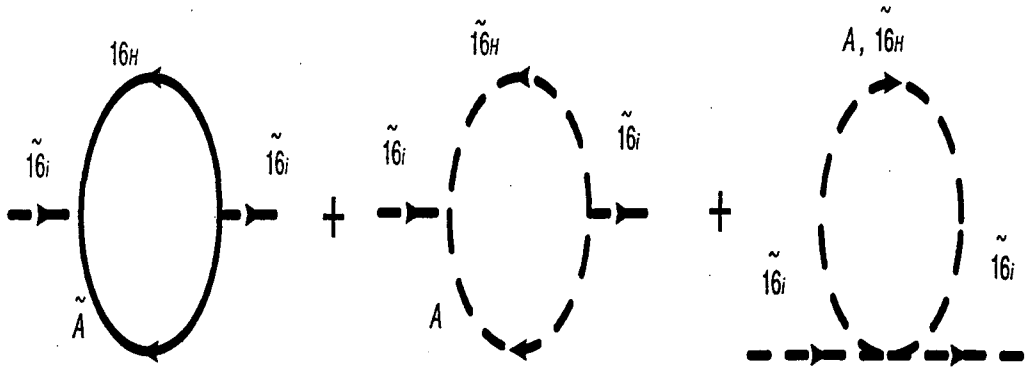

Figure 5.2: Feynman diagrams which contribute to the radiative squark masses.

move to lower generations.

In the ADHRS model, the light 16 multiplets, which contain the known quarks, couple to heavy $\overline{16}$s. The relevant terms in the superpotential are of the form

$$\lambda \; 16 \; \sigma_{ij} \overline{16}_H \; A_{ij}, \tag{5.36}$$

where A_{ij} is one of the 45 representations of $SO(10)$ which takes a vev (see equation (5.6)), the σ_{ij} are the 16 dimensional spinor $SO(10)$ matrices (normalized so that trace$(\sigma_{ij}\sigma_{ij}) = 16$ with no sum on ij), and λ is a dimensionless coupling constant not much smaller than one. The field $\overline{16}_H$ is heavy, taking a mass of the order λv_{10}.

Diagrams, such as those in Figure 5.2, which enter in the renormalization group scaling of squark masses for energies between the Planck and GUT scales, lead to possibly large squark mass corrections. These radiative effects primarily contribute to diagonal squark mass terms in the flavor basis - the basis singled out by diagonalizing the exotic couplings in the theory. Such corrections can lead to unacceptably large flavor changing neutral current (FCNC) effects, as well as to changes in the proton decay expectations.

We can get a rough idea of the size of these corrections by looking at the one loop effects. From the coupling in equation (5.36), we get one loop corrections

to the diagonal elements of the squark matrix on the order of

$$\Delta\tilde{M}_q^2 \approx -\frac{1}{16\pi^2}\, m_o^2\, \lambda^2\, 45\, (3 + A^2)\, \ln\left(\frac{M_p}{m_H}\right)^2 , \tag{5.37}$$

where Am_0^2 is the trilinear soft supersymmetry breaking parameter, and m_H is the mass of the heavy field $\overline{16}_H$. If λ is approximately one, then this correction is disastrously large, in fact too large for perturbation theory to be valid. One way to avoid violating FCNC limits is to just assume λ is of order 1/10. This insures that the squark masses don't differ significantly from those computed using the MSSM. (Although it does lower the mass of the heavy 16s by a factor of 10 while keeping the mass of the heavy gauge bosons in the theory fixed.)[2]

Meeting FCNC Limits

Limits from FCNC processes are most severe for mixing between the first two down squark generations [62].

$$(\Delta_M^d)_{12} < 0.008, \qquad (\Delta_L^d)_{12}(\Delta_R^d)_{12} < (0.0005)^2 , \tag{5.38}$$

where M stands for either L or R, and the precise limits, here and below, can differ by up to a factor of 3 to 4 because of hadronic uncertainties. These limits come from experimental results on CP violation in the $K - \overline{K}$ system when one assumes the relevant phases are large. For very small phases, we can ignore the limits in equation (5.38). However there are other limits from ΔM_K measurements;

$$(\Delta_M^d)_{12} < 0.1, \qquad (\Delta_L^d)_{12}(\Delta_R^d)_{12} < (0.006)^2. \tag{5.39}$$

We also have limits for the other mixing elements [70],

$$\begin{aligned} (\Delta_M^d)_{13} < 0.27, \qquad & (\Delta_L^d)_{13}(\Delta_R^d)_{13} < (0.07)^2 \\ (\Delta_M^u)_{12} < 0.1, \qquad & (\Delta_L^u)_{12}(\Delta_R^u)_{12} < (0.04)^2 \end{aligned} \tag{5.40}$$

Even small diagonal (in the flavor basis) radiative corrections to squark matrices can violate some of the limits above. For example, if the second generation

[2]We require an even smaller coupling constant for operators such as $16_i\, \overline{126}\, 16_j$ which can be used to give large majorana masses to right handed neutrinos.

squarks receive a correction of order ϵm_0^2, then the mixing matrix Δ_M^d is given approximately by

$$(\Delta_M^d)_{12} \approx \epsilon (V_L^d)_{12} (V_L^{d\dagger})_{22}. \tag{5.41}$$

For $(\Delta_M^d)_{12} < 0.0005$ and $(V_L^d)_{12} \approx \sin\theta_c$, we require $\epsilon < 2 \times 10^{-3}$, implying very small contributions to the first two generation down squark masses.

There are ways, however, to accommodate large diagonal radiative corrections without violating the FCNC limits above. One method is to align down squark and down quark mass eigenstates. The only natural way to accomplish this is to assume very nearly unbroken flavor symmetries in the down sector, leading to negligible off diagonal couplings for the down flavor eigenstates. This unavoidably leads to the relation $V_L^u \approx K$. Nir and Seiberg apply such a scheme in reference [70] where they address the problem of nonminimal soft supersymmetry breaking squark masses. In Section 5.7, we will see that such a solution naturally leads to large gluino dressed diagrams for proton decay.

Nonminimal Boundary Conditions

There is a separate problem with the MSGUT squark mass assumptions as we mention above. Besides flavor symmetries, there is no theoretical reason why at the Planck scale the squarks should be degenerate. Recently, various authors have used flavor symmetries to limit the form of Planck scale squark mass matrices [70, 71, 72]. Dine, Leigh, and Nelson have applied a spontaneously broken $SU(2)$ flavor symmetry to insure near degeneracy of the first two generation squarks [71]. If we are to take seriously the possibility of nonminimal soft supersymmetry breaking squark masses, we must employ a method similar to that used by Dine et al., Nir and Seiberg, or the authors of reference [72].

In our calculations, below, we will examine the consequences of various squark mass assumptions. We note that, even with standard MSGUT squark masses, our Yukawa matrices lead to increased gluino contributions which challenge the dominance of charged wino diagrams. If we allow for even moderate squark mixing, gluino diagrams will very likely surpass the wino contributions.

5.6 Calculational Preliminaries

In the remainder of this chapter, we we will be concerned primarily with the proton decay modes ($p \to K^+\overline{\nu_\mu}$), ($p \to K^+\overline{\nu_\tau}$), and ($p \to K^0\mu^+$), which are the dominant proton decay modes to neutrinos and charged leptons in the MSGUT calculations [63]. We leave the other modes, which are simply related to these, for Appendix B, where we also list neutron decay results.

As discussed in Section 5.3, we will make use of our approximate Yukawa matrices given in equation (5.16). This makes apparent the flavor symmetry structure of our theory, and allows one to easily determine how that structure effects proton decay. Although the Yukawa matrices in a specific ADHRS model may differ from this ansatz, the variation over the models is slight in many cases, and we indicate the exact values of important quantities where appropriate. We also make a few approximations which reduce the complexity of our calculation, but which have very little effect on our conclusions.

First, except for higgsino dressed diagrams, we will ignore left-right mixing in the squark matrices. Such mixing, expected to be small for all but the third generation, will not change our general results. Second, we will neglect certain renormalization effects, namely the running of the dimension-five operators from the $SU(5)$ breaking scale down to the SUSY breaking scale and the running of the four-fermion operators from the SUSY scale down to $1GeV$. Since we are concerned with ratios of diagrams, our approximation leads to very small quantitative errors (and no error for ratios involving dimension-five operators with the same superfield flavor content).

In the following section, we examine the possibility of large gluino dressed diagrams. We begin by using typical minimal supersymmetric standard model[73, 74] (MSSM) squark masses. We find that our Yukawa ansatz greatly increases the chances that gluino contributions to the decay $p \to K^+\overline{\nu}_\tau$ are large. In certain ADHRS models, the ν_μ mode also receives big gluino contributions. We also examine the consequences of nonstandard squark masses and find that small flavor changing effects in squark propagators can lead to a great enhancement of all gluino

dressed diagrams.

In Section 5.8, we discus chargino and neutralino diagrams. Using the ADHRS Yukawa couplings, we find that, out of these dressings, charged wino diagrams are the largest sources of proton decay, although neutral wino diagrams can contribute significantly. In addition, these diagrams give a larger branching ratio for charged lepton modes than one finds using MSGUT couplings. Unfortunately, the charged lepton modes are still sufficiently suppressed so that they will probably not be among the first modes observed. However, this result is sensitive to the exact structure of the ADHRS effective operators. We point out that very simple and reasonable changes in this structure are enough to make the charged lepton modes among the first observed.

5.7 Gluino Dressed Diagrams

Derivation and General Result

In this section, we will examine the dressing of dimension-five nucleon decay operators by gluinos. We wish to determine the relevance of these gluino diagrams given our nonstandard Higgs triplet couplings. We show that, in contrast to the MSGUT situation, certain gluino diagrams become important even when MSSM squark masses are used. In addition, we examine the increased importance of the gluino dressed diagrams for the case of non-MSSM squark masses.

The most significant result of this section is the marked increase in the branching ratio for the gluino dressed diagram leading to the decay ($p \to K^+\overline{\nu_\tau}$) when we use our Yukawa ansatz rather than MSSM couplings. For MSGUT squárk and gaugino masses favored by experimental limits on proton decay, we conclude that this gluino contribution is larger than the normally dominant charged wino diagram. In addition, we examine the possibility that flavor changing effects in squark mass matrices make all gluino diagrams large. We show that FCNC data does not imply that these effects are negligible. On the contrary, allowed flavor changing effects can easily make gluino diagrams the dominant source for all nucleon

decay modes.

5.7.1 Neutrino Modes

We first examine proton decay modes with neutrinos in the final state. Only the left handed dimension-five operators of equation (5.20) contribute to these neutrino modes. In superfield notation, we have

$$\mathcal{L}_5 = \frac{1}{M_{H_c}} U^Q_{ij}\, U^L_{lm}\, \left[(u_i d'_j)(u_l e_m \;-\; d'_l \nu_m)\right]_F, \tag{5.42}$$

where we have suppressed $SU(3)$ indices, and the subscript F indicates that one should take the F-term in the square brackets[3] For example, we have

$$\begin{aligned}(u_i d_j d_l \nu_m)_F \;&=\; (u_i d_j)(\tilde{d}_l \tilde{\nu}_m) + (u_i d_l)(\tilde{d}_j \tilde{\nu}_m) + (d_j d_l)(\tilde{u}_i \tilde{\nu}_m) \\ &\quad + (u_i \nu_m)(\tilde{d}_l \tilde{d}_j) + (d_j \nu_m)(\tilde{u}_i \tilde{d}_l) + (d_l \nu_m)(\tilde{u}_i \tilde{d}_j),\end{aligned} \tag{5.43}$$

where a tilde signifies a sfermion field.

Gluinos can dress the last three terms in equation (5.43). The relevant couplings in the Lagrangian are given in four component notation by

$$\mathcal{L} = -\frac{g_3}{\sqrt{2}} \lambda^a_{\alpha\beta} \left(\overline{\tilde{G}^a} L Q_\alpha\, \tilde{Q}^*_\beta - \overline{Q_\alpha} R \tilde{G}^a\, \tilde{Q}_\beta \right), \tag{5.44}$$

where Q is a quark field, $L = \frac{1}{2}(1-\gamma_5)$, $R = \frac{1}{2}(1+\gamma_5)$, the majorana gluino spinor $\tilde{G}^a$ is related to the the two component gluino spinor $\tilde{g}^a$ by

$$\tilde{G}^a = \begin{pmatrix} -i\tilde{g}^a \\ i\overline{\tilde{g}^a} \end{pmatrix}, \tag{5.45}$$

and λ^a are the $SU(3)$ matrices normalized such that trace$(\lambda^2) = 2$.

Dressing the scalars $(\tilde{u}_i \tilde{d}_j)$, for example, involves the triangle diagram pictured in Figure 5.3. This diagram converts the squark fields to quark fields

$$(\tilde{u}_i \tilde{d}_j) \longrightarrow \frac{4}{3}\frac{\alpha_3}{2\pi}\; (u_s\, d_t)\; (K^\dagger_{\tilde{u}})_{ik}\, (K_{\tilde{u}})_{ks}\, (K^\dagger_{\tilde{d}})_{jl}\, (K_{\tilde{d}})_{lt}\; f(\tilde{m}^2_{u_k}, \tilde{m}^2_{d_l}, m_{\tilde{g}}), \tag{5.46}$$

[3]In equation (5.42), we have used the fact that U^Q is symmetric.

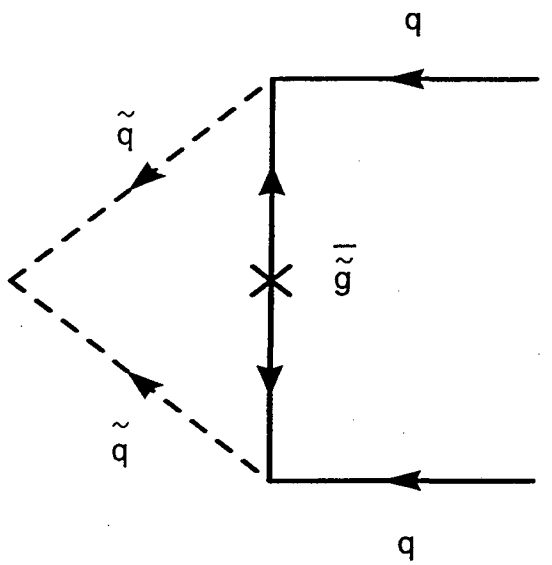

Figure 5.3: A triangle diagram, which converts squark fields into quark fields by the exchange of a gluino.

where $m_{\tilde{g}}$ is the mass of the gluino and we have suppressed Lorentz indices. Above, we have used the $K_{\tilde{q}}$ matrixes of equation (5.30), but have ignored the chirality flipping components of the squark mass matrices. The function f is the so called triangle diagram factor [75] giving the contribution from the loop integral in Figure 5.3:

$$\frac{\alpha_3}{2\pi} f(\tilde{m}_u^2, \tilde{m}_d^2, m_{\tilde{g}}) = -(i)^3 \varsigma_3^2 \int \frac{d^4k}{(2\pi)^4} \frac{1}{k^2 - \tilde{m}_u^2} \frac{1}{k^2 - \tilde{m}_d^2} \frac{m_{\tilde{g}}}{k^2 - m_{\tilde{g}}^2} \tag{5.47}$$

This gives

$$f(m_1^2, m_2^2, m_{\tilde{g}}) = \frac{m_{\tilde{g}}}{(m_1^2 - m_2^2)} \left(\frac{m_1^2}{m_1^2 - m_{\tilde{g}}^2} \ln \frac{m_1^2}{m_{\tilde{g}}^2} - \frac{m_2^2}{m_2^2 - m_{\tilde{g}}^2} \ln \frac{m_2^2}{m_{\tilde{g}}^2} \right). \tag{5.48}$$

By dressing equation (5.42) and using the Fierz identity to combine terms, we arrive at the following four-fermion operator responsible for gluino mediated proton decay to neutrino modes.

$$\mathcal{L}_{\tilde{g}}(p,n \to \nu_m) = \frac{1}{M_{H_c}} \frac{\alpha_3}{2\pi} \frac{4}{3} \epsilon^{\alpha\beta\gamma} (d_q'^{\alpha} u_s^{\beta})(d_t'^{\gamma} \nu_m) \left[U_{ij}^Q U_{lm}^L - U_{il}^Q U_{jm}^L \right]$$
$$\cdot (K_{\tilde{d}}^\dagger)_{la} (K_{\tilde{d}})_{aq} \left[(K_{\tilde{d}}^\dagger)_{jb} (K_{\tilde{d}})_{bt} f(\tilde{m}_{d_a}^2, \tilde{m}_{d_b}^2) \delta_{is} - (K_{\tilde{u}}^\dagger)_{ib} (K_{\tilde{u}})_{bs} f(\tilde{m}_{d_a}^2, \tilde{m}_{u_b}^2) \delta_{jt} \right], \tag{5.49}$$

where we have reintroduced color indices (Greek letters) and have dropped the explicit dependence on $m_{\tilde{g}}$ in the function f. Equation (5.49) includes a factor of $-\frac{8}{3}$ from a trace over $SU(3)$ matrices and a factor of $\frac{1}{2}$ from $(c_3/\sqrt{2})^2$.

The squark mixing matrices $K_{\tilde{q}}$ in equation (5.49) are in the d' basis of equation (5.3), so we have;

$$K_{\tilde{q}} = V^{\tilde{q}} \begin{pmatrix} V_L^{u\dagger} & 0 \\ 0 & V_R^{q\dagger} \end{pmatrix}. \tag{5.50}$$

It is easy to see from equation (5.49) how degenerate squarks lead to the vanishing of gluino dressed diagrams. For degenerate squarks, the $K_{\tilde{q}}$ matrices can be chosen to be the identity, and the last factor of equation (5.49) in square brackets is zero.

Using MSSM Squark Masses

We will return to the more general case below, but first, let us examine the implications of equation (5.49) when squark masses are given by a MSSM calculation. Unless $\tan\beta \gg 1$, the down quark Yukawa coupling contributions to squark masses can be treated as perturbations, and the squark mass matrices are very close to being diagonalized in the d' basis above, ie. $K_{\tilde{q}} \approx \mathbf{1}$. This is a well known MSSM result, and it leads to negligible gluino amplitudes when MSGUT Yukawa matrices are used [73]. Setting $K_{\tilde{q}} \approx \mathbf{1}$, we can rewrite equation (5.49) in the following form.

$$\begin{aligned} \mathcal{L}_{\tilde{g}}(p,n \to \nu_m) &= \frac{1}{M_{H_c}} \frac{\alpha_3}{2\pi} \frac{4}{3} \epsilon^{\alpha\beta\gamma} (d_l'^{\alpha} u_i^{\beta})(d_j'^{\gamma} \nu_m) \\ &\quad \cdot \left[U_{ij}^Q U_{lm}^L - U_{il}^Q U_{jm}^L \right] \left[f(\tilde{m}_{d_l}^2, \tilde{m}_{d_j}^2) - f(\tilde{m}_{d_l}^2, \tilde{m}_{u_i}^2) \right]. \end{aligned} \tag{5.51}$$

We now use equation (5.51) to compute the relevant 4-fermion operators for the decay $\Gamma(p \to K^+ \overline{\nu}_m)$. Borrowing the notation of reference [63],

$$\mathcal{L}_{p \to K^+ \overline{\nu}_m} = \epsilon_{\alpha\beta\gamma} \left[C(sud\nu_m)(s^\alpha u^\beta)(d^\gamma \nu_m) + C(dus\nu_m)(d^\alpha u^\beta)(s^\gamma \nu_m) \right] \tag{5.52}$$

The gluino contributions to the constants C are given by

$$C_{\tilde{g}}(sud\nu_m) = \frac{1}{M_{H_c}}\frac{\alpha_3}{2\pi}\frac{4}{3}\, K_{l2}\, K_{j1}\, \left[U^Q_{1j}U^L_{lm} - U^Q_{1l}U^L_{jm}\right]\left[f(\tilde{m}^2_{d_l},\tilde{m}^2_{d_j}) - f(\tilde{m}^2_{d_l},\tilde{m}^2_{u_1})\right], \tag{5.53}$$

and $C_{\tilde{g}}(dus\nu_m)$ is equal to the same thing with $K_{l2}K_{j1} \rightarrow K_{l1}K_{j2}$.

Nucleon decay rates predicted by minimal SUSY GUT theories are already severely constrained by experiment. These constraints restrict the allowed values for the function f in equation (5.53). If we wish to keep SUSY particle masses below $1TeV$, then these limits favor large squark masses, on the order of $1TeV$, and small gaugino masses on the order of $100GeV$ [63]. Similarly, since the decay rate in these theories goes as $(\sin 2\beta)^2$, smaller values for $\tan\beta$ are desirable. Thus, we tend to lean towards small gaugino masses, large squark masses, and $\tan\beta \approx 1$.

For the MSSM with $\tan\beta \approx 1$, we expect near degeneracy for the squarks of the first two generations. Even for large values of $\tan\beta$, the splitting between these generations is small enough so that the combination

$$f(\tilde{m}^2_{d_l},\tilde{m}^2_{d_j}) - f(\tilde{m}^2_{d_l},\tilde{m}^2_{u_1}), \tag{5.54}$$

appearing in the previous equation, is negligible unless $j = 3$.

Using this fact and our approximate Yukawa matrices from equation (5.16), we see the largest gluino contribution is to the ν_τ decay mode. An example of the relevant diagrams is given in Figure 5.4.

In equations (5.78) and (5.79), we write the corresponding contributions from charged wino diagrams. By using the approximate Yukawa matrices of equation (5.16), one can determine that the flavor factors are of the same order for both gluino and wino diagrams. Numerical calculations verify this, giving a ratio which varies from 1.2 to 0.84 over the different ADHRS models of Appendix A. We thus arrive at the following;

$$\left|\frac{C_{\tilde{g}}(sud\nu_\tau)}{C_{\tilde{w}^+}(sud\nu_\tau)}\right| \approx \left|\frac{C_{\tilde{g}}(dus\nu_\tau)}{C_{\tilde{w}^+}(dus\nu_\tau)}\right| \approx \left|\frac{2}{3}\frac{\alpha_3}{\alpha_2}\frac{\Delta f}{f}\right|, \tag{5.55}$$

where

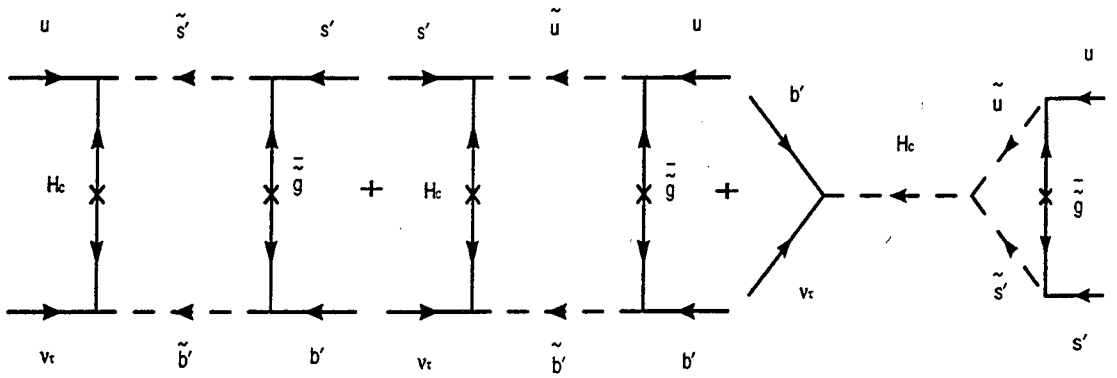

Figure 5.4: These are the gluino dressed diagrams which contribute to four-fermion operators with the flavor factor $U^Q_{12}U^L_{33}$. They cancel among themselves to lowest order in $M_{H_c}^{-2}$ if $\tilde{m}^2_u = \tilde{m}^2_{b'} = \tilde{m}^2_{s'}$.

$$f = f(\overline{m}^2, \overline{m}^2, m_{\tilde{w}^+}) \tag{5.56}$$

$$= \frac{1}{m_{\tilde{w}^+}} \frac{1}{x-1} \left[1 - \frac{\ln x}{x-1}\right]\Bigg|_{x=\overline{m}^2/m^2_{\tilde{w}^+}}, \tag{5.57}$$

$$\Delta f = f(\overline{m}^2, m^2_{\tilde{d}_3}, m_{\tilde{g}}) - f(\overline{m}^2, \overline{m}^2, m_{\tilde{g}}), \tag{5.58}$$

and $\overline{m}$ is the common squark mass for the first two generations[4].

The ratio $\frac{\Delta f}{f}$ depends on the specifics of the superpartner spectrum. As long as $\tan\beta$ is not very large, the mass $m_{\tilde{d}_3}$ in Δf is the mass of the left handed b squark, which receives radiative corrections of order $-\frac{1}{2}\lambda_t^2\ m_0^2$. These radiative corrections lower its mass below $\overline{m}$. Since all squark masses also receive positive radiative corrections proportional to gaugino masses, the factor Δf depends critically on the ratio of m_0 to the gaugino masses.

For typical models in which the universal Planck scale gaugino mass $m_{\frac{1}{2}}$ is approximately one tenth of the universal scalar mass m_0 [76], the ratio $\frac{\Delta f}{f}$ is about one. As discussed above, experimental constraints favor this sparticle spectrum. In such models, gluino diagrams are twice as large as charged wino diagrams for the

[4]The term with $l = 3$ in equation (5.53) vanishes when $j = 3$.

decay ($p \to K^+\overline{\nu}_\tau$). On the other hand, if $m_0 \approx m_{\frac{1}{2}}$, then $\frac{\Delta f}{f}$ is usually of order $10\% - 20\%$, and the ratio in equation (5.55) is twice this. For no-scale models, in which $m_0 = 0$, the gluino contribution above is negligible.

The enhancement of this gluino mode is a definite consequence of our nonminimal Yukawa matrices. If we use MSSM Yukawa matrices in our four-fermion operators, then we recover the standard result; the matrix U^Q is proportional to the diagonal up quark mass matrix m^u, charged wino diagrams have a contribution proportional to U^Q_{22}, all gluino diagrams are proportional to U^Q_{11}. This leads to an additional suppression factor in equation (5.55) on the order of $\frac{m_u}{m_c}\sin^{-2}\theta_c$. Thus, with MSSM squark masses, it is the violation of the $SU(5)$ relations of equation (5.4) which allows for a potentially large gluino contribution.

From equations (5.53), (5.78), and (5.79), and using our approximate Yukawa matrices, we deduce that for ν_μ modes gluino diagrams receive an additional suppression relative to wino diagrams which is usually of the order $\sin^2\theta_c$. Numerical calculations, however, show that there are ADHRS models in which this additional suppression, in effect, is absent, being as small as 0.83. In general we have

$$\left|\frac{C_{\tilde{g}}(sud\nu_\mu)}{C_{\tilde{w}^+}(sud\nu_\mu)}\right| \approx \left|a_1\frac{2}{3}\frac{\alpha_3}{\alpha_2}\frac{\Delta f}{f}\right|, \tag{5.59}$$

$$\left|\frac{C_{\tilde{g}}(dus\nu_\mu)}{C_{\tilde{w}^+}(dus\nu_\mu)}\right| \approx \left|a_2\frac{2}{3}\frac{\alpha_3}{\alpha_2}\frac{\Delta f}{f}\right|, \tag{5.60}$$

where the coefficient a_1 ranges over values from 0.83 to 2.3×10^{-4} and the coefficient a_2 ranges over values from 0.53 to 7.6×10^{-6} for the different ADHRS models. Thus, there are models in which the gluino diagrams for ν_μ modes are as large or larger than charged wino diagrams. The gluino contribution to the ν_e mode can also be as large as the charged wino contribution in some ADHRS models.

We conclude that, just by employing a flavor symmetry structure which corrects the fermion mass relations in an $SO(10)$ GUT theory, gluino mediated diagrams for the decay ($p \to K^+\overline{\nu_\tau}$) can easily become twice as large as the wino contributions. Similarly, certain, flavor symmetry structures lead to equally large gluino mediated diagrams for the decay ($p \to K^+\overline{\nu_\mu}$). When one allows for nonstan-

dard squark masses, the deviation from MSGUT predictions is even more marked.

Nonstandard Squark Masses

Let us suppose that we allow for large corrections to the squark mass matrices as discussed in Section 5.5. We can meet FCNC limits by aligning the down squark and down quark mass basis. In such a scenario, squark degeneracy is no longer a problem. If the mass splittings are of order the squark masses, in most situations gluino diagrams will dominate for all neutrino modes. In fact, even for moderate squark flavor changing effects, well within FCNC data limits, gluino diagrams are dominant.

Since these effects are actually necessary to avoid the vanishing of gluino dressed diagrams for charged lepton modes, we leave their analysis for the next section. Although we do not explicitly show that similar results hold for neutrino modes, it should be obvious from our discussion.

5.7.2 Charged Lepton Modes

The situation for charged lepton decay modes differs in important ways from the neutrino case. We will focus on the left handed dimension-five operators of equation (5.20), later discussing the right handed operators. Using the same notation as in equation (5.52), we have

$$\begin{aligned}\mathcal{L}_{\tilde{g}}(p,n \to K e_m) = \tfrac{1}{M_{H_c}} \tfrac{\alpha_3}{2\pi} \tfrac{4}{3}\, \epsilon^{\alpha\beta\gamma}(d_t'^{\alpha} u_q^{\beta})(u_s^{\gamma} e_m)\ \left[U^Q_{ij} U^L_{lm} - U^Q_{lj} U^L_{im}\right] \\ \cdot (K^\dagger_{\tilde{u}})_{la}(K_{\tilde{u}})_{aq}\ \left[(K^\dagger_{\tilde{d}})_{jb}(K_{\tilde{d}})_{bt}\, f(\tilde{m}^2_{u_a}, \tilde{m}^2_{d_b})\delta_{is} - (K^\dagger_{\tilde{u}})_{ib}(K_{\tilde{u}})_{bs}\, f(\tilde{m}^2_{u_a}, \tilde{m}^2_{u_b})\delta_{jt}\right]\end{aligned} \tag{5.61}$$

For MSSM squark masses with $\tan\beta \ll \frac{m_t}{m_b}$, the $K_{\tilde{q}}$ are very close to the identity in the basis of equation (5.3) (the d' basis). This forces $i = l = 1$, and the first term in squark brackets vanishes. In such a situation, there is no flavor changing for up squarks, so the original dimension-five operator of equation (5.20) vanishes due to color antisymmetrization.

In the MSSM, off-diagonal corrections in the triangle factor are proportional to Δ^u_{ij} from equation (5.34);

$$\Delta^u_L = c_2 V^u_l \lambda_d \lambda^\dagger_d V^{u\dagger}_L. \tag{5.62}$$

Thus, it is possible for equation (5.61) to contribute if the down quark Yukawa couplings are big, ie. for large $\tan\beta$. (Large values for the Yukawa couplings λ_d also increase the overall proton decay rate. As discussed in the last section, this consideration argues for small $\tan\beta$.)

To examine the effects of off-diagonal triangle factors for more general squark masses, we make the approximation that the squark eigenmasses can be expanded in the form

$$\tilde{m}^2_{q_k} = \overline{m}^2 + \delta\tilde{m}^2_{q_k}, \tag{5.63}$$

where $\overline{m}$ is an average squark mass and $\delta\tilde{m}^2_{q_k}$ is assumed to be small. Although this is not a very good approximation for the third generation, it suffices when determining the relative importance of gluino diagrams.

We expand the function f in terms of $\delta\tilde{m}^2_q$

$$\begin{aligned} f(\tilde{m}^2_1, \tilde{m}^2_2, m_{\tilde{g}}) &= f(\overline{m}^2, \overline{m}^2, m_{\tilde{g}}) \\ &\quad + f'(\overline{m}^2, m_{\tilde{g}}) \left(\frac{\delta\tilde{m}^2_1}{\overline{m}^2} + \frac{\delta\tilde{m}^2_2}{\overline{m}^2}\right) + o\left(\left(\frac{\delta\tilde{m}^2_2}{\overline{m}^2}\right)^2\right), \end{aligned} \tag{5.64}$$

where

$$f'(\overline{m}^2, m_{\tilde{g}}) = \frac{1}{m_{\tilde{g}}} \frac{1}{(x-1)^2} \left[\frac{x \ln x}{x+1} - \tfrac{1}{2}(x-1)\right]\Bigg|_{x=\overline{m}^2/m^2_{\tilde{g}}}. \tag{5.65}$$

Substituting equation (5.65) into equation (5.61), and keeping only the lowest order terms in $\delta\tilde{m}^2$, we get

$$\mathcal{L}_{\tilde{g}}(p, n \to K e_m) = -\frac{1}{M_{H_c}} \frac{\alpha_3}{2\pi} \frac{4}{3}\, \epsilon^{\alpha\beta\gamma} (d'^\alpha_j u^\beta)(u^\gamma e_m)\ (\Delta^u_L)_{i1}\, f' \ \left[U^Q_{ij} U^L_{1m} - U^Q_{1j} U^L_{im}\right], \tag{5.66}$$

where $f' = f'(\overline{m}^2, m_{\tilde{g}})$, and we have used the notation of equation (5.33).

Using the same notation as in equation (5.52), we have

$$\mathcal{L}(p \to K^0 e^+_m) = \epsilon_{\alpha\beta\gamma} C (suue_m)(s^\alpha u^\beta)(u^\gamma e_m), \tag{5.67}$$

with

$$C_{\tilde{g}}(suue_m) = -\frac{1}{M_{H_c}}\frac{\alpha_3}{2\pi}\frac{4}{3}\,K_{t2}\,(\Delta_L^u)_{i1}\,f'\;\left[U_{it}^Q U_{1m}^L - U_{1t}^Q U_{im}^L\right]. \tag{5.68}$$

To get an idea of how important this operator is, we compare it to the corresponding charged wino contribution given in equation (5.81), in which we have neglected squark mixing effects. Of course, if our comparison indicates that the gluino dressed operator is of the same order, squark mixing effects will also be important for the wino dressed operators. Using our approximate Yukawa matrices of equation (5.16), we see that

$$\frac{C_{\tilde{g}}(suu\mu)}{C_{\tilde{w}^+}(sud\mu)} \approx \frac{2}{3}\frac{\alpha_3}{\alpha_2}\frac{f'}{f}\;(a(\Delta_L^u)_{21}\;+\;b\,(\Delta_L^u)_{31}), \tag{5.69}$$

where the coefficients a and b are roughly given by

$$\begin{aligned} |a| &\approx \tfrac{3}{\sin\theta_c} \\ |b| &\approx \tfrac{6}{\sin\theta_c}. \end{aligned} \tag{5.70}$$

Our approximation is fairly good for $|a|$, which we find varies from 13 to 30 over the different ADHRS models. However, for $|b|$, the approximation is not as good. For the different ADHRS models we find values of $|b|$, as large as 181 and as small as 13. FCNC limits for the factors $(\Delta_L^u)_{21}$ and $(\Delta_L^u)_{31}$ were given in equation (5.40). We see that the term in brackets in equation (5.69) can be of order one for relatively small values of $(\Delta_L^u)_{31}$. For models in which $|b| \approx 180$, values of $(\Delta_L^u)_{31}$ an order of magnitude smaller than the most conservative experimental limit are large enough.

We do not have enough information about the squark mass matrices to determine how gluino dressed operators will compare to wino dressed ones when squark mixing is taken into account for both. But, since gluino couplings are larger than wino couplings, a value for the ratio in equation (5.69) larger than one indicates that it is likely that gluino diagrams play the dominant role in these decays.

The factor $\frac{f'}{f}$ depends on the sparticle spectrum, but is of order 1 in most models. For $m_{\frac{1}{2}} \ll m_0$ it is given by

$$\begin{aligned} \frac{f'}{f} &= -\tfrac{1}{2}\frac{m_{\tilde{g}}}{m_{\tilde{w}^+}} \\ &\approx -\tfrac{1}{2}\frac{\alpha_3}{\alpha_2}, \end{aligned} \tag{5.71}$$

with the last equality following from the well known result $\frac{m_{\tilde{g}}}{m_{\tilde{w}^+}} \approx \frac{\alpha_3}{\alpha_2}$.

As argued in Section 5.5, large squark mass splittings are possible in many models. If there are corrections to the MSSM squark masses of the form $\Delta\tilde{M}_q^2$, we have

$$\Delta_L^u = V_L^u \left(c_2 \, \lambda_d \lambda_d^\dagger \, + \, \frac{\Delta\tilde{M}_u^2}{\overline{m}^2} \right) V_L^{u\dagger}. \tag{5.72}$$

If we accommodate large flavor diagonal corrections by aligning down squarks and quarks, then $(\Delta_L^u)_{21}$ is approximately $\sin\theta_c$, slightly larger than its experimental limit[5], and $(\Delta_L^u)_{31}$ is of order K_{31}.

From equation (5.69), we see that if either Δ_L^u factor is this large, then gluino diagrams are of the same order or larger than wino diagrams. For models in which $|b|$ is large, we only require a radiative correction on the order $\frac{(\Delta\tilde{M}_u^2)_{33}}{\overline{m}^2} \approx 15\%$ to make the ratio in equation (5.69) of order one, assuming $V_{13}^u \approx K_{13}$.

We note that it is possible for gluino mediated charged lepton modes to become dominant even when one uses MSGUT Yukawa matrices [64]. This is because MSGUT Yukawa matrices not only suppress the gluino contributions to these modes, but also the charged wino contributions (See Section 5.8). One only requires a large enough value for Δ_L^u. This can be realized using MSSM squark masses if $\tan\beta \approx \frac{m_t}{m_b}$, which implies that the term proportional to $\lambda_d\lambda_d^\dagger$ in equation (5.72) is large[64].

The right-handed dimension-five operators of equation (5.20) lead to very similar 4-fermion operators. One arrives at these operators by making the following replacement in the equations above;

$$\begin{gathered} U^Q \to U^{D*}, \qquad U^L \to U^{E*}, \qquad \Delta_L^q \to \Delta_R^q, \qquad K \to \mathbf{1} \\ u, d, e \to \overline{u^c}, \overline{d^c}, \overline{e^c}, \end{gathered} \tag{5.73}$$

where the bar in $\overline{q^c}$ denotes Hermitian conjugation.

Let us, once again, get an idea of the importance of these operators by comparing them to the corresponding charged wino contribution given in equa-

[5]Recall that the limits in equation (5.40) are uncertain by a factor of 3 to 4.

tion (5.81). We have

$$\frac{C_{\tilde{g}}(suu\mu)_R}{C_{\tilde{w}^+}(sud\mu)} \approx \frac{2}{3}\frac{\alpha_3}{\alpha_2}\frac{f'}{f}\left(a_R(\Delta_R^u)_{21} + b_R\,(\Delta_R^u)_{31}\right). \tag{5.74}$$

Because of the large $(3,2)$ and $(2,3)$ entries of $\hat{U}^E$ (See Appendix A), we find that a_R can be as large as 70 and b_R as large as 1500 for certain ADHRS models. Thus, very small values of $(\Delta_R^u)_{21}$ and $(\Delta_R^u)_{31}$ are required to induce large gluino dressed right handed operators.

5.7.3 Gluino Conclusions

We have seen that the introduction of our Yukawa matrices has increased the possibility of large gluino mediated proton decay. This is most dramatic in the tau neutrino decay mode where in many cases, even with $\tan\beta \approx 1$ and MSSM squark masses, gluino diagrams are of the same order as, or larger than wino diagrams.

Allowing for non-MSSM squark masses greatly increases the chances of gluino dominance. We have shown that gluino contributions to charged lepton modes are likely to be at least as important as the wino contributions for relatively small squark flavor changing effects. The same holds true for the neutrino modes.

5.8 Chargino and Neutralino Dressed Diagrams

We now examine the other possible dressings for the dimension-five operators, paying particular attention to pure wino diagrams. In most instances, these diagrams give larger contributions than other chargino and neutralino dressings. We concentrate on diagrams which have the possibility of being the dominant source of a primary nucleon decay mode. Thus, for example, we ignore pure bino dressed diagrams which will always be smaller than their gluino counterparts.

The most important conclusion we reach concerns the relative branching ratio of charged lepton decay modes versus neutrino modes for pure wino diagrams. While this branching ratio is of the order 10^{-3} in MSGUT calculations, it is an order of magnitude larger when we use our Yukawa matrix ansatz.

5.8.1 Chargino Dressing

For chargino dressing, squark mass degeneracy does not cause a cancellation among the diagrams. From the discussion in Section 5.5, we conclude that any flavor changing effects from squark matrices are expected to be at most of order the KM matrix. Using our Yukawa matrix ansatz, chargino diagrams already have flavor mixing effects of this order, so we will ignore squark mass splittings in most of our discussion. If splittings are large enough to dramatically effect chargino diagrams, we certainly expect that gluino diagrams will be much larger.

Charged Wino Dressing

We first examine charged wino exchange diagrams. Proceeding as we did for gluino diagrams, we arrive at the following relevant Lagrangian terms;

$$\mathcal{L}_{\tilde{w}^+}(\nu_m) = \frac{1}{M_{H_c}} \frac{\alpha_2}{2\pi} (d_i' u_l)(d_j' \nu_m) \left[U^Q_{ij} U^L_{lm} - U^Q_{il} U^L_{jm} \right] U^*_{k1} V^*_{k1} \, 2 f(m_{\chi_k^+}), \qquad (5.75)$$

where f is the triangle diagram function of equation (5.48) for average squark mass $\overline{m}$ and chargino mass eigenstate χ_k^+,

$$f(m_{\chi_k^+}) = f(\overline{m}^2, \overline{m}^2, m_{\chi_k^+}), \qquad (5.76)$$

and U and V are the 2×2 unitary matrices which diagonalize the chargino mass matrix

$$\begin{pmatrix} m_{\tilde{w}^+} & m_W\sqrt{2}\,\cos\beta \\ m_W\sqrt{2}\,\sin\beta & \mu \end{pmatrix}. \tag{5.77}$$

(We have used the notation of reference [77]). The mass μ is a pure higgsino mass. Below, we approximate $U^*_{k1}\,V^*_{k1}\,f(m_{\chi^+_k})$ by $f(m_{\tilde{w}^+})$, valid for $m_{\chi^+_k} \ll \overline{m}$.

Once again, we will examine the Kaon decay modes. Using the same notation as in equation (5.52), we have

$$C_{\tilde{w}^+}(sud\nu_m) = \frac{1}{M_{H_c}}\frac{\alpha_2}{2\pi}\,2\,f(m_{\tilde{w}^+})\left\{\left[K^TU^QK\right]_{21}\left[U^L\right]_{1m} - \left[K^TU^Q\right]_{21}\left[K^TU^L\right]_{1m}\right\}, \tag{5.78}$$

$$C_{\tilde{w}^+}(dus\nu_m) = \frac{1}{M_{H_c}}\frac{\alpha_2}{2\pi}\,2\,f(m_{\tilde{w}^+})\left\{\left[K^TU^QK\right]_{12}\left[U^L\right]_{1m} - \left[K^TU^Q\right]_{11}\left[K^TU^L\right]_{2m}\right\}, \tag{5.79}$$

where K^T denotes the transpose of the KM matrix, K.

The wino dressed operator leading to charged lepton decay modes is

$$\mathcal{L}_{\tilde{w}^+}(e_m) = \frac{1}{M_{H_c}}\frac{\alpha_2}{2\pi}\,(d_ju_i)(d_le_m)\left[U^Q_{ij}U^L_{lm} - U^Q_{il}U^L_{jm}\right]\,U^*_{k1}\,V^*_{k1}\,2\,f(m_{\chi^+_k}), \tag{5.80}$$

with the corresponding result

$$C_{\tilde{w}^+}(suue_m) = \frac{1}{M_{H_c}}\frac{\alpha_2}{2\pi}\,2\,f(m_{\tilde{w}^+})\left\{\left[U^QK\right]_{12}\left[U^L\right]_{1m} - \left[U^Q\right]_{11}\left[K^TU^L\right]_{2m}\right\}. \tag{5.81}$$

Using MSGUT Yukawa Couplings

As explained in Section 5.4, when one assumes squark degeneracy, charged wino diagrams dominate the nucleon decay process. If one also uses the MSGUT Yukawa matrices of equation (5.16), then neutrino decay modes have a much larger branching fraction then those of charged leptons. In the d' basis of that equation, U^Q is diagonal and proportional to the up quark mass matrix. From equations (5.78), (5.79), and (5.81), we see that charged lepton decay modes involve $U^Q_{11} \propto m_u$ while neutrino modes have terms, such as

$$\left[K^TU^QK\right]_{21}, \tag{5.82}$$

which are proportional to $m_c \sin\theta_c$.

It is a simple matter to conclude that the neutrino modes are enhanced by a factor of

$$\left|\frac{m_c}{m_u}\sin^2\theta_c\right|^2 \tag{5.83}$$

relative to the charged lepton modes. Chiral Lagrangian coefficients in Equations (B.1) and (B.2) of Appendix A add an additional enhancement factor of $(2.02/0.70)^2$. The result is a relative branching fraction

$$\frac{\Gamma(p \to K^+\overline{\nu}_\mu)}{\Gamma(p \to K^0\mu^+)} = 1.4 \times 10^3. \tag{5.84}$$

Using ADHRS Yukawa Couplings

What value do we expect for the previous ratio when we use our Yukawa matrix ansatz (again assuming small gluino diagrams)? For our matrices, U^Q is no longer diagonal, and it is possible that the first term in the curly brackets of equation (5.81) is dominant. In fact, if we naively assume that $\left|\frac{U^Q_{12}}{U^Q_{22}}\right| \approx \sin\theta_c$, then the only enhancement for neutrino modes comes from the chiral lagrangian factor, and the ratio in the previous equation is of order 10. This naive guess is incorrect, however. We see from our approximate Yukawa matrices of equation(5.16) that $\left|\frac{U^Q_{12}}{U^Q_{22}}\right| \approx \frac{1}{3}\sin\theta_c$. In the discussion following that equation, we examined the origin of this extra factor of one third.

We conclude that

$$\left[K^T U^Q K\right]_{21} = \left[K^T U^Q K\right]_{12} \approx \tfrac{1}{3}\left[U^Q K\right]_{12}, \tag{5.85}$$

in sharp contrast with the MSGUT results;

$$\left[K^T U^Q K\right]_{12} \approx \frac{m_c}{m_u}\left[U^Q K\right]_{12}. \tag{5.86}$$

Using our Yukawa matrices, we calculate the size of the flavor factors for the ν_μ mode relative to the μ^+ mode;

$$\frac{\left[K^T U^Q K\right]_{12}\left[U^L\right]_{1m} - \left[K^T U^Q\right]_{11}\left[K^T U^L\right]_{2m}}{\left[U^Q K\right]_{12}\left[U^L\right]_{1m} - \left[U^Q\right]_{11}\left[K^T U^L\right]_{2m}} \approx 3. \tag{5.87}$$

Combined with the chiral Lagrangian enhancement factor (2.02/0.70), which also appeared in the MSGUT calculation, we find that, for charged wino dressed diagrams,

$$\frac{\Gamma(p \to K^+\nu_\mu)}{\Gamma(p \to K^0\mu)} \approx 75. \tag{5.88}$$

Using our Yukawa ansatz, we find that the charged wino contribution to the mode $(p \to K^+\nu_\tau)$ is roughly equal to the ν_μ mode, while the ν_e mode is much smaller. Thus we have

$$R \equiv \frac{\sum_i \Gamma(p \to K^+\nu_i)}{\Gamma(p \to K^0\mu)} \approx 150. \tag{5.89}$$

As we have stated previously, we expect the exact value of R above to vary with the different ADHRS models. A detailed numerical calculation gives values that range between 92 and 400 for the models in Appendix A.

Large Charged Lepton Modes

To what extent are the results above general? All we really can conclude from these calculations is that the large suppression factor in equation (5.83) is a special case of the MSGUT Yukawa couplings. It is true that the ADHRS Yukawa matrices also give a suppression which implies that the charged lepton modes will not be among the first observed in such models. However, it is easy to avoid this conclusion. After all, as we have just seen, it is a simple factor of three in the amplitude which means the difference between the observability or invisibility of the charged lepton modes. We give some examples of models which lead to large charged lepton branching fractions.

Let us insert a 45 multiplet which takes a vev in the T_{3R} direction into the operator O_{22} in the ADHRS models. This makes the Clebsch factors y_Q and y_L equal to zero. By examining our Yukawa structure, we see that this can increase the ratio in equation (5.87). If we make no other changes, our numerical calculations indicate that, in certain ADHRS models, this scheme leads to

$$R \equiv \frac{\sum_i \Gamma(p \to K^+\nu_i)}{\Gamma(p \to K^0\mu)} \approx 20, \tag{5.90}$$

where we have included diagrams dressed by pure neutral winos also (See below). Since experiments are more sensitive to charged lepton modes by a factor of about three, they may be seen in the first few proton decay observations in such models.

Unfortunately, inserting this factor of $< 45_{T_3R} >$ will ruin the fermion mass predictions for the basic ADHRS models. However, one need not assume, as ADHRS do, that the model one uses is maximally predictive. By adding extra effective operators, we can increase the degrees of freedom and allow for more complex flavor structures. Although we lose the ability to make all the predictions which ADHRS make, we can see from the above example that arranging for large charged lepton modes is not difficult.

If one is willing to allow different group contractions in the effective operators of the theory, it is even simpler to generate large charged lepton amplitudes. For example, one can introduce the effective operator

$$\frac{1}{M}\ (16_1\, C\Gamma_i\, 16_2)\, A_{ij}\, T_j, \tag{5.91}$$

where A is a 45 of $SO(10)$, T is the Higgs multiplet, 16_k is the kth generation fermion multiplet, Γ_i are the $SO(10)$ gamma matrices, C is the $SO(10)$ charge conjugation matrix, and M is a GUT scale mass. If A takes a vev in the $B-L$ direction then this operator only contributes to the Higgs triplet Yukawa matrices[78]. Thus, one can generate large values of U^Q_{12} without disturbing the fermion mass predictions. As we discussed above, one only needs $U^Q_{12} \approx \sin\theta_c\, U^Q_{22}$ to make charged lepton modes visible.

Charged Higgsino Dressing

Most diagrams which involve charged higgsino interactions are negligible in comparison to the pure charged wino diagrams. In contrast to the weak gauge coupling constant, the Higgsino couplings, being proportional to fermion masses, are very small for the lighter generations. The exceptions are diagrams with top-bottom-higgsino vertices which have the large coupling λ_t or the possibly large coupling λ_b, the latter being large only for $\tan\beta \approx \frac{m_t}{m_b}$. Since this last possibility is disfavored, we will assume $\lambda_b < g_2$, and keep only diagrams with λ_t couplings.

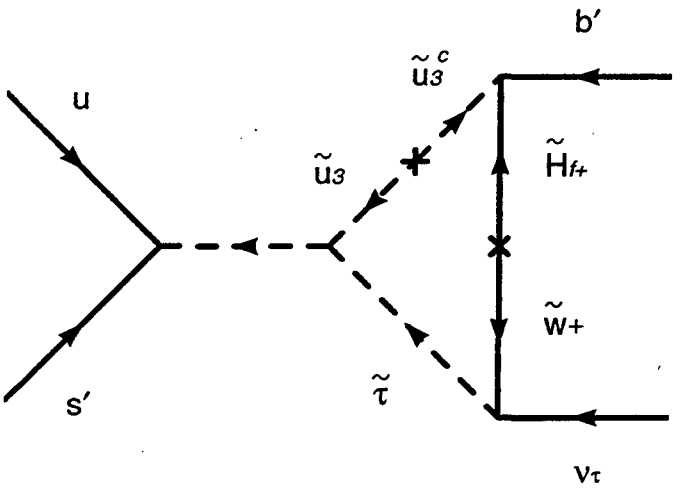

Figure 5.5: This chargino diagram containing a higgsino vertex is the dominant such diagram in the ADHRS model.

We conclude that the only possible large higgsino diagrams require a higgsino coupling at one of the dressing vertices and a wino coupling at the other. Such diagrams must include a chirality flip in one of the squark propagators. The dominant diagrams of this type come from the dressing of the left-handed dimension-five operators with a chirality flip in the stop leg. (Right-handed dimension-five operators with λ_t require a chirality flip in the down squark sector and additional small mixing angles.) Out of these diagrams, the only one which does not suffer a flavor symmetry suppression due to our Yukawa matrices is the diagram in Figure 5.5 for the decay ($p \to K^+\nu_\tau$). However, in addition to requiring a chirality flip in the stop leg, this diagram is proportional to the off diagonal element of the chargino mass matrix. Thus, although it is enhanced relative to the corresponding pure wino diagram by a factor λ_t/ϱ_2, it has a suppression factor of the order

$$\sqrt{2}\,\sin\beta\,\frac{m_W}{m_{\tilde{w}+}}\frac{(\tilde{M}^2_{u,LR})_{33}}{(\tilde{M}^2_{u,L})_{33}}. \tag{5.92}$$

We expect this factor will more than compensate for the coupling constant enhancement in most models, the exception being those models in which squark and gaugino masses are not much larger than the weak scale.

5.8.2 Neutralino Dressing

Most neutralino dressed diagrams are also quite small in our model. Diagrams with neutral higgsino couplings in the dressing process always involve small higgs doublet Yukawa couplings, and thus are negligible. The only possibly large diagrams involve the neutral gaugino particles. In the limit of squark degeneracy, diagrams dressed by pure bino exchange vanish just as in the gluino case. Since the couplings of binos are smaller than gluinos, gluino diagrams will always be larger. We, thus, do not examine pure bino contributions here.

Dressings with a bino at one vertex and a neutral wino at the other are small due to the structure of the neutralino mass matrix. At the tree level, there is no mass term which directly connects neutral binos and winos. Thus, the neutralino propagator is suppressed by at least three mass insertions. We conclude that the dominant neutralino diagrams have neutral winos at both dressing vertices.

Using the notation of equations (5.75) and (5.76), the neutral wino four-fermion operators responsible for neutrino decay modes are given by

$$\mathcal{L}_{\tilde{w}}(\nu_m) = -\frac{1}{M_{H_c}}\frac{\alpha_2}{2\pi}\,(d_j u_i)(d_l \nu_m)\left[U^Q_{ij}U^L_{lm} - U^Q_{il}U^L_{jm}\right]\, N^*_{2k}\, N^*_{2k}\, 2\, f(m_k), \qquad (5.93)$$

where, using the notation of reference [77], N is the 4×4 unitary matrix which diagonalizes the neutralino mass matrix, m_k are the neutralino mass eigenvalues, and the combination

$$N^*_{2k}\, N^*_{2k}\, m_k \qquad (5.94)$$

picks out the pure wino mass, M_2. As in equation (5.75), we have neglected squark mixing.

Approximating $N^*_{2k}\, N^*_{2k}\, f(m_k)$ by $f(M_2)$, valid for $m_k \ll \overline{m}$, we arrive at the relevant amplitudes

$$C_{\tilde{w}}(sud\nu_m) = -\frac{1}{M_{H_c}}\frac{\alpha_2}{2\pi}\, 2\, f(M_2)\left\{\left[U^Q K\right]_{12}\left[K^T U^L\right]_{1m} - \left[U^Q K\right]_{11}\left[K^T U^L\right]_{2m}\right\} \qquad (5.95)$$

$$C_{\tilde{w}}(dus\nu_m) = -C_{\tilde{w}}(sud\nu_m). \qquad (5.96)$$

Our approximate Yukawa matrices work well when comparing the ν_μ and ν_e modes above with the corresponding charged wino four-fermion operator. They indicate

that the neutral wino operator is approximately one third of the charged wino one. Detailed numerical calculations show that the actual ratio varies between 0.23 and 0.40 over the different ADHRS models for the ν_μ mode, and between 0.21 and 0.45 for the ν_e mode. Our calculations indicate that the neutral wino operator for the ν_τ mode is even further suppressed relative to the charged wino one, the least suppression being by a factor of 5.1×10^{-2}.

When we include neutral wino diagrams in our calculation of the ratio in equation (5.89), the range of possible values changes little. R now runs over values from 92 to 280. The value for individual models changes by about five to ten percent. However, in models like those discussed in Section 5.8.1, the neutral wino diagrams can alter the ratio significantly.

The neutral wino amplitude for charged lepton decay modes vanishes in this approximation since there is no flavor changing in the dressing process. This same phenomenon was seen in the corresponding gluino diagrams. Non-minimal squark masses will lead to nonzero contributions, but, as in the bino case, gluino diagrams will always be larger.

5.8.3 Chargino and Neutralino Conclusions

Pure charged wino dressing is the dominant type of chargino diagram in most models. Although our Yukawa matrix ansatz has lead to the result that neutrino modes dominate the decay rate for these diagrams, we find that charged lepton modes are not as suppressed as in the MSGUT case and that it is a simple matter to arrange for even less of a suppression by altering the flavor structure of the theory. In addition, diagrams dressed by neutral winos contribute a larger fraction of the neutrino mode decay rates than in the MSGUT case.

5.9 Discussion of Branching Ratios

In the previous two sections, we have shown that MSGUT calculations for proton decay are likely to be wrong in GUT theories such as ours which accurately predict the mass spectrum of the SM fermions. Unfortunately, the specific way in which they differ from MSGUT results depends critically on the superpartner spectrum. Thus, it is difficult to make any definitive predictions, although we can discuss branching ratios in particular cases.

An issue of importance is the relative branching ratios one expects for the charged lepton versus the neutrino modes. One need not fine tune the parameters of a theory to get much larger charged lepton mode decay rates. One can assume that squarks are very degenerate in mass, so that gluino diagrams are negligible. If one imposes a flavor ansatz, for example, with $U^Q_{12} = \sin\theta_c\, U^Q_{22}$, then, as we showed in Section 5.8, charged wino diagrams give the same order flavor factors for both ν_μ and μ modes. Nuclear matrix elements lead to a very modest relative suppression, on the order of a tenth, for the μ mode. This would imply that this mode would be one of the first to be observed, since experiments are about a factor of three more sensitive to it than to the neutrino modes.

Our lack of knowledge about squark masses makes it particularly difficult to predict these ratios if squark flavor mixing is large. In such a circumstance, we expect gluino diagrams to dominate all proton decay modes, and the branching fractions to be dependant on squark masses in a complicated way. Comparable flavor factors for the charged lepton and neutrino modes are certainly not ruled out, however, and, if realized, lead to relatively large charged lepton branching fractions as in the wino dominated case above.

One can even arrange for partial cancellation of neutrino modes between gluino and wino diagrams. This can be accomplished using basic MSSM squark masses. For example, in specific ADHRS models where the ratios in equations (5.55), (5.59), and (5.60) are large, one can arrange for such a cancellation.

Thus, the common assumption, that charged lepton modes will be swamped in most cases, is far less certain.

5.10 Conclusion

We have examined proton decay in a class of SUSY GUT models which accurately predict the SM fermion spectrum. Previously, SUSY GUT proton decay calculations have been based, almost exclusively, on the minimal supersymmetric standard model, with little regard for the fact that the Yukawa couplings of this theory are known to be incorrect.

Flavor symmetries are the natural mechanism by which one fixes the Yukawa couplings. In this chapter, we looked in detail at a particular flavor symmetry scheme, the ADHRS scheme. We found that the mechanism by which the Yukawa matrices are corrected in the ADHRS model alters the couplings responsible for proton decay in SUSY theories. In many other models, a similar result holds.

In addition, we discussed the repercussions for squark masses of schemes, such as the ADHRS scheme, which attempt to explain the hierarchical nature of the Yukawa couplings. The squark spectrum is important in determining the relative importance of gluino dressed diagrams in the proton decay process. We found that radiative running of squark masses for energies above the GUT scale can very easily cause large squark mass splittings, posing a threat to limits from various FCNC processes. We discussed the possibility of meeting these limits while still allowing the large splittings.

We then used the new Yukawa couplings and various assumptions concerning the mass spectrum of the supersymmetric particles to determine the relative importance of different dressing processes and the relative branching fractions for certain key proton decay modes.

In Section 5.7, we examined gluino dressed diagrams. First assuming typical MSGUT squark masses, we determined that these diagrams will be the dominant source for the decay modes ($p \to K^+\overline{\nu_\tau}$) and ($p \to K^+\overline{\nu_\mu}$) in certain ADHRS models. Next, we discussed the consequences of non-MSGUT squark masses for the charged lepton decay modes. We found that flavor mixing effects in the up squark mass matrices can very easily lead to gluino dominance for these modes as well.

In Section 5.8, we examined proton decay modes dressed by neutralinos and charginos. We found that pure wino dressed diagrams are the dominant diagrams of each kind. Assuming small squark mass effects, we determined that, for these diagrams, in contrast to calculations based on the MSGUT, our Yukawa structure gives a larger branching fraction for the dominant charged lepton mode, $(p \to K^0\mu^+)$, relative to the dominant neutrino modes.

In Sections 5.8.1 and 5.9, we discussed the possibility that charged lepton modes will be among the first proton decays to be seen. With sufficient squark flavor mixing, gluino diagrams will be the dominant source for all proton decay modes. In this circumstance, the charged lepton mode $(p \to K^0\mu^+)$ can be large enough to be seen in the first proton decay observations. If we assume wino dominance, it is unlikely that the charged lepton modes will be large enough in the ADHRS models. However, we pointed out that flavor symmetry schemes exist which lead to large enough charged lepton modes even for wino dominance.

Unfortunately, definitive conclusions are impossible to make without limiting oneself to a particular model in all its detail. However, it is clear that many past proton decay calculations have relied on faulty assumptions. Relaxing these assumptions opens the possibility of very different proton decay signatures.

Bibliography

[1] R. Davis,Jr. in Proceedings of Seventh Workshop on Grand Unification, ICOBAN1986, Toyama, Japan, edited by J. Arafune, World Scientific, Singapore (1986), p.237.

[2] S. P. Mikheyev and A. Y. Smirnov Sov. J. Nucl. Phys. **42**, 913 (1985); Nuovo Cimento C **9**, 17 (1986); Sov. Phys. JETP **64**, 4 (1986); L. Wolfenstein, Phys. Rev. D **17**, 2369 (1978); Phys. Rev. D **20**, 2634 (1979).

[3] A. Zee, Phys. Lett. B **93**, 389, (1980); Phys. Lett. B **161**, 141, (1985).

[4] L. Hall and S. Weinberg, Phys. Rev. D **48**, R979 (1993);

[5] S.L.Glashow and S. Weinberg, Phys. Rev. **D15** 1958 (1977).

[6] For any given four fermions the exchanged scalar could induce several four-fermion operators with different helicity structures. According to our ansatz they could have slightly different coupling constants. Since we do not know the relative coefficients by which these operators enter the theory, we decided to use in our estimates the operator with the "average" Yukawa coupling (e.q. in $\Delta m(K^0 - \bar{K}^0)$ we use $\bar{s}_R d_L \bar{s}_L d_R$ rather than $(\bar{s}_R d_L)^2$ or $(\bar{s}_L d_R)^2$).

[7] R.N. Cahn and H. Harari, Nucl. Phys. **B176** 135 (1980); S. Dimopoulos and J. Ellis, Nucl. Phys. **B182** 505 (1981).

[8] Proposal For An Upgraded CDF Detector, CDF/DOC/PUBLIC/1172 (1990).

[9] M. Savage, Phys. Lett. **B266** 135 (1991); A. Ali, Deutsches Electronen Synchotron, Hamburg, Germany, Preprint number: DESY-91-080.

[10] For a review see L.J. Hall, Mod. Phys. Lett. **A5** 467 (1990) which cites the original literature.

[11] T.P. Cheng and M. Sher, Phys. Rev. **D35** 3484 (1987).

[12] G. t'Hooft in Recent Developments in Gauge Theories, Cargése Summer Institute Lectures, 1979, eds. G. t'Hooft et al (Plenum Press, New York, 1980).

[13] J. N. Bahcall and R.K. Ulrich, Rev. Mod. Phys. **60**, 297 (1988); Turk-Chieze et al, Astrophys. J. **335**, 415 (1988).

[14] see J. N. Bahcall in Neutrino Astrophysics, Cambridge University Press, Cambridge (1989); D.S. Dearborn and G.M. Fuller, Phys. Rev. **D39**, 3543 (1989).

[15] S. P. Mikheyev and A. Y. Smirnov Sov. J. Nucl. Phys. **42**, 913; Nuovo Cimento **9C**, 17 (1986); Sov. JETP **64**, 64 (1986); in Proceedings of Twelfth International Conference on Neutrino Physics and Astrophysics, edited by T. Hitaki and H. Yuta, World Scientific, Singapore (1986), p. 177; L. Wolfenstein, Phys. Rev. **D20**, 2369 (1979); M.B. Voloshin et al., Sov. JETP **64**, 446 (1986).

[16] A. Zee, Phys. Lett. **93B**, 389, (1980); Phys. Lett. **161B**, 141, (1985). S.T. Petcov, Phys. Lett **115B**, 401 (1982).

[17] L. Wolfenstein, Nucl. Phys. **B175**, 93 (1980).

[18] Particle Data Group, Phys. Lett. **239B**, 1 (1990).

[19] A.E. Nelson and S.M. Barr, Phys. Lett. **246B**, 141 (1990).

[20] M. Doi et al., Phys. Lett. B **102**, 323 1989.

[21] B. Kayser, PRD **24**, 110 1981.

[22] P. D. Mannheim, PRD **37**, 1935 1988.

[23] J. Bouchez et al., Z. Phys. C **32** ,499 1986.

[24] S. M. Bilensky and S. T. Petcov, Rev. Mod. Phys. **59** ,671 1987.

[25] A. Suzuki, KEK-PREPRINT-93-96, Aug 1993.

[26] H. Anada and H. Nishimura, PRD **41**, 2379 1990.

[27] V. Barger, R. J. N. Phillips, and K. Whisnant, Phys. Rev. Lett. **65**, 3084 1990.

[28] D. N. Spergel and J. N. Bahcall, Phys. Lett. B **200**, 366 1987.

[29] S. R. Mishra et al., Phys. Lett. B **252**, 170 1990; D. Geiregat et al., Phys. Lett. B **249**, 131 1990.

[30] B. Balke et al., PRD **37**, 587 1988.

[31] W. C. Haxton, J. Stephenson, Jr., and D. Strottman, Prog. Part. Nucl. Phys. **12**, 132 1984; M. Doi, T. Kotani, and T. Takasugi, Prog. Theor. Phys. Suppl. **83**, 1985.

[32] S. T. Petcov, Phys. Lett. B **115**, 401 1982.

[33] J. N. Bahcall and M. H. Pinsonneault, Rev. Mod. Phys. **64**,885 (1992).

[34] GALLEX Collaboration (P. Anselmann, et al.), Phys. Lett. **B327**, 377 (1994).

[35] SAGE collaberation, Talk at International Conference on Non-Accelerator Particle Physics, Bangalore, India 1994. See R.J.N. Phillips, RAL-94-017, Jan. 1994.

[36] S. Turck-Chièze, S. Cahen, M. Casse, and C. Doom, Astrophys. J. **335**, 415 (1988); S. Turck-Chièze and I. Lopes, Astrophys. J. **408**, 347 (1993).

[37] E. Bellotti, Talk given at 27th International Conference on High Energy Physics, Glasgow, (1994).

[38] M. Fukugita and T. Yanagida, Phys. Rev. D **42**, 1285 (1990); B. Campbell, S. Davidson, J. Ellis and K.A. Olive, Phys. Lett. B **256**, 457 (1991); Astropart. Phys. **1**, 77 (1992); J. A. Harvey and M. S. Turner, Phys. Rev. D **42**, 3344 (1990).

[39] A.E. Nelson and S.M. Barr, Phys. Lett. B **246**, 141 (1991); W. Fischler, G.F. Giudice, R.G. Leigh and S. Paban, Phys. Lett. B **258**, 45 (1991).

[40] G. 't Hooft, Phys. Rev. Lett. **37**, 8 (1976); Phys. Rev. D **14**, 3432 (1976).

[41] V. Kuzmin, V. Rubakov, M. Shaposhnikov, Phys. Lett. B **155**, 36 (1985); P. Arnold, L. McLerran, Phys. Rev. D **37**, 1020 (1988); N. S. Manton, Phys. Rev. D **28**, 2019 (1983); F. R. Klinkhammer and N. S. Manton, Phys. Rev. D **30**, 2212 (1984).

[42] L.J. Hall and Suzuki, Nucl. Phys. B **231**, 419 (1984); C. Aulakh and R. Mohapatra, Phys. Lett. B **119**, 136 (1983); I.H. Lee, Nucl. Phys. B **246**, 120 (1984); G.G. Ross and J.W.F. Valle, Phys. Lett. B **151**, 375 (1985); S.Dawson, Nucl. Phys. B **261**, 297 (1985); F. Zwirner, Phys. Lett. B **132**, 103 (1983); R. Barbieri, and A. Masiero, Nucl. Phys. B **267**, 679 (1986); S. Dimopoulos and L. J. Hall, Phys. Lett. B **196**, 135 (1987).

[43] L. E. Ibáñez and Fernando Quevedo, Phys. Lett. B **283**, 261 (1992).

[44] J. Cline, K Kainulainen, K. A. Olive, Phys. Rev. Lett. **71**, 2372 (1993);

[45] H. Dreiner and G.G. Ross, Nucl. Phys. **B410**, 188 (1993).

[46] S.M. Barr, Phys. Rev. D **44**, 3062 (1991); D.B. Kaplan, Phys. Rev. Lett. **68**, 741 (1992).

[47] S. Dodelson, B.R. Greene, L.M. Widrow, Nuc. Phys. B **372**, 467 (1992).

[48] D.O. Caldwell *et al.*, Phys. Rev. Lett. **61**, 510 (1988).

[49] S.P. Ahlen *et al.*, Phys. Lett. B **195**, 603 (1987).

[50] E.W. Kolb and M. S. Turner, The Early Universe (Addison-Wesley, Redwood City, CA, 1990) and references therein.

[51] D. Lindley, Astrophys. J. **294**, 1 (1985); J. Audouze, D. Lindley and J. Silk, Astrophys. J. **293**, L53 (1985).

[52] J. Ellis, G. Gelmini, C. Jarlskog, G.G. Ross and J.W.F. Valle, Phys. Lett. B **150**, 142 (1985).

[53] S. M. Barr, R. S. Chivukula and E. Fahri, Phys. Lett. B **241**, 387 (1991); S. M. Barr, Phys. Rev. D **44**, 3062 (1992); D. Kaplan, Phys. Rev. Lett. **68**, 741 (1992).

[54] S. Dimiopoulos, S. Raby, and F. Wilczek, Phys. Rev. D **24**, 1681 (1981); L.. Ibanez and G. G. Ross, Phys. Lett. **105B**, 439 (1981); M. B. Einhorn and D. R. T. Jones, Nucl. Phys. B **196**, 475 (1982); W. J. Marciano and G. Senjanovic, Phys. Rev. D **25**, 3092 (1982).

[55] H. Georgi and L. Glashow, Phys. Rev. Lett. **32**, 438 (1974);
M.J.G. Veltman, Acta Phys. Pol. **B12**, 437 (1981);
L. Maiani, Gif-sur-Yvette Summer School on Particle Physics 11th, Gif-sur-Yvette, France, 1979 (Inst. Nat. Phys. Nucl. Phys. Particules, Paris, 1979);
S. Dimopoulos and S. Raby, Nucl. Phys. **B192**, 353 (1981);
E. Witten, Nucl. Phys. **B188**, 513 (1981);
M. Dine, W. Fischler, and M. Srednicki, Nucl. Phys. **B189**, 575 (1981).

[56] N. Sakai and T. Yanagida, Nucl. Phys. **B197**, 533 (1982);
S. Weinberg, Phys. Rev. **D26**, 287 (1982).

[57] E. Witten, in Ref. [55];
S. Dimopoulos, S. Raby, and F. Wilczek, Phys. Rev. **D24**, 1681 (1981);
S. Dimopoulos and H. Georgi, Nucl. Phys.**B193**, 150 (1981);
N. Sakai, Zeit. Phys.**C11**, 153 (1981).

[58] J. Ellis, D.V. Nanopoulos, and S. Rudaz, Nucl. Phys.**B202**, 43 (1982);
P. Nath, A.H. Chamseddine, and R. Arnowitt, Phys. Rev. **D32**, 2348 (1985);
P. Nath and R. Arnowitt, Phys. Rev.**D38**, 1479 (1988).

[59] G. Anderson, S. Dimiopoulos, L. J. Hall, S. Raby, and G. D. Starkman, Phys. Rev. D **49**, 3660 (1994).

[60] M. Kobayashi and T. Maskawa, Prog. Th. Phys. **49**, 652 (1973).

[61] L. Wolfenstein, Phys. Rev. Lett. **51**, 1945 (1983).

[62] J. S. Hagelin, S. Keely, and T. Tanaka, Nucl. Phys. **B415**, 293 (1994).

[63] J. Hisano, H. Murayama, and T. Yanagida, Nucl. Phys. B **402**, 46 (1993).

[64] T. Goto, T. Nihei, and J Arafune, University of Tokyo Preprint, ICRR-Report-317-94-12, April 1994.

[65] P. Nath, A.H. Chamseddine, and R. Arnowitt, Phys. Rev. **D32**, 2348 (1985).

[66] A. Bouquet, J. Kaplan, and C. A. Savoy, Phys. Lett. B **148**, 69 (1984);
G.G. Ross and S. K.. Wilkinson, Nucl. Phys. **B282**, 382 (1987).

[67] A. Bouquet, J. Kaplan, and C. A. Savoy, Phys. Lett. B **148**, 69 (1984); Nucl. Phys. **B262**, 299 (1985);
B. Gato, J. Leon, J. Perez-Mercader, and M Quiros, Nucl. Phys.. **b253**, 285 (1985);
N. K. Falck, Z. Phys. **C30**, 247 (1986);
M. Drees and M. M. Nojiri, Nucl. Phys. **B369**, 54 (1992);
D.J. Castano, E.J. Piard, P. Ramond, Phys. Rev. **D47**, 232 (1992);
H. Baer et al., Florida State University Preprint, FSU-HEP-940311, June 1994;
J. S. Hagelin, S. Keely, and T. Tanaka, Nucl. Phys. **B415**, 293 (1994).

[68] L.J. Hall, V.A. Kostelecky, and S. Raby, Nucl. Phys. **B267**, 415 (1986).

[69] G.G. Ross and S. K.. Wilkinson, Nucl. Phys. **B282**, 382 (1987);
F. Gabbiani and A. Masiero, Nucl. Phys. **B322**, 235 (1989);
S.P. Martin and P. Ramond, Phys. Rev. **D48**, 5365 (1993).

[70] Y. Nir and N. Seiberg, Phys. Lett. **B309**, 337 (1993).

[71] M. Dine, R. Leigh, and A. Kagan, Phys. Rev. **D48**, 4369 (1993).

[72] P. Pouliot and N. Seiberg, Phys. Lett. **B318**, 169 (1993);
D. A. Kaplan and M. Schmaltz, Phys. Rev. **D49**, 3741 (1994).

[73] A. Bouquet, J. Kaplan, and C. A. Savoy, Phys. Lett. B **148**, 69 (1984); Nucl. Phys. **B262**, 299 (1985).

[74] J.F. Donoghue, H.P. Nilles, and D. Wyler, Phys. Lett. B **128**, 55 (1983);
M.J Duncan, Nucl. Phys. **B221**, 285 (1983);
M.J Duncan and J. Trampetic, Phys. Lett. **B134**, 439 (1984);
R. Barbieri and R. Gatto, Phys. Lett. **B110**, 210 (1982).

[75] P. Nath and R. Arnowitt, Phys. Rev.**D38**, 1479 (1988).

[76] H. Baer et al., Florida State University Preprint, FSU-HEP-94031, June 1994.

[77] H.E. Haber and G.L. Kane, Phys. Rep. (Phys. Lett. C) **117**, 75 (1985).

[78] I thank Hitoshi Murayama for suggesting this operator.

Appendix A

Yukawa Matrices

We list the 54 ADHRS models which we use in the main text. They differ by the choice of O_{22} and O_{23} operator used. All have the same O_{33} and O_{12} operator given in equation (5.7). The notation is explained in the text and in reference [59].

The six choices for O_{22} are

$$\begin{aligned}
&16_2\, 45_X\, 10\, \tfrac{45_{B-L}}{45_X}\, 16_2 \\
&16_2\, \tfrac{1}{45_X}\, 10\, 45_{B-L}\, 16_2 \\
&16_2\, 45_X\, 10\, 45_{B-L}\, 16_2 \\
&16_2\, 10\, \tfrac{45_{B-L}}{45_X}\, 16_2 \\
&16_2\, 10\, 45_X\, 45_{B-L}\, 16_2 \\
&16_2\, 10\, \tfrac{45_{B-L}}{45_X^2}\, 16_2
\end{aligned} \tag{A.1}$$

The nine choices for O_{23} are

$$
\begin{aligned}
&16_2\ 45_Y\ 10\ \tfrac{1}{45_X}\ 16_3\\
&16_2\ 45_Y\ 10\ \tfrac{45_{B-L}}{45_X}\ 16_3\\
&16_2\ \tfrac{45_Y}{45_X}\ 10\ \tfrac{1}{45_X}\ 16_3\\
&16_2\ \tfrac{45_Y}{45_X}\ 10\ \tfrac{45_{B-L}}{45_X}\ 16_3\\
&16_2\ 45_Y\ 10\ \tfrac{45_Y}{45_X}\ 16_3\\
&16_2\ \tfrac{45_Y}{45_X}\ 10\ \tfrac{45_Y}{45_X}\ 16_3\\
&16_2\ 10\ \tfrac{1}{45_X^2}\ 16_3\\
&16_2\ 10\ \tfrac{45_{B-L}}{45_X^2}\ 16_3\\
&16_2\ 10\ \tfrac{45^2_{B-L}}{45_X^2}\ 16_3
\end{aligned}
\tag{A.2}
$$

For the possible choices above, we list the Yukawa matrices $\hat{\lambda}^g$, $g = u, d, e$, which are defined in the text.

$$
\hat{\lambda}^u = \begin{pmatrix} 0 & -\frac{C}{27} & 0 \\ -\frac{C}{27} & 0 & (-4,-4,-4,-4,-4,-4,1,1,1)B \\ 0 & (1,-1,1,-1,-4,-4,1,-1,1)B & A \end{pmatrix} \tag{A.3}
$$

$$
\hat{\lambda}^d = \begin{pmatrix} 0 & C & 0 \\ C & Ee^{i\phi} & (2,2,-\frac{2}{3},-\frac{2}{3},2,-\frac{2}{3},1,1,1)B \\ 0 & (-\frac{1}{3},\frac{1}{3},-\frac{1}{3},\frac{1}{3},-\frac{2}{3},-\frac{2}{3},\frac{1}{9},-\frac{1}{9},\frac{1}{9})B & A \end{pmatrix} \tag{A.4}
$$

$$
\hat{\lambda}^e = \begin{pmatrix} 0 & C & 0 \\ C & 3Ee^{i\phi} & (-2,6,-2,6,6,6,\frac{1}{9},-\frac{1}{3},1)B \\ 0 & (-3,-9,1,3,-18,6,1,3,9)B & A \end{pmatrix} \tag{A.5}
$$

Similarly, For the possible choices above, we list the Yukawa matrices $\hat{U}^G$, $G = Q, L, D, E$, which are defined in the text.

$$\hat{U}^Q = \begin{pmatrix} 0 & -\frac{C}{27} & 0 \\ -\frac{C}{27} & (-\frac{3}{4}, -\frac{3}{2}, -\frac{1}{2}, \frac{3}{2}, \frac{1}{2}, \frac{9}{4})Ee^{i\phi} & (1,1,1,1,1,1,1,1,1)B \\ 0 & (1,1,1,1,1,1,1,1,1)B & A \end{pmatrix} \tag{A.6}$$

$$\hat{U}^L = \begin{pmatrix} 0 & C & 0 \\ C & (\frac{3}{4}, \frac{5}{2}, \frac{3}{2}, \frac{3}{2}, \frac{5}{2}, \frac{3}{4})Ee^{i\phi} & (-\frac{1}{3}, 1, -\frac{1}{3}, 1, 1, 1, \frac{1}{9}, -\frac{1}{3}, 1)B \\ 0 & (-3,-3,1,1,-3,1,1,1,1)B & A \end{pmatrix} \tag{A.7}$$

$$\hat{U}^D = \begin{pmatrix} 0 & C & 0 \\ C & (-\frac{5}{4}, \frac{1}{2}, -\frac{1}{2}, -\frac{1}{2}, \frac{1}{2}, -\frac{5}{4})Ee^{i\phi} & (\frac{4}{3}, -\frac{4}{3}, \frac{4}{3}, -\frac{4}{3}, \frac{8}{3}, \frac{8}{3}, \frac{1}{9}, -\frac{1}{9}, \frac{1}{9})B \\ 0 & (2, -2, -\frac{2}{3}, \frac{2}{3}, -8, \frac{8}{3}, 1, -1, 1)B & A \end{pmatrix} \tag{A.8}$$

$$\hat{U}^E = \frac{1}{2}\begin{pmatrix} 0 & -\frac{C}{27} & 0 \\ -\frac{C}{27} & (-\frac{3}{4}, -\frac{3}{2}, -\frac{1}{2}, \frac{3}{2}, \frac{1}{2}, \frac{9}{4})Ee^{i\phi} & (-4,-12,-4,-12,-24,-24,1,3,9)B \\ 0 & (6,-6,6,-6,-24,-24,1,-1,1)B & A \end{pmatrix} \tag{A.9}$$

Appendix B

Branching Ratios

We list some of the branching ratios for proton and neutron decays in the table below. For the neutrino modes we have normalized by the rate for ($p \to K^+\overline{\nu}_\mu$). For the charged lepton modes we have normalized by the rate for ($p \to K^0\mu^+$). The relative branching ratio of these reference modes is discussed in the text in Sections 5.8, 5.8.1, and 5.9.

Replacing ν_μ by ν_e or μ by e introduces two extra factor of $\sin\theta_1 \approx 0.2$ in the branching ratios. The ν_τ modes are also discussed in the text in Sections 5.7 and 5.8.

In arriving at our result, we have used the Chiral lagrangian analysis of reference [63]. For example,

$$\Gamma(p \to K^+\nu_i) = \frac{(m_p^2 - m_K^2)^2}{32\pi m_p^3 f_\pi^2}\left|C(sud\nu_i)\frac{2m_p}{3m_B}D + C(dus\nu_i)\left(1 + \frac{m_p}{3m_B}(D+3F)\right)\right|^2, \tag{B.1}$$

$$\Gamma(p \to K^0 e_i) = \frac{(m_p^2 - m_K^2)^2}{32\pi m_p^3 f_\pi^2}\left|C(suue_i)\left(1 - \frac{m_n}{m_B}(D-F)\right)\right|^2, \tag{B.2}$$

where the chiral lagrangian factors are estimated to be $m_B = 1150 MeV$, $D = 0.81$ and $F = 0.44$. Similar results for the other possible decays are listed in reference [63].

$\overline{\nu}_\mu$	$\frac{\Gamma(\overline{\nu}_\mu mode)}{\Gamma(p \to K^+\overline{\nu}_\mu)}$
$p \to \pi^+\overline{\nu}_\mu$	1.2×10^{-1}
$n \to \pi^0\overline{\nu}_\mu$	5.8×10^{-2}
$n \to \eta\overline{\nu}_\mu$	2.1×10^{-2}
$n \to K^0\overline{\nu}_\mu$	1.8

(B.3)

μ^+	$\frac{\Gamma(\mu^+ mode)}{\Gamma(p \to K^0\mu^+)}$
$p \to \pi^0\mu^+$	4.8×10^{-1}
$n \to \pi^-\mu^+$	1.0
$p \to \eta\mu^+$	1.7×10^{-1}

(B.4)

LAWRENCE BERKELEY LABORATORY
UNIVERSITY OF CALIFORNIA
TECHNICAL INFORMATION DEPARTMENT
BERKELEY, CALIFORNIA 94720